



Cationic micelles and methods for using them

Halldóttir, Hólmfríður Rósa; Andresen, Thomas Lars; Henriksen, Jonas Rosager; Hansen, Anders Elias; Bak, Martin; Jensen, Andreas Tue Ingemann; Petersen, Lars Ringgaard; Jæhger, Ditte Elisabeth; Melander, Carl Frederik; Eliassen, Rasmus

Total number of authors:
11

Publication date:
2020

Document Version
Publisher's PDF, also known as Version of record

[Link back to DTU Orbit](#)

Citation (APA):
Halldóttir, H. R., Andresen, T. L., Henriksen, J. R., Hansen, A. E., Bak, M., Jensen, A. T. I., Petersen, L. R., Jæhger, D. E., Melander, C. F., Eliassen, R., & Larsen, J. B. (2020). Cationic micelles and methods for using them. (Patent No. WO2020249745).

General rights

Copyright and moral rights for the publications made accessible in the public portal are retained by the authors and/or other copyright owners and it is a condition of accessing publications that users recognise and abide by the legal requirements associated with these rights.

- Users may download and print one copy of any publication from the public portal for the purpose of private study or research.
- You may not further distribute the material or use it for any profit-making activity or commercial gain
- You may freely distribute the URL identifying the publication in the public portal

If you believe that this document breaches copyright please contact us providing details, and we will remove access to the work immediately and investigate your claim.



(51) International Patent Classification:

A61K 51/12 (2006.01) C07K 5/072 (2006.01)

A61K 51/08 (2006.01) C07K 5/09 (2006.01)

A61K 49/00 (2006.01) C07K 5/11 (2006.01)

A61K 51/04 (2006.01) G01N 33/58 (2006.01)

(21) International Application Number:

PCT/EP2020/066328

(22) International Filing Date:

12 June 2020 (12.06.2020)

(25) Filing Language:

English

(26) Publication Language:

English

(30) Priority Data:

19179716.6 12 June 2019 (12.06.2019) EP

19208070.3 08 November 2019 (08.11.2019) EP

(71) Applicant: DANMARKS TEKNISKE UNIVERSITET

[DK/DK]; Anker Engelunds Vej 101 A, 2800 Kgs. Lyngby (DK).

(72) Inventors: ANDRESEN, Thomas Lars; Kroegebjerg 68,

2720 Vanløse (DK). HENRIKSEN, Jonas Rosager;

Gravenstensvej 14, 3450 Allerød (DK). HANSEN, Anders

Elias; Snickaregatan 9, 21618 Linhamm (SE). BAK, Mar-

tin; Peter Sabroes Gade 8, 2.tv, 2450 Copenhagen SV (DK). JENSEN, Andreas Tue Ingemann; Engbakken 40, 2840 Virum (DK). PETERSEN, Lars Ringgaard; Kongensvej 2, 1.mf, 2000 Frederiksberg (DK). JÆHGER, Ditte Elisabeth; Richard Mortensens Vej 71.5.3, 2300 Copenhagen S (DK). MELANDER, Carl Frederik; Korpvägen 16, 218 33 Bunkflostrand (SE). ELIASSEN, Rasmus; Harmonivej 3, 3650 Ølstykke (DK). LARSEN, Jannik Bruun; Tjørnevænget 1, 2800 Kgs. Lyngby (DK). HALLDÓTTIR, Hólmfríður Rósa; Vanløse Torv 217, 3.tv, 2720 Vanløse (DK).

(74) Agent: HØIBERG P/S; Adelgade 12, 1304 Copenhagen K (DK).

(81) Designated States (unless otherwise indicated, for every kind of national protection available): AE, AG, AL, AM, AO, AT, AU, AZ, BA, BB, BG, BH, BN, BR, BW, BY, BZ, CA, CH, CL, CN, CO, CR, CU, CZ, DE, DJ, DK, DM, DO, DZ, EC, EE, EG, ES, FI, GB, GD, GE, GH, GM, GT, HN, HR, HU, ID, IL, IN, IR, IS, JO, JP, KE, KG, KH, KN, KP, KR, KW, KZ, LA, LC, LK, LR, LS, LU, LY, MA, MD, ME, MG, MK, MN, MW, MX, MY, MZ, NA, NG, NI, NO, NZ, OM, PA, PE, PG, PH, PL, PT, QA, RO, RS, RU, RW, SA,

(54) Title: CATIONIC MICELLES AND METHODS FOR USING THEM

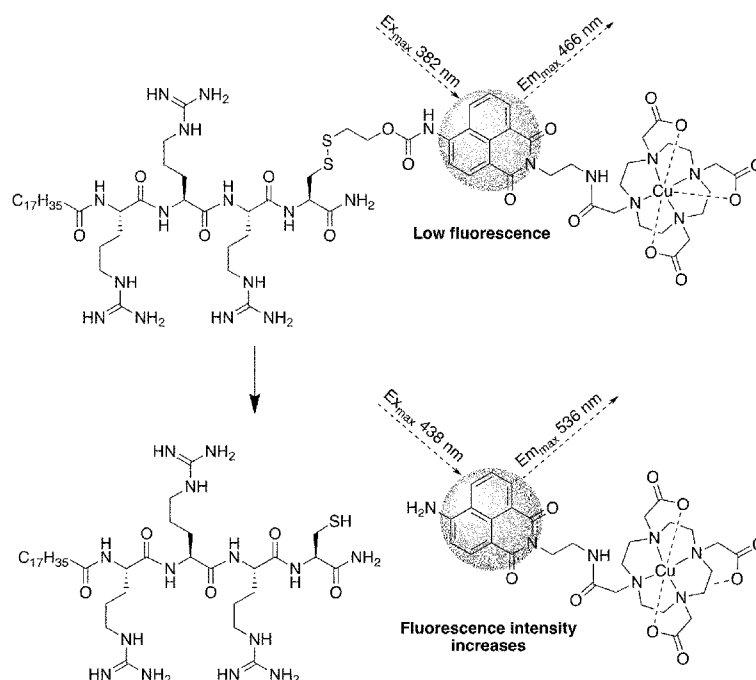


Fig. 2

(57) Abstract: The present invention relates to cationic micelles, and in particular the compounds capable of forming such cationic micelles for use in cell tracking.



SC, SD, SE, SG, SK, SL, ST, SV, SY, TH, TJ, TM, TN, TR,
TT, TZ, UA, UG, US, UZ, VC, VN, WS, ZA, ZM, ZW.

(84) Designated States (*unless otherwise indicated, for every kind of regional protection available*): ARIPO (BW, GH, GM, KE, LR, LS, MW, MZ, NA, RW, SD, SL, ST, SZ, TZ, UG, ZM, ZW), Eurasian (AM, AZ, BY, KG, KZ, RU, TJ, TM), European (AL, AT, BE, BG, CH, CY, CZ, DE, DK, EE, ES, FI, FR, GB, GR, HR, HU, IE, IS, IT, LT, LU, LV, MC, MK, MT, NL, NO, PL, PT, RO, RS, SE, SI, SK, SM, TR), OAPI (BF, BJ, CF, CG, CI, CM, GA, GN, GQ, GW, KM, ML, MR, NE, SN, TD, TG).

Declarations under Rule 4.17:

— *of inventorship (Rule 4.17(iv))*

Published:

— *with international search report (Art. 21(3))*

Cationic micelles and methods for using them

Technical field

- 5 The present invention relates to cationic micelles, and in particular compounds capable of forming such cationic micelles for use in cell tracking.

Background

- 10 The ability to specifically label a distinct cell population in the laboratory (*in vitro*) and subsequently non-invasively study the distribution in the body (*in vivo*) can provide important information for diagnostic and therapeutic interventions.

- Radiolabeling provides the possibility to non-invasively determine the biodistribution and kinetics of radioactivity-labeled cell by means of nuclear medicine imaging technologies with high sensitivity and spatial resolution, including; positron emission tomography (PET), single photon emission computed tomography (SPECT) and gamma camera imaging. Nuclear medicine imaging techniques (i.e. PET and SPECT) have much better clinical potential than optical imaging in that they have long range tissue penetration capability and they are highly quantitative. Bioluminescence imaging with use of luciferase reporter genes and optical imaging with use of dye-labeled cells are not practical for whole-body imaging because of the limited tissue penetration of light. Moreover, bioluminescence imaging requires transfection of luciferase, whose immunogenicity cannot be excluded. Magnetic resonance (MR) imaging with iron nanoparticle-loaded cells has limited sensitivity due to the negative contrast of iron superimposed on a highly heterogeneous background.
- 15
20
25

- Although techniques that use perfluorocarbon agents to label cells *ex vivo* and visualize positive signals with fluorine 19 (^{19}F) MR imaging have been rapidly developing, the requirement of a dedicated coil installation and relatively weak signal of ^{19}F is a significant constraint.
- 30

On the contrary, optical imaging properties provide the possibility to study e.g. labeling efficacy, distribution, division of label between progeny cells and kinetics *in vitro* and in cell product harvested after *in vivo* administration.

The clinical application of a flexible cell labeling technology can be divided into procedures for diagnostics and therapeutic purposes. From a diagnostic perspective the technology can include labeling of leukocytes that are recruited to sites of inflammation. Leukocyte imaging is used to localize acute infections, where neutrophils are still rapidly and actively localizing to the infection, e.g. for imaging for osteomyelitis that does not involve the spine, and for locating abdominal and pelvic infections and patients with a fever of unknown origin or suspected inflammatory or infectious foci. Modern cell sorting technologies are furthermore providing the possibility to accurately isolate specific cell populations and phenotypes of, e.g. natural killer cells (NK-cells), dendritic cells (DCs), B lymphocytes, regulatory T lymphocytes (Treg), cytotoxic T lymphocytes (cTL) and helper T lymphocytes (Th). This allows for studying disease mechanisms for research and diagnostic purposes in animal models and diseased individuals. The cells may be isolated from the individual to be investigated (autologous cell product) or in cases where the products do not need to be autologous to the individual to be investigated, be collected from a donor (allogenic cell product).

Cell-based therapies (also termed cellular therapy or cytotherapy) have been demonstrated to hold tremendous potential in the treatment of various cancers and other uses are also emerging, including stem cell therapies. Cell-based therapy holds great promise for cancer treatment. The ability to non-invasively by nuclear imaging technology track, in real-time, the delivery of various therapeutic cells (e.g. T cells and stem cells) to the tumor site, and/or subsequent differentiation/proliferation of these cells, would allow better understanding the molecular basis of immune cell trafficking and biodistribution of these immune cells is critical for developing more efficacious immunotherapies. Cell-based therapies are highly heterogeneous in terms of technology and obtaining direct information on cell trafficking after administration to an experimental model or diseased individual is vital to decipher and identify the optimal approach. A flexible cell labeling system that does not alter cell functionality, phenotype and trafficking is highly attractive for this evaluation. The biocompatibility, toxicity, and safety are paramount for, not only the labeled cell product, but also the recipient to assure clinical and translational value. Various approaches have been applied for radiolabeling of specific cells in the laboratory (*in vitro*). These can generally be divided into direct and indirect methods. In direct labeling, cells are labeled with certain tags that can be detected directly with suitable imaging equipment, whereas the indirect technique typically uses a reporter gene approach. Direct cell labeling does not involve

genetic modification of the cell. Instead cells are actively labeled with the appropriate method *in vitro* and are administered to a recipient. Optimally, this should allow for labeling of cell with minimal influence on their behavior and thus provides the most reliable read-out for evaluation of the therapeutic cell product. The two most commonly applied technologies are based on oxines and on radiolabeled antibody attachment to the cell product before injection into the subject of interest. In the case of oxine labeling this has mostly been performed using zirconium 89 (^{89}Zr), copper 64 (^{64}Cu) and indium 111 (^{111}In) as radioisotopes. However, the cellular toxicity of oxine and radioisotopes has limited their clinical advancement beyond leukocytes scintigraphy.

In the case of antibodies, the specific ligands available to antibody targeting have generally been associated with problems in terms of cell functionality and the amount of radioactivity that can be attached. In the specific case of T cell labeling of the T cell receptor it was demonstrated that the receptor was lost 24 hours after labeling and antigen binding was subsequently very low. These features are highly problematic for evaluation of the cell product behavior. Furthermore, the antibody-based radiolabeling requires that a specific antibody and ligand are used, and are available, for the cell type of interest, which is limiting for the clinical application of the technology.

Hence, there is a need in the art for a flexible cell labeling system that is able to efficiently label a broad range of cells by a highly tolerated, with importance both for the advancement and understanding of cell-based therapies but equally for diagnostic purposes. Any flexible cell labeling system must furthermore involve simple procedures that allows for the implementation into routine laboratory processes for clinical applicability.

Summary

The present inventors have developed a flexible system, comprising a compound as disclosed herein, for well tolerated *in vitro* radiolabeling of cells for subsequent administration to a subject for the study of e.g. cell kinetics and biodistribution in relation to the cell type labeled and diagnostic or therapeutic evaluation intended. The present disclosure provides an improved method for labeling cells with minimal influence on biological properties and thereby solves the discussed limitations of currently applied technology known in the art. The flexible labeling technology is based on partitioning between cationic micelles and negatively charged cell membranes

which provides a broadly applicable and highly effective cell labeling system. The labeling technology is solely dependent on the partitioning effect and as such does not require or interfere with cellular receptors or signaling ligands.

- 5 In a first aspect, a compound is provided, comprising:
- a. a chelator group (Z_1),
 - b. a cationic peptide sequence (P_1) comprising amide-bonded amino acids, and
 - c. a lipophilic aliphatic group (A_1).
- 10 In a second aspect, a method for labelling cells is provided comprising the steps of:
- a. providing a compound as defined herein,
 - b. providing cells from a subject, and
 - c. contacting the compound with the cells in vitro.
- 15 In a third aspect, use of a compound as defined herein is provided for tracking cell proliferation, differentiation, and/or function.
- In a fourth aspect, a composition comprising a micelle is provided, wherein the micelle comprises a plurality of compounds as defined herein.
- 20 In a fifth aspect, a kit is provided for tracking cell proliferation, differentiation, and/or function, comprising:
- a. a compound as defined herein,
 - b. a solvent, and optionally
 - c. instructions for use
- 25

Description of Drawings

Fig. 1: Surface tension plotted against the concentration of D3R-C16 (A) and D3R-C18 (B). The results are presented as mean \pm SEM, $n = 3$. The CMC is the intersection between the regression straight line (grey dashed lines) and the straight line passing through the plateau (black dashed lines).

30

Fig. 2: Conceptual drawing of the mode of action of the redox-induced cleavage of the disulphide-bridge of the DFSS3R-C18 compound.

35

Fig. 3: A: Emission and excitation scanning of the intact DFSS3R-C18 construct giving an excitation / emission maximum of 382 nm / 466 nm. B: Emission and excitation scanning of the cleaved DFSS3R-C18 construct giving an excitation / emission maximum of 438 nm / 536 nm. C: Emission profile with an excitation of 405 nm. D: Emission profile with an excitation of 438 nm. E: Emission profile with an excitation of 488 nm. In this experiment, DFSS3R-C18 was dissolved in ISO-TRIS-NaCl (10mM TRIS, 150mM NaCl, pH 7.8).

Fig. 4: Fluorescence response/standard curve of the intact DFSSR3-C18 analogue in ISO-TRIS-NaCl buffer (10 mM / 150 mM, pH 7.8) (black flat 96-well plate, 80 μ L per well, Conc. 50, 25, 10, 5, 2.5, 1, 0.5, 0.25, 0.1 μ M). A: Ex382 nm and Em466 nm, B: Ex438 nm and Em545 nm with a bandwidth of 10 nm.

Fig. 5: Activation kinetics of DFSSR3-C18 studied via fluorescence emission. DTT or Cys was added (C_{final} 10 mM) to DFSSR3-C18 (50 μ M, 100 μ L) in ISO-TRIS-NaCl (10mM TRIS, 150mM NaCl, pH 7.8, 37 $^{\circ}$ C) with and without one equivalent of $CuCl_2$.

Fig. 6: Solvent effect on the fluorescence emission. DFSSR3-C18 (25 μ M, 100 μ L) in either TRIS, TRIS:DMSO or TRIS liposomes (Lipoid Stealth formulation comprising HSPC:Cholesterol:DSPE-PEG2000 in the molar ratio 56.5 to 38.2 to 5.3) at 37 $^{\circ}$ C with $CuCl_2$ (2.5 mg/mL, 1 eq.) added DTT (100 eq., 10 mM) ($n = 2$).

Fig. 7: pH dependency of the fluorescence emission of the cleaved and intact DFSS3R-C18 compound. A: The intact DFSSR3-C18 (5 μ L, 50 μ M) with Cu (1 eq., 2.5 mg/mL) was diluted in ISO-TRIS-NaCl (95 μ L, 10mM TRIS, 150mM NaCl, pH 2, 3, 4, 5, 6, 7, 7.8, 8, 9, 10 and 11 (HCl/NaOH)). Ex488nm and Em545nm, bandwidth: 20nm, Temp.: 22 $^{\circ}$ C ($n = 1$). B: The fully cleaved DFSSR3-C18 (5 μ L, 50 μ M) with Cu (1 eq., 2.5 mg/mL), and DTT (100 eq., 10 mM) was diluted in ISO-TRIS-NaCl (95 μ L, 10mM TRIS, 150mM NaCl, pH 2, 3, 4, 5, 6, 7, 7.8, 8, 9, 10 and 11 (HCl/NaOH)). Ex488nm and Em545nm, bandwidth: 20nm, Temp.: 22 $^{\circ}$ C (Std., $n = 2$).

Fig. 8: Partitioning into liposomes of ^{64}Cu -D3R-C16 (A) and ^{64}Cu -D3R-C18 (B). Comparison of liposome partitioning of D3R-C16 (C) and D3R-C18 (D) labelled with $^{64}Cu^{2+}$ or $^{177}Lu^{3+}$. The results are presented as mean \pm SEM, $n = 3$. POPC is the phosphatidylcholine, 1-palmitoyl-2-oleoyl-sn-glycero-3-phosphocholine. POPG is

palmitoyllecithin phosphatidylglycerol. The “stealth” liposomes have a polymer, PEG on their outer membrane and comprise HSPC:Cholesterol:DSPE-PEG2000 in the molar ratio 56.5 to 38.2 to 5.3.

5 **Fig. 9:** Flow cytometric characteristics of murine T lymphocytes (A) and human leukocytes (B) displaying loading efficiency in terms of mean fluorescence intensity (MFI) and percent positively labelled cells (% DFSS3R-C18+) and fraction of viable cells (% Viability) after incubation with DFSS3R-C18 at increasing concentrations.

10 **Fig. 10:** Murine T lymphocytes display increased viability at shorter incubation periods for all DFSS3R-C18 micelle concentrations investigated (A). The percentage of murine T lymphocytes positive for DFSS3R-C18 fluorescent signal is comparable between incubation periods of 20 minutes and 60 minutes across the investigated micelle concentrations (B). Mean fluorescence intensity is comparable between murine T
15 lymphocytes incubated for 20 minutes, 40 minutes and 60 minutes (C).

Fig. 11: Viability of murine T lymphocytes incubated for 1 hour with D3R-C18 or D3R-C16 micelles with saturated (+Cu) DOTA-chelator and unsaturated chelator.

20 **Fig. 12:** The influence of cellular density of murine T lymphocytes during incubation with DFSS3R-C18 at a micelle concentration of 40 μ M on cellular viability (% viability), percentage cells positive for fluorescent signal (% DFSS3R-C18 +) and mean fluorescence intensity (MFI). The viability of unloaded control was 81.5%. 0% viability was obtained at a cell density of 0.1×10^6 and 10^6 cells/mL.

25 **Fig. 13:** Murine T lymphocytes were radiolabelled using ^{64}Cu -D3R-C18 micelles and co-incubated with cell trace stained splenocytes for 2 hours. After co-incubation cell population were sorted by FACS based on cell trace staining. The sorted population were gamma counted to determine specific radioactivity in each population.

30 **Fig. 14:** ^{64}Cu -D3R-C18 micelle labelled T cells (5×10^6 Murine T lymphocytes) were injected intravenously in mice 24 hours after 5Gy whole body irradiation and compared to untreated controls by PET/CT scanning 16 and 40 hours after injection of T cells. Mice having received whole body irradiation displayed activity in thymus (5Gy TBI, dashed ellipse) whereas un-irradiated controls did not display accumulation in the thymus
35

(Control, dashed ellipse). Whole body irradiated mice displayed significantly higher ($p < 0.05$; un-paired t-test) activity compared to un-irradiated mice at PET scans performed 16 and 40 hours after injection of ^{64}Cu -D3R-C18 micelle labelled T cells.

5 **Fig. 15:** Bright field and MIP (maximum intensity projection) images of HT1080 cells in the presence of no micelles, DFSS3R-C18, or Cu-DFSS3R-C18.

Fig. 16: A: Summed intensity projection images of HT1080 cells after incubation with either no micelles, DFSS3R-C18 for 12 and 48 hours or DFSS3R-C18 for 24 hours and then 24 hours in non-micelle medium. B: Histogram depicting the $\text{Int}_{\text{AvrPix}}$ histogram for 114 individual cells and the mean $\text{Int}_{\text{AvrPix}}$ quantified using the gaussian fit. C: Mean $\text{Int}_{\text{AvrPix}}$ for the no micelle control, various incubation times and the retention after 24 hour incubation with and without micelles.

15 **Fig. 17:** Loading of activated T cells with D3R-C18 micelles does not change the composition (phenotype of CD8+ T cells). The barplots show mean and SEM ($n=6$). A: Barplot showing the % of naïve, central memory (T central memory), effector T cells (Teff/em) and CD44 and CD62L negative T cells (DN) from the viable population. B: MFI of PD1 in the populations. C: Viability of T cells 72 hours after loading with D3R-C18 micelles

Fig. 18: Activity acquired by well-counting is reported as function of the number of infused radiolabeled T cells for the thymus (A), spleen (B) and Tumor (C). Infusion was conducted in mice ($n=2$). PET ROI activity and well counting activity ratio between 5 and 25 10 million infused T cells is shown for the thymus, spleen and tumor in D.

Fig. 19: Biodistribution of T cells labeled (loaded) with ^{64}Cu -D3R-C18 and ^{64}Cu -D3R-C18 micelles as control. Accumulation is given for the spleen (A), lungs (B), blood (C), liver (D), tumor (E), bladder (F) as % ID/ cm^3 and as function of time. The overall whole-body radioactivity normalized to the activity at $t=0$ is given in (G).

Fig. 20: PET/CT images of mice treated with TLR7 agonist immunogel (left) and untreated control (right). The mean and maximum accumulation is presented as %ID/g.

Fig. 21: Conceptual drawing of the mode of action of the non-cleavable DF3R-C18 compound.

Fig. 22: Emission and excitation scanning of the DF3R-C18 construct giving an
5 excitation / emission maximum of 434 nm / 546 nm.

Detailed description

Definitions

10 The term “aliphatic” is used herein to describe any compound or part of a compound (group within a compound) that is aliphatic. Aliphatic in the present context shall refer to any hydrocarbon based molecule which is non-aromatic. Aliphatic molecules can be non-cyclic or cyclic, and can be unsaturated or saturated, and/or straight or branched. In the present context, an aliphatic group includes gonane-based structures, such as steroids. Aliphatic compounds can be saturated, joined by single bonds (alkanes), or
15 unsaturated, with double bonds (alkenes) or triple bonds (alkynes). Besides hydrogen, other elements can be bound to the carbon chain, the most common being oxygen, nitrogen, sulfur, and chlorine.

20 The term “lipophilic aliphatic” is used herein to describe any compound or part of a compound that is aliphatic as defined above, and also lipophilic. The term “lipophilic” as used herein, refers to the ability of a compound or part of a compound to dissolve in fats, oils, lipids, and non-polar solvents such as hexane or toluene. Such non-polar solvents are themselves lipophilic. Lipophilic substances tend to dissolve in other lipophilic substances. A non-limiting example of a “lipophilic aliphatic” group is an acyl
25 group, such as a C18 acyl.

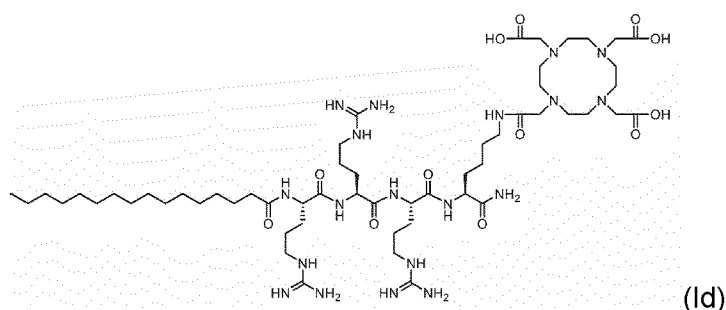
The term “chelator group” as used herein, refers to any moiety within a compound capable of chelating an ion to form a chelate. Chelation, by the chelator group, involves the formation or presence of two or more separate coordinate bonds between a
30 polydentate (multiple bonded) ligand and a single central atom.

The term “functional group” as used herein, refers to a specific grouping of atoms within molecules that has its own characteristic properties, regardless of the other atoms present in a molecule. Common non-limiting examples are alcohols, amines,
35 carboxylic acids, ketones, ethers, and amides,

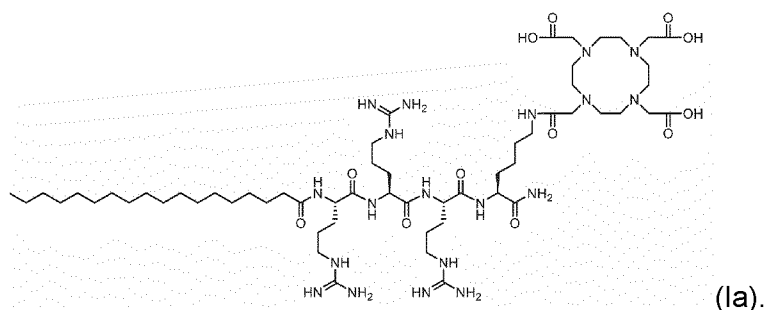
The term “PEG”, as used herein, refers to the polyether compound polyethylene glycol. PEG is currently available in several sizes and may e.g. be selected from PEG350, PEG550, PEG750, PEG1000, PEG2000, PEG3000, PEG5000, PEG10000, PEG20000 and PEG30000. The number refers to the molecular weight of the ethylene units.

The term “physiological conditions”, as used herein, refers to conditions simulating *in vivo* conditions or being *in vivo* conditions. Physiological systems are generally considered to be comprised of an aqueous system having a pH of about 7.

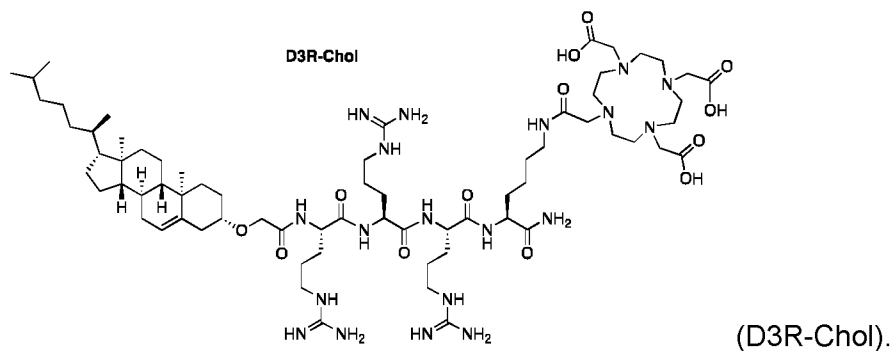
The term “D3R-C16” as used herein, refers to a compound of the present disclosure where “D” indicates that the chelator group (Z_1) is DOTA, and “3R” indicates that the cationic peptide sequence (P_1) is a triarginine sequence, and “C16” refers to a 16-carbon acyl chain of the compound, i.e. the lipophilic aliphatic group A_1 is a C15 alkyl, which is linked through a carbonyl group to P_1 . An example of D3R-C18 is shown below as compound (Id),



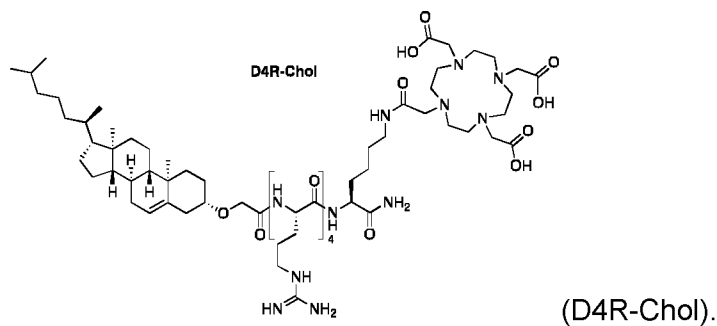
The term “D3R-C18” as used herein, refers to a compound of the present disclosure where “D” indicates that the chelator group (Z_1) is DOTA, and “3R” indicates that the cationic peptide sequence (P_1) is a triarginine sequence, and “C18” refers to an 18-carbon acyl chain of the compound, i.e. the lipophilic aliphatic group A_1 is a C17 alkyl, which is linked through a carbonyl group to P_1 . An example of D3R-C18 is shown below as compound (Ia),



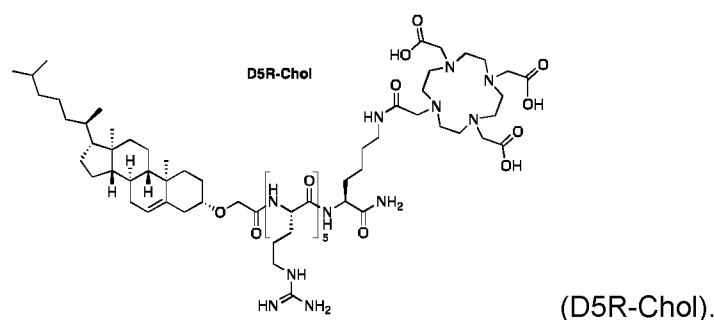
The term “D3R-Chol” as used herein, refers to a compound of the present disclosure where “D” indicates that the chelator group (Z_1) is DOTA, and “3R” indicates that the cationic peptide sequence (P_1) is a triarginine sequence, and “Chol” refers to a cholesterol part of the compound, i.e. the lipophilic aliphatic group A_1 is cholesterol, which is linked through its secondary alcohol to P_1 . D3R-Chol is shown below,



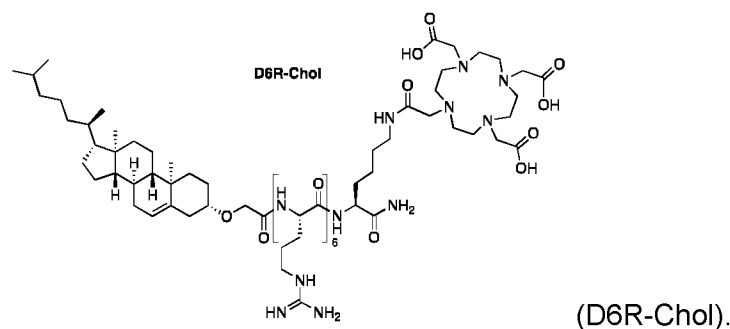
The term “D4R-Chol” as used herein, refers to a compound of the present disclosure where “D” indicates that the chelator group (Z_1) is DOTA, and “4R” indicates that the cationic peptide sequence (P_1) is an arginine sequence of four arginine residues, and “Chol” refers to a cholesterol part of the compound, i.e. the lipophilic aliphatic group A_1 is cholesterol, which is linked through its secondary alcohol to P_1 . D4R-Chol is shown below,



The term “D5R-Chol” as used herein, refers to a compound of the present disclosure where “D” indicates that the chelator group (Z_1) is DOTA, and “5R” indicates that the cationic peptide sequence (P_1) is an arginine sequence of five arginine residues, and “Chol” refers to a cholesterol part of the compound, i.e. the lipophilic aliphatic group A_1 is cholesterol, which is linked through its secondary alcohol to P_1 . D5R-Chol is shown below,



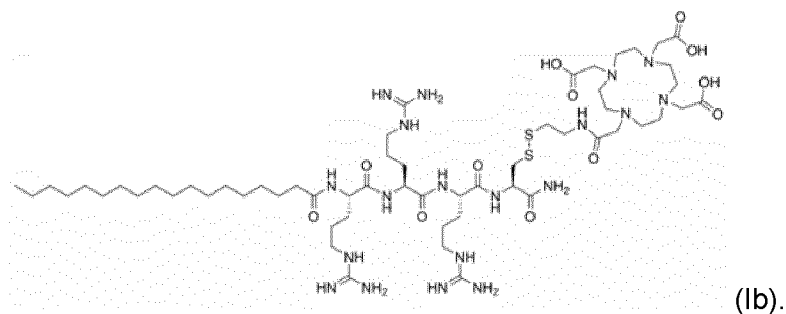
The term “D6R-Chol” as used herein, refers to a compound of the present disclosure where “D” indicates that the chelator group (Z_1) is DOTA, and “6R” indicates that the cationic peptide sequence (P_1) is an arginine sequence of six arginine residues, and “Chol” refers to a cholesterol part of the compound, i.e. the lipophilic aliphatic group A_1 is cholesterol, which is linked through its secondary alcohol to P_1 . D5R-Chol is shown below,



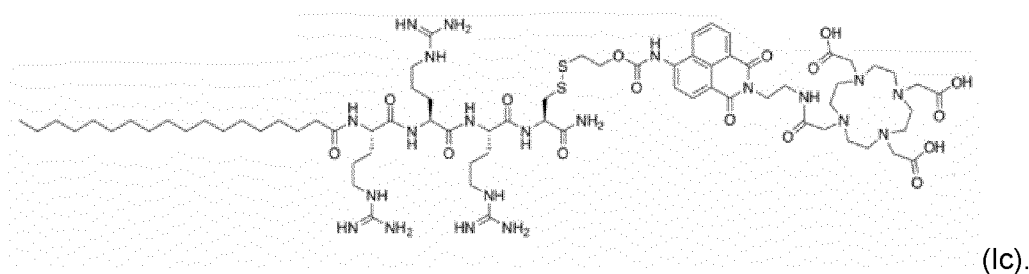
The term “D n R” as used herein refers to a compound of the present disclosure where “D” indicates that the chelator group (Z_1) is DOTA, and “ n R” indicates that the cationic peptide sequence (P_1) is an arginine sequence of “ n ” arginine residues, where n is an integer, such as 3, 4, 5, 6, 7, or 8.

The term “DSS3R-C18” as used herein, refers to a compound of the present disclosure where “D” indicates that the chelator group (Z_1) is DOTA, “SS” indicates that the compound comprises a cleavable disulfide bridge, and “3R” indicates that the cationic

peptide sequence (P_1) is a triarginine sequence, and “C18” to an 18-carbon acyl chain of the compound, i.e. the lipophilic aliphatic group A_1 is a C17 alkyl, which is linked through a carbonyl group to P_1 . An example of DSS3R-C18 is shown below as compound (1b),



The term “DFSS3R-C18” as used herein, refers to a compound of the present disclosure where “D” indicates that the chelator group (Z_1) is DOTA, F refers to presence of a fluorescent linker, “SS” indicates that the compound comprises a disulfide bridge, and “3R” indicates that the cationic peptide sequence (P_1) is a triarginine sequence, and “C18” to an 18-carbon acyl chain of the compound, i.e. the lipophilic aliphatic group A_1 is a C17 alkyl, which is linked through a carbonyl group to P_1 . An example of DFSS3R-C18 is shown below as compound (1c),



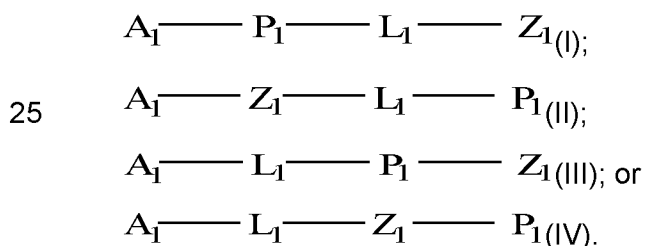
The term “D3R analogue”, as used herein, refers to compounds of the present disclosure comprising a chelator group (Z_1), an arginine sequence as the cationic peptide sequence (P_1), and a lipophilic aliphatic group (A_1). This class of compounds encompass, without limitation, the D3R-C16 and D3R-C18 compounds, but also compounds with cleavable and fluorescent linkers, such as DSS3R-C18 and DFSS3R-C18. In particular, the term “D3R analogue” covers compounds of the present disclosure that have three, four, five, or six cationic amino acid residues in the cationic peptide sequence (P_1), such as three arginine residues, four arginine residues, five arginine residues, or six arginine residues.

The term "alkyl" group refers to a saturated hydrocarbyl group having from one to thirty carbon atoms in a linear, branched or cyclic arrangement, preferably linear or branched.

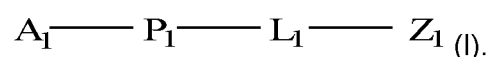
- 5 The term "stealth liposome" or "Lipoid Stealth formulation" as used herein refers to a formulation comprising HSPC:Cholesterol:DSPE-PEG2000 in the molar ratio 56.5 to 38.2 to 5.3. The term "HSPC" is L- α -phosphatidylcholine, hydrogenated Soy.

Compounds of the disclosure

- 10 The compound as defined herein is by design suitable for forming micelles, and comprises three essential structural units i.e. a chelator group (Z_1), a cationic peptide sequence (P_1) comprising amide-bonded amino acids, and a lipophilic aliphatic group (A_1).
- 15 In one embodiment, a compound is provided, comprising:
- a chelator group (Z_1),
 - a cationic peptide sequence (P_1) comprising amide-bonded amino acids, and
 - a lipophilic aliphatic group (A_1).
- 20 In one embodiment, the compound as defined herein is provided, wherein the chelator group (Z_1), the cationic peptide sequence (P_1), and the lipophilic aliphatic group (A_1), are covalently connected via a linker (L_1) according to any one of formulas (I) to (IV):



- 30 In one embodiment, the compound as defined herein is provided, wherein the chelator group (Z_1) is bound via a linker (L_1) to the N-terminus or the C-terminus of the cationic peptide sequence (P_1), and the compound is represented by formula (I):



In one embodiment, the compound as defined herein is provided, wherein the lipophilic aliphatic group (A_1) is bound via a functional group to the N-terminus or C-terminus of the cationic peptide sequence (P_1).

5

In one embodiment, the compound as defined herein is provided, wherein the lipophilic aliphatic group (A_1) is bound via a carbonyl group to the N-terminus of the cationic peptide sequence (P_1), wherein the carbonyl group and the amine of the N-terminus together forms an amide.

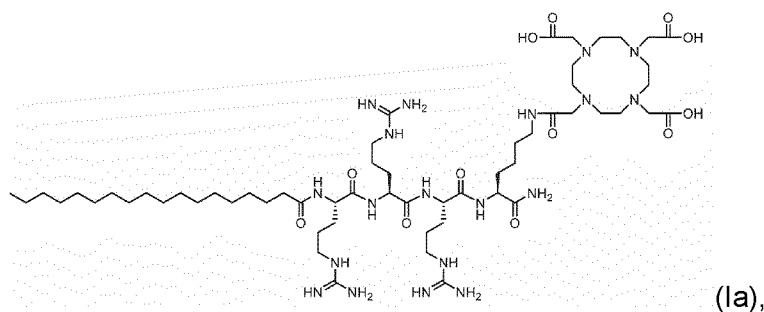
10

In one embodiment, the compound as defined herein is provided, wherein:

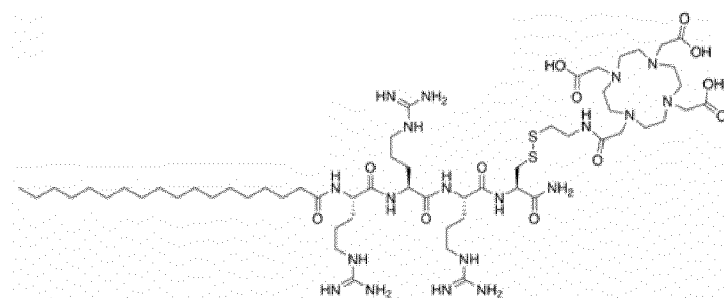
- a. the chelator group (Z_1) is DOTA,
- b. the cationic peptide sequence (P_1) is RRR, and
- c. the lipophilic aliphatic group (A_1) is a non-branched C17 alkyl.

15

In one embodiment, the compound as defined herein is provided, wherein the compound is selected from the group consisting of:

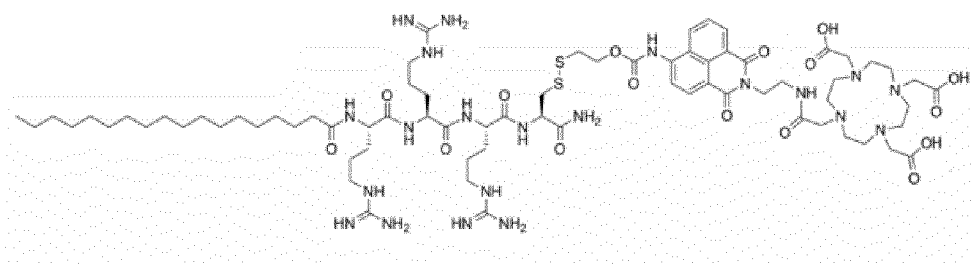


(Ia),



(Ib), and

20

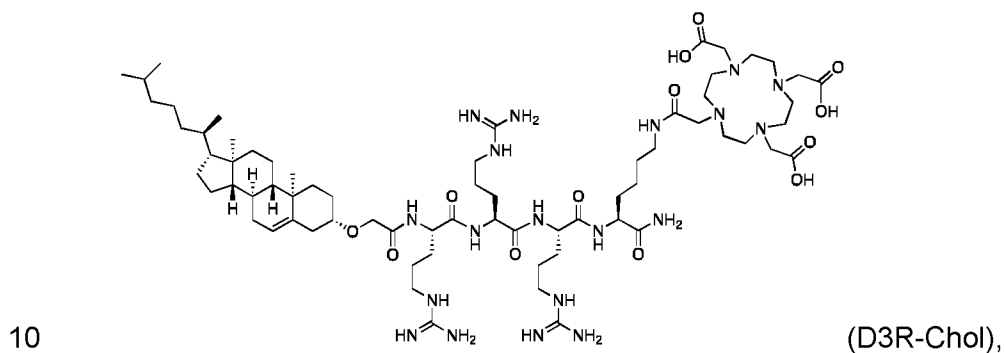


(Ic).

In one embodiment, the compound is provided, wherein:

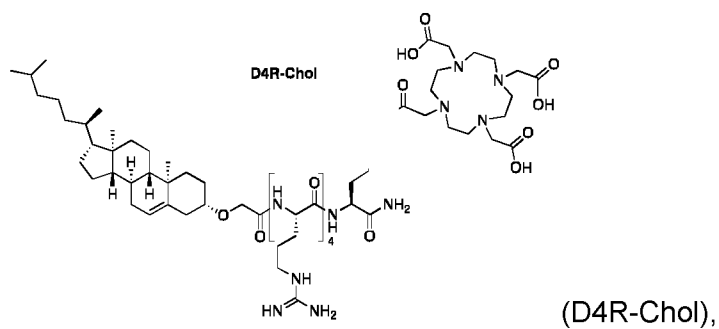
- a. the chelator group (Z₁) is DOTA,
- 5 b. the cationic peptide sequence (P₁) is RRR, RRRR, RRRRR, or RRRRRR
and
- c. the lipophilic aliphatic group (A₁) is a sterol.

In one embodiment, the compound is selected from the group consisting of:

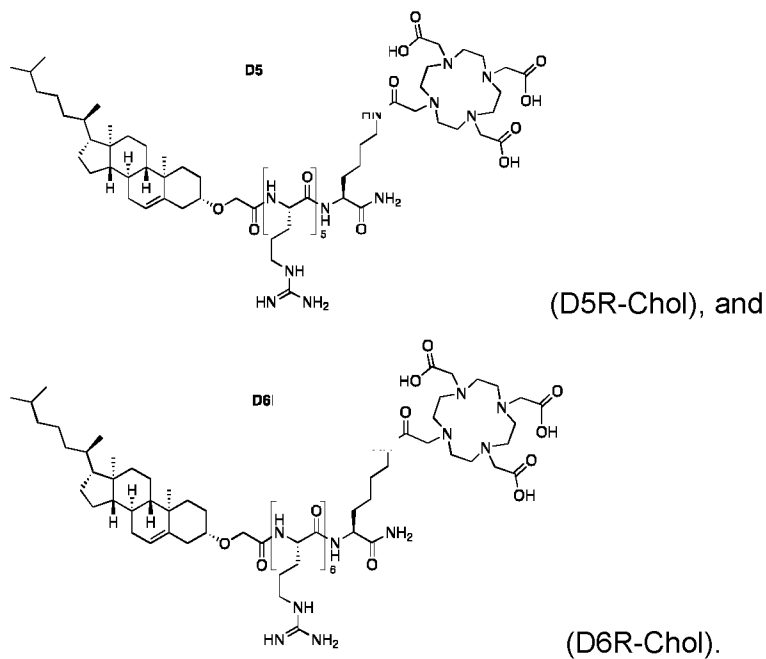


(D3R-Chol),

10



(D4R-Chol),



In one embodiment, the compound as defined herein is provided, wherein:

5

- the chelator group (Z_1) is DOTA,
- the cationic peptide sequence (P_1) is RRR, and
- the lipophilic aliphatic group (A_1) is an aliphatic cycle comprising a gonane structure.

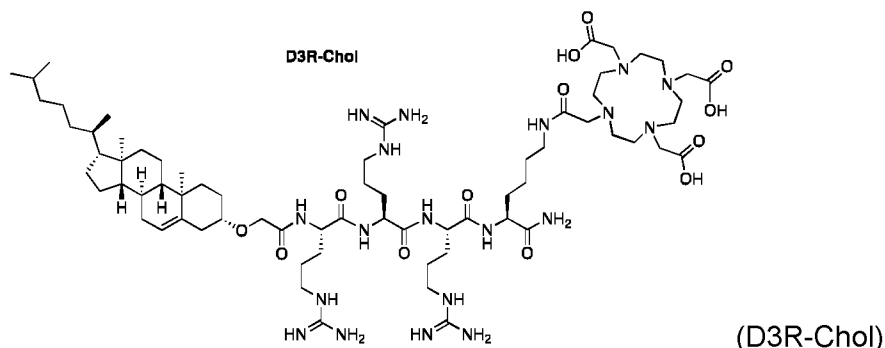
10

In one embodiment, the compound as defined herein is provided, wherein:

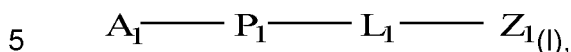
- the chelator group (Z_1) is DOTA,
- the cationic peptide sequence (P_1) is RRR, and
- the lipophilic aliphatic group (A_1) is cholesterol, optionally linked to P_1 as cholesteroxy acetic acid by condensation.

15

In one embodiment, the compound as defined herein is provided, wherein the compound is:



The compound D3R-Chol can be synthesized as described in Example 19. A person of skill in the art understands that in D3R-Chol, A_1 of formula (I),



is connected to the cationic peptide sequence P_1 via a “ $-\text{CH}_2(\text{C}=\text{O})-$ ” fragment. This connection may result from a condensation reaction between an amino group, such as the N-terminal amino group of the cationic peptide sequence, and the carboxylic acid moiety of cholesteroxy acetic acid.

10

Micelles

Micelles are aggregates of amphipathic molecules composed of hydrophilic and hydrophobic moieties. Examples are lysolipids, fatty acids, pegylated lipids, ionic and non-ionic surfactant that commonly consist of e.g. hydrophobic hydrocarbon chains, lipids or sterols that are non-soluble in water and hydrophilic polymers like PEG, sugars, or charged groups that are readily soluble in water. In an example of the present disclosure, the amphipathic structure is composed of hydrocarbon chains (fatty acids) chemically linked to a charged tri-arginine peptide sequence that is chemically linked to a DOTA chelator (Fig. 2). Micelles consist of aggregated amphiphiles, and in a micellar solution these are in equilibrium with free, unaggregated amphiphiles. Micellar solutions form when the concentration of amphiphile exceeds the critical micellar concentration (CMC) or critical aggregation concentration (CAC), and persist until the amphiphile concentration becomes sufficiently high to form a lyotropic liquid crystal phase.

25

In colloidal and surface chemistry, the critical micelle concentration (CMC) is defined as the concentration of surfactants above which micelles form and all additional surfactants added to the system go to micelles. The CMC is an important characteristic

of a surfactant. Before reaching the CMC, the surface tension changes strongly with the concentration of the surfactant. After reaching the CMC, the surface tension remains relatively constant or changes with a lower slope. Furthermore, micelles only form above critical micelle temperature. Although micelles are often depicted as being spherical, they can be cylindrical or oblate depending on the chemical structure of the amphiphile.

In one embodiment, a composition comprising a micelle is provided, wherein the micelle comprises a plurality of compounds as defined herein. In one embodiment, the micelle comprises a compound as defined herein and one or more other micelle-forming lipids.

Charged micelles

For charged micelles such as SDS (sodium dodecyl sulfate) or for the compound of the present disclosure, the ionic strength and thereby charge screening is important for the formation of micelles. At low ionic strengths present in e.g. sugar based buffers (ISO-TRIS-Sucrose), the charges of the monomers are unscreened, and formation of micellar structures are hindered due to high electrostatic repulsion between these. At higher ionic strengths present in e.g. salt based buffers (ISO-TRIS-NaCl), the charges of the monomers are screened by counterions, and formation of micellar structures/aggregates is more pronounced. Ionic strength of the aqueous media thus impacts the CMC leading to lowering of the CMC in buffers with increased ionic strength.

The cationic peptide sequence (P₁)

In one embodiment, the compound as defined herein is provided, wherein the cationic peptide sequence (P₁) comprises an amino acid selected from the group consisting of: L-arginine (R), L-homoarginine (hArg), L-histidine (H), L-homohistidine (hHis), L-lysine (K), L-homolysine (hLys), L-ornithine (Orn), D-ornithine (orn), D-arginine (r), D-homoarginine (harg), D-histidine (h), D-homohistidine (hhis), D-Lysine (k), and D-homolysine (hlys).

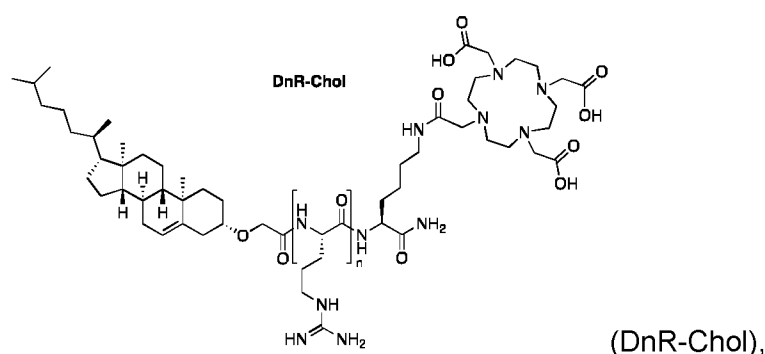
In one embodiment, the compound as defined herein is provided, wherein the cationic peptide sequence (P₁) comprises an amino acid selected from the group consisting of: L-arginine (R), and D-arginine (r).

In one embodiment, the compound as defined herein is provided, wherein the cationic peptide sequence (P_1) comprises at least two amide bonded amino acids, such as at least three amino acids, such as at least four amino acids, such as at least five amino acids, such as at least six amino acids, such as at least seven amino acids, such as at least eight amino acids, such as at least nine amino acids, such as at least ten amino acids.

In one embodiment, the compound as defined herein is provided, wherein the cationic peptide sequence (P_1) comprises from two amino acids to five amino acids, such as three amino acids.

In one embodiment, the compound as defined herein is provided, wherein the cationic peptide sequence (P_1) is selected from the group consisting of: RR, rr, RRR, rrr, RRRR, rrrr, RRRRR, rrrrr, RRRRRR, rrrrrr, RRRRRRR, rrrrrrr, RRRRRRRR, rrrrrrrr, RRRRRRRRR, rrrrrrrrr, RRRRRRRRRR, and rrrrrrrrrr. According to the present disclosure, the term "RR" means that two L-arginine residues are connected by an amide bond to form a dipeptide sequence. The term "RRR" means that three L-arginine residues are connected by amide bonds to form a tripeptide sequence. The same terminology applies to peptide sequences of other lengths.

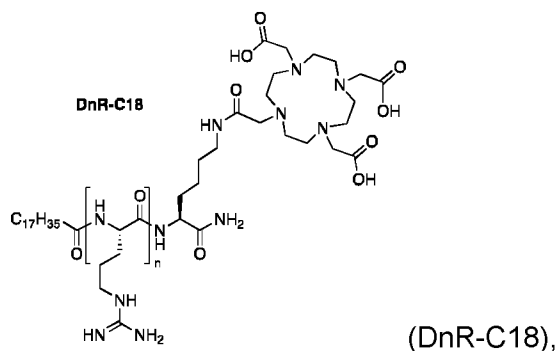
In one embodiment, the length of the cationic peptide sequence (P_1) is "n" according to the formula (DnR-Chol):



25

wherein n is 2, 3, 4, 5, 6, 7, 8, 9 or 10.

In one embodiment, the length of the cationic peptide sequence (P_1) is "n" according to the formula



wherein n is 2, 3, 4, 5, 6, 7, 8, 9 or 10.

The lipophilic aliphatic group (A₁)

- 5 In one embodiment, the compound as defined herein is provided, wherein the lipophilic aliphatic group (A₁) comprises at least 8 carbon atoms, such as at least 9 carbon atoms, such as at least 10 carbon atoms, such as at least 11 carbon atoms, such as at least 12 carbon atoms, such as at least 13 carbon atoms, such as at least 14 carbon atoms, such as at least 15 carbon atoms, such as at least 16 carbon atoms, such as at least 17 carbon atoms, such as at least 18 carbon atoms, such as at least 19 carbon atoms, such as at least 20 carbon atoms, such as at least 21 carbon atoms, such as at least 22 carbon atoms, such as at least 23 carbon atoms, such as at least 24 carbon atoms, such as at least 25 carbon atoms, such as at least 26 carbon atoms, such as at least 27 carbon atoms, such as at least 28 carbon atoms, such as at least 29 carbon atoms, such as at least 30 carbon atoms, such as at least 31 carbon atoms, such as at least 32 carbon atoms, such as at least 33 carbon atoms, such as at least 34 carbon atoms, such as at least 35 carbon atoms.

- 20 In one embodiment, the compound as defined herein is provided, wherein the lipophilic aliphatic group (A₁) is an aliphatic chain or an aliphatic cycle.

Aliphatic cycles

- In one embodiment, the compound as defined herein is provided, wherein the lipophilic aliphatic group (A₁) is an aliphatic cycle comprising a gonane structure.

25

In one embodiment, the compound as defined herein is provided, wherein A₁ is a sterol. In one embodiment, the sterol is selected from the group consisting of: cholesterol, campesterol, sitosterol, stigmasterol, and ergosterol.

In one embodiment, the compound as defined herein is provided, wherein the lipophilic aliphatic group (A_1) is an aliphatic cycle comprising a steroid, such as cholesterol.

5 In one embodiment, the compound as defined herein is provided, wherein the lipophilic aliphatic group (A_1) comprises two adjacent carbon atoms connected by a double bond.

Aliphatic chains

10 In one embodiment, the compound as defined herein is provided, wherein the lipophilic aliphatic group (A_1) is an aliphatic branched or non-branched chain.

In one embodiment, the compound as defined herein is provided, wherein the lipophilic aliphatic group (A_1) is a non-branched C15 to C20 alkyl, such as C15, C16, C17, C18, C19 or C20 alkyl.

15 In one embodiment, the compound as defined herein is provided, wherein the lipophilic aliphatic group (A_1) is a non-branched C17 alkyl.

Membrane partitioning

20 Amphipathic molecules are interfacial-active and therefore accumulate at water-air and water-oil interphases. In the presence of a lipid membrane (water-oil interphase), these amphiphiles partitions into the lipid membrane by embedding the hydrophobic segments in the oily interior of the bilayer, and positions the hydrophilic segments at the interphase of the bilayer. The degree of partitioning is quantified by the partitioning coefficient, and is governed by the relative size or hydrophobicity/hydrophilicity ratio of the amphiphile. For the present disclosure, the hydrophobicity/hydrophilicity ratio may be modified by varying the acyl-chain length from C8-C24, using different aliphatic cycles, such as different sterols, and varying the poly-arginine sequence from 1-10 arginine.

30 For charged amphiphiles, such as the compound of the present disclosure, electrostatic interactions may further drive the partitioning into membranes of the opposite charge, i.e. cationic amphiphiles may partition to larger extent into anionic lipid membranes. This rationale also governs the behavior of the D3R-analogues as the cationic arginine peptide sequence interacts favorably with the anionic surface charge of the cellular plasma membrane of e.g. T lymphocytes or leucocytes. The electrostatic

35

interaction with lipid or plasma membranes of cells may be tuned with the cationic charge of the amphiphiles, e.g. increasing the cationic charge increases the electrostatic interaction with anionic lipid membranes but also increases the solubility in the aqueous phase. Higher partitioning into anionic lipid membranes is thus achieved by increasing both the charge and magnitude of the hydrophobic segments of the amphiphile.

Membrane translocation

Cationic peptide sequences, such as the tri-arginine sequences of the D3R-analogues are known to facilitate membrane translocation e.g. of antimicrobial or cell penetrating peptides (AMPs and CPPs). CPPs typically have an amino acid composition that either contains a high relative abundance of positively charged amino acids such as lysine or arginine or has sequences that contain an alternating pattern of polar/charged amino acids and non-polar, hydrophobic amino acids. These two types of structures are referred to as polycationic or amphipathic, respectively. A third class of CPPs are the hydrophobic peptides, containing only apolar residues, with low net charge or have hydrophobic amino acid groups that are crucial for cellular uptake. Unlike the majority of conventional antibiotics, it appears that antimicrobial peptides frequently destabilize biological membranes, can form transmembrane channels, and may also have the ability to enhance immunity by functioning as immunomodulators.

The constructs of the current disclosure therefore may translocate lipid membranes or plasma membranes of cells after which the compound accumulates inside the cells. AMP and CPP sequences are known to promote membrane translocation and may be part of the chelator – peptide – hydrophobic segment constructs of the current disclosure.

The chelator group (Z_1)

The compounds of the present disclosure are constructed as carriers/vehicles of metal ion chelators, also referred to as chelator groups (Z_1) herein, with the purpose of transporting radionuclides across plasma membranes into cells. While the peptide – hydrophobic segment part of the constructs facilitates partitioning and translocation of cell membranes, a high affinity chelator chemically linked to the construct enables co-transport of cations and metal cationic radionuclides. The full chelator – peptide – hydrophobic segment construct thus facilitates electrostatic attraction to anionic cell

membranes, membrane partitioning, membrane translocation and effective co-transport of metal cations via the chelator into cells. The chelators used in the present disclosure have high thermodynamic and high kinetic stability to ensure low degree of transmetallation or other forms of loss of the radionuclide. Some examples of such
5 chelators are CbTETA, TETA, DOTA, NOTA, DTPA, EDTA, and DF (deferoxamine).

In one embodiment, the compound as defined herein is provided, wherein the chelator group (Z_1) is a polydentate hydrophilic chelator group. In one embodiment, the chelator group (Z_1) is linear or cyclic. In one embodiment, the chelator group (Z_1) comprises
10 ethylene diamine.

In one embodiment, the compound as defined herein is provided, wherein the chelator group (Z_1) is selected from the group consisting of: 1,4,7,10-tetraazacyclododecane-1,4,7,10-tetraacetic acid (DOTA), 1,4,7,10-tetrazacyclododecane (Cyclen), 1,4,8,11-tetraazacyclotetradecane (cyclam), 1,4-ethano-1,4,8,11-tetraazacyclotetradecane (et-cyclam), 1,4,7,11-tetra-azacyclotetradecane (isocyclam), 1,4,7,10-tetraazacyclotridecane ([13]aneN₄), 1,4,7,10-tetraazacyclododecane-1,7-diacetic acid (DO2A), 1,4,7,10-tetraazacyclododecane-1,4,7-triacetic acid (DO3A), 1,4,7,10-tetraazacyclododecane-1,7-di(methanephosphonic acid) (DO2P), 1,4,7,10-tetraazacyclododecane-1,4,7-tri(methanephosphonic acid) (DO3P), 1,4,7,10-tetraazacyclododecane-1,4,7,10-tetra(methanephosphonic acid) (DOTP), diethylenetriaminepentaacetic acid (DTPA), 1,4,8,11-tetraazacyclotetradecane-1,4,8,11-tetraacetic acid (TETA), and ethylenediaminetetraacetic acid (EDTA).

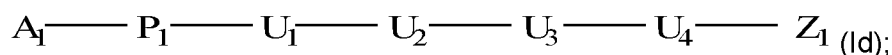
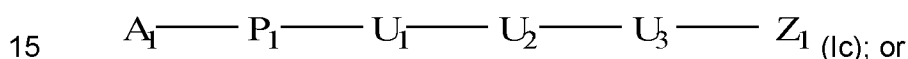
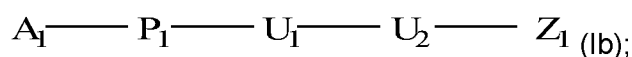
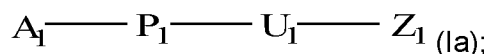
25 In one embodiment, the compound is saturated by one or more cations, optionally chelating to the chelator. In one embodiment, the one or more cations are radioactive or stable isotopes. In one embodiment, the stable isotopes are Cu-63 and/or Cu-65.

Cleavable linkers

30 The compound of the current disclosure can be dispersed in water either as monomers or micelles depending on their concentration and the ionic strength of the buffer, and may upon interaction with cell membranes be internalized by translocation of the lipid bilayer. Once the compound has been internalized or taken up by the cell, it may reside in the cytosol, in cellular compartments or in cellular membranes of various
35 organelles. To enhance the retention of the compound inside the cells and avoid

exocytosis, cleavable linkers may be included that detach the cargo (radionuclide + chelator) from the transporting unit, which according to the current disclosure may be poly arginine coupled to a hydrophobic segment such as an acyl chain. In this manner, the cargo (chelate + radionuclide) is separated from the vehicle (e.g. 3R-C18) upon
 5 activation of the cleavable linker. In this process, the chelator changes physiochemical characteristics from being amphipathic to hydrophilic and purely water soluble, which increases the retention of the radionuclide and chelate inside the cell.

10 In one embodiment, the compound as defined herein is provided, wherein the linker (L_1) consists of one or more linking units (U_1) to (U_4), connecting the chelator group (Z_1) with the cationic peptide sequence (P_1), according to formula (Ia), (Ib), (Ic), or (Id):



wherein (A_1), (P_1) and (Z_1) are defined as in any one of the preceding claims.

20 In one embodiment, the compound as defined herein is provided, wherein at least one of the linking units (U_1) to (U_4) is a proteinogenic or non-proteinogenic amino acid.

In one embodiment, the compound as defined herein is provided, wherein the proteinogenic amino acid is selected from: L-cysteine (C), D-cysteine (d), L-lysine (K), and D-lysine (d).

25

In one embodiment, the compound as defined herein is provided, wherein the linker (L_1) of formula (I) is cleavable, covalently disconnecting any one of the linking units (U_1) to (U_4) by reduction, photolysis, a change in pH and/or an enzymatic process.

30 In one embodiment, the compound as defined herein is provided, wherein the compound of formula (Ib) is cleavable between linking units (U_1) and (U_2).

In one embodiment, the compound as defined herein is provided, wherein the compound of formula (Ic) is cleavable between linking units (U₁) and (U₂).

5 In one embodiment, the compound as defined herein is provided, wherein the compound of formula (Id) is cleavable between linking units (U₁) and (U₂).

In one embodiment, the compound as defined herein is provided, wherein the bond between any one of (U₁) and (U₂), (U₂) and (U₃), (U₃) and (U₄), is a disulfide bond.

10 In one embodiment, the compound as defined herein is provided, wherein at least one of the linking units (U₁) to (U₄) is a fluorophore (F₁).

Activation of cleavable linkers by external stimuli

15 The current disclosure includes chemical linkers that can be activated by external stimuli, such as cleavage (disruption of chemical bonds) induced by an external light source (photolysis) or by externally applied chemical gradients. Examples of the latter are click or 'declick' reactions where the use of a very simple conjugate acceptor, derived from e.g. Meldrum's acid, for the sequential 'clicking' together of an amine and a thiol in aqueous conditions at neutral pH. Subsequently, this linkage can be
20 'declicked' by a chemical trigger to release the original amine and thiol undisturbed.

Activation of cleavable linkers by internal stimuli

Activation of redox-sensitive linkers, such as disulfide bridges (R-S-S-R') may occur once these constructs are internalized by the cells. Upon reduction, the disulfide linker
25 is cleaved ($R-S-S-R' \rightleftharpoons R-S + S-R'$) and the construct is split in two. These processes are governed e.g. by intracellularly located glutathione (GSH), Thioredoxin (Trx) and Protein Disulfide Isomerase (PDI*).

30 Intracellularly, GSH is found in cytosol, mitochondria, endoplasmatic reticulum (ER) and nucleus. In the cytosol, GSH de novo synthesis occurs and 90 % of the total cell GSH is found here. The amount of GSH in the nucleus varies with cell cycle progression, where it seems to be most important during cell proliferation.

Intracellularly, Trx acts as the major disulfide reductase and is responsible for maintaining proteins in their reduced state. There are two forms of Trx; Trx1 is found within the cytosol and the nucleus, whereas Trx2 is found in the mitochondria.

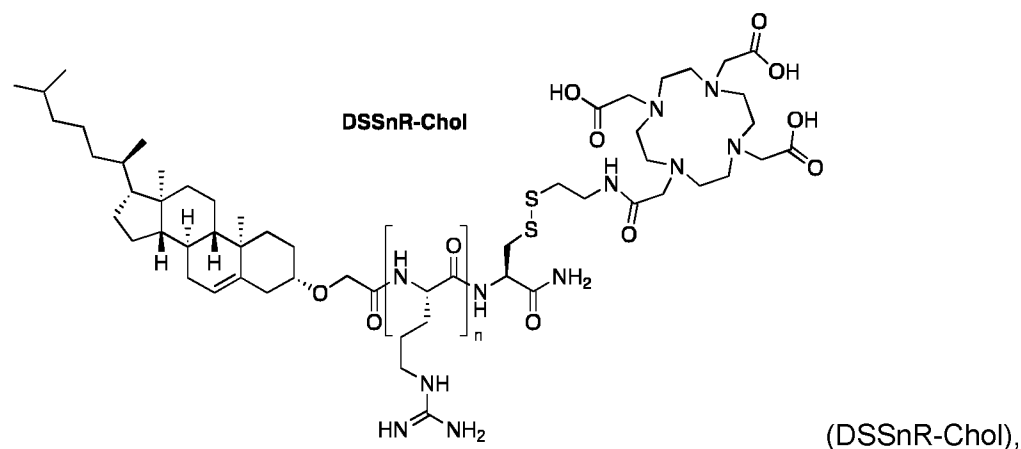
5 Intracellularly, PDI* is mainly located to the ER, where it is involved in stable native protein folding. PDI*, in collaboration with GSH, catalyzes cycles of thiol oxidation-reductions with great efficiency and substantially increase correct disulfide introduction into proteins. Apart from its function as oxidizer and reducer, PDI* also has isomerase activity which means that it can relocate disulfide bonds. Although PDI* is mainly an
10 ER-located protein, it has also been found in other cellular compartments where the physiological role is not clear. At the cell surface, however, PDI* localization is well documented and is thought to play a role in reductions of membrane-specific thiols. PDI* may also exert its isomerase activity at the membrane to relocate regulatory disulfides in response to the redox state.

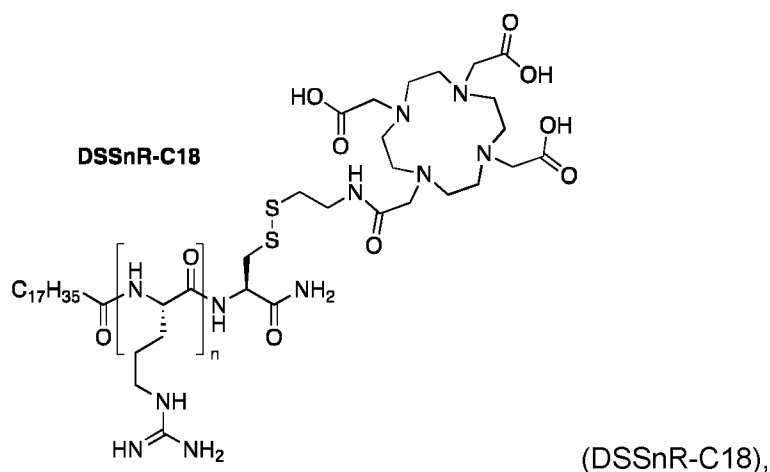
15

Protease sensitive linkers composed of amino acid (A) sequences (peptides) are also considered part of the current disclosure. Upon activation of such linkers (R-A-A-R') by proteases an amide bond is disrupted and the construct is split in two (R-A-A-R' \leftrightarrow R-A + A-R'). Proteases such as Matrix Metalloproteinases (MMPs), Chymase and tryptase
20 are present intracellularly in the cytosol and endosomes of several cell types.

Esterases such as lipases also present endogenously available enzymes that may catalyze cleavage of ester-based linkers.

25 In one embodiment, the compound is provided according to formula DSSnR-Chol or formula DSSnR-C18,





wherein n is 2, 3, 4, 5, 6, 7, 8, 9, or 10.

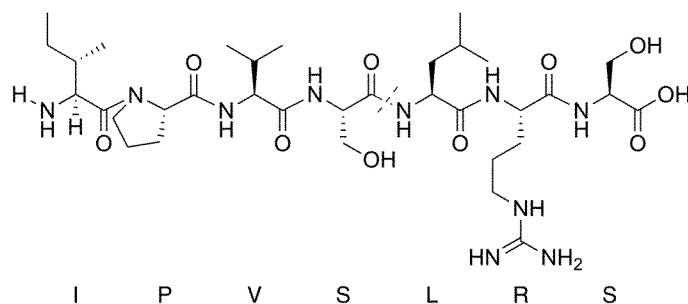
In a particular embodiment, the compound is provided according to formula DSSnR-
 5 Chol or DSSnR-C18, wherein n is 3.

Further cleavable linkers

Targetability can be achieved, by having stimuli-responsive mechanisms within the
 structure of the compound of the present disclosure. Systemically administered
 10 compounds encounter many different stimuli along the way, so by tuning the compounds
 of the disclosure to respond to one specific biological stimulus could generate a desired
 targeting effect. This research area is already vast expanding, making the compounds
 sensitive to endogenous or exogenous factors such as pH, enzymes, redox potential and
 temperature. External stimuli can also be applied in the sense of e.g. inducing a magnetic
 15 field, ultrasound or various types of radiation.

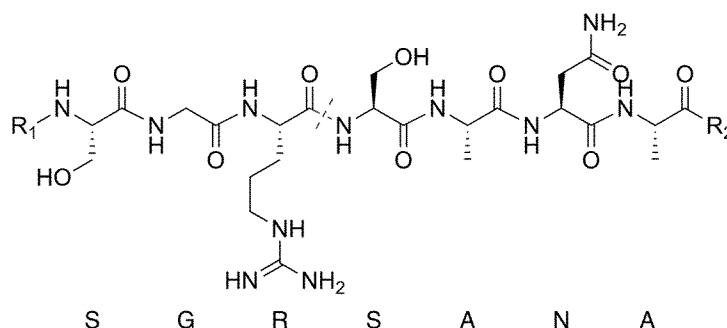
Protease sensitive linkers

Matrix metalloproteases (MMP)



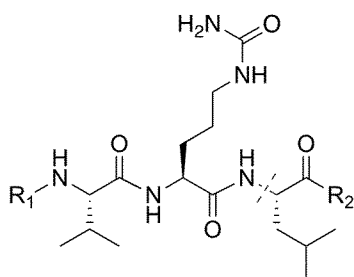
For decades now, thorough investigations have been conducted, to map the expression of specific enzymes, present in association with diseased states, e.g. enzymes involved in substantial tissue remodelling such as inflammatory diseases or cancer. One of the enzymes presented in tumors, are the MMP, which is known to regulate multiple cell processes such as growth, differentiation, apoptosis, migration, and invasion. Furthermore, it is part of the angiogenic mechanism. Under normal physiological conditions, the MMPs are tightly regulated, but they are up-regulated during tissue remodelling. MMPs are a Zn-dependent endopeptidase, which are secreted into the ECM in most cancer types, following the degradation of the normal surrounding tissue of the tumor.

Urokinase sensitive linker



Plasminogen activators, such as urokinase plasminogen activator (uPA), also play an important role in the extravasation of tumor cells. Like MMPs, uPA is closely associated with tumor growth, invasion, metastasis, and recurrence of tumors. Urokinase-type plasminogen-activator receptor (uPAR) is a cell-surface receptor for uPA, which is a serine protease that catalyses the formation of plasmin from plasminogen. Converting the plasminogens into proteolytic active plasmins, makes the uPA capable of degrading ECM. The proteolytic degradation of ECM paves the way for tumor progression, which constitutes the invasive nature of the tumor.

A Cathepsin sensitive linker



The Valine-Citrulline linker system is cleaved by various cysteine cathepsins, which is found in all animals. Most of these cathepsins are activated by low pH within lysosomes.

pH sensitivity

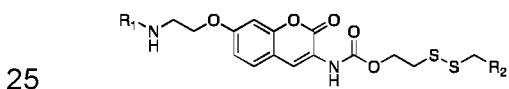
5 Differences in pH have been vastly exploited to control the delivery of drugs, including intracellular compartments (such as endosomes or lysosomes). The acidification of endosomes (pH ~5–6) and lysosomes (pH ~4–5) gives a natural pH-change that can be used for effective intracellular drug accumulation. Thus the presence of acid-sensitive functional groups, such as hydrozones, oxime, esters, phosphoramidates or acetals can
10 lead to a compound disassembly and release.

Several drug delivery systems and pro-drug strategies have utilized ester linkers to implement pH-sensitivity into the delivery mechanism.

15 Cleavable fluorescent linkers

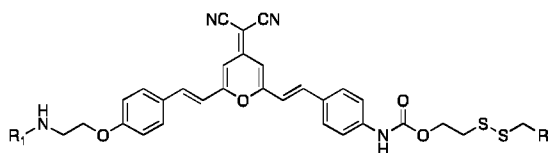
In some embodiments of the disclosure, the cleavable linker contains a chromophore that upon cleavage changes its optical properties. Upon cleavage of such construct, the construct is split in two, leading to formation of two fragments where one is fluorescent. Cleavage of the linker may lead to activation of the fluorophore resulting in
20 changed excitation or emission properties as well as changes in quantum yield of the fluorescent fragment. Examples of chemical structures are shown below i.e. the coumarin-like setup and the dicyanomethylene-4H-pyran setup.

Coumarin-like setup (Two-photon probe)



Coumarin is a fluorophore that offers an emission maximum in the range of 400-475 nm, and has previously been shown to a redox sensitive probe in a similar concept at seen with the naphthalimide. Coumarin is not a particular strong fluorophore but it offers the ability to act as a two-photon probe, which potentially can facilitate high-resolution
30 imaging within the near infrared range. The synthesis routes of coumarin-probes have been thoroughly investigated and can be obtained within approx. 5 steps.

A dicyanomethylene-4H-pyran setup (NIR-I)



The bis-condensed dicyanomethylene-4H-pyran derivative has previously been used as an activatable near-infrared fluorophore. The compound can be obtained via approx. 5 steps synthesis. The excitation will be approx. 500 nm with an emission placed in the near-infrared spectrum of approx. 650-700 nm.

The near-infrared I (NIR-I) window spans from 700 nm to 900 nm, whereas the near-infrared II (NIR-II) windows spans from 900 nm to 1700 nm, approximately.

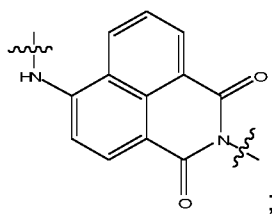
The chromophores may absorb and emit light in the visible part of the spectrum (<700nm) as well as in the NIR region (>700nm).

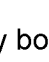
Including a fluorescently active linker as part of the compound of the present disclosure provides the advantage of monitoring cell uptake and intracellular linker cleavage using non-radioactive micelles via fluorescence microscopy, spectroscopy and FACS analysis.

In one embodiment, the compound as defined herein is provided, wherein the fluorophore (F₁) emits light at a wavelength between 500 and 2600 nm.

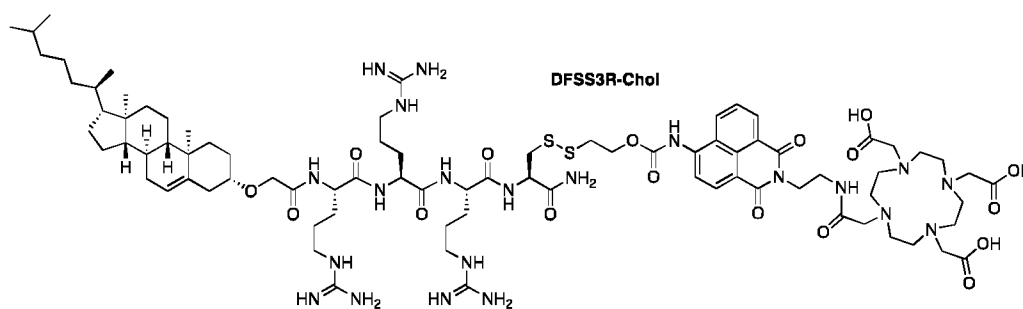
In one embodiment, the compound as defined herein is provided, wherein the fluorophore (F₁) is selected from the group consisting of: a naphthalene derivative, a squaraine derivative, a xanthene derivative, a cyanine derivative, a coumarine derivative, an oxadiazole derivative, an anthracene derivative, a pyrene derivative, an oxazine derivative, an acridine derivative, an arylmethine derivative, and a tetrapyrrole derivative.

In one embodiment, the compound as defined herein is provided, wherein the fluorophore (F₁) is:



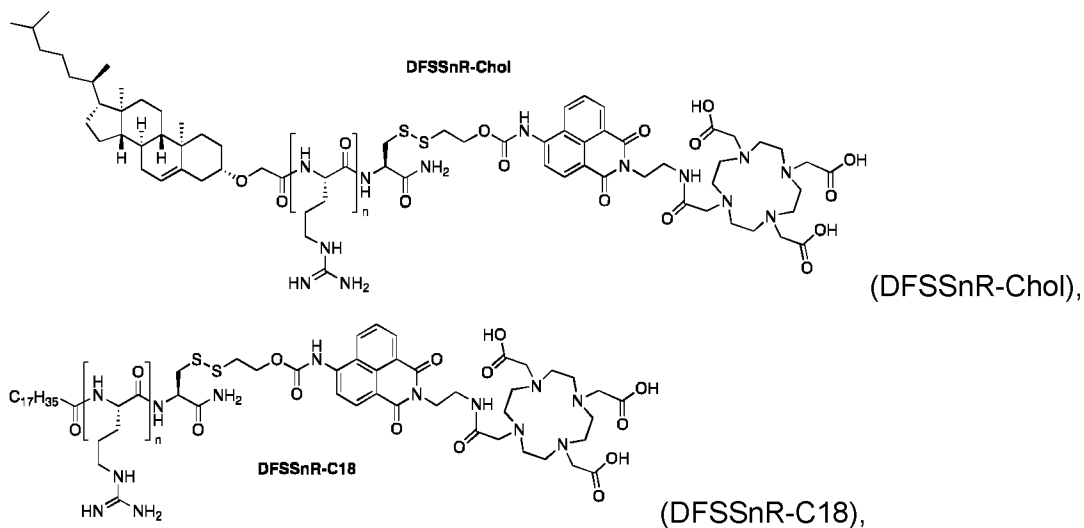
wherein a wavy bond “” indicates by intersection the bond connected to L₁ or Z₁ of the compound as represented by formula (I).

- 5 In one embodiment, the compound as defined herein is provided, wherein the compound is of formula DFSS3R-Chol,



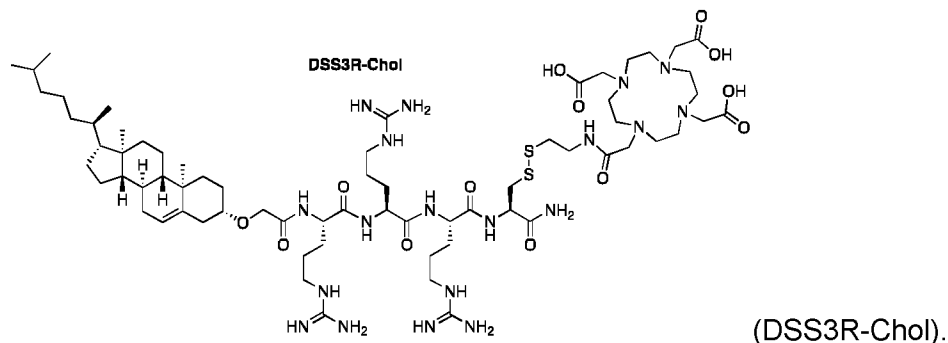
(DFSS3R-Chol).

- 10 In one embodiment, the compound as defined herein is provided, wherein the compound is of formula DFSSnR-Chol or formula DFSSnR-C18,



wherein n is 2, 3, 4, 5, 6, 7, 8, 9, or 10.

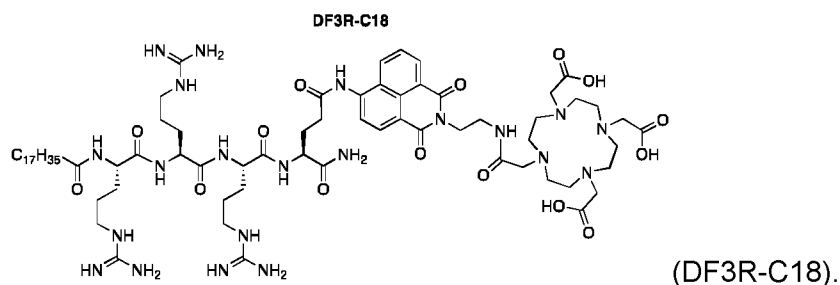
In one embodiment, the compound according to the present disclosure is DSS3R-Chol,



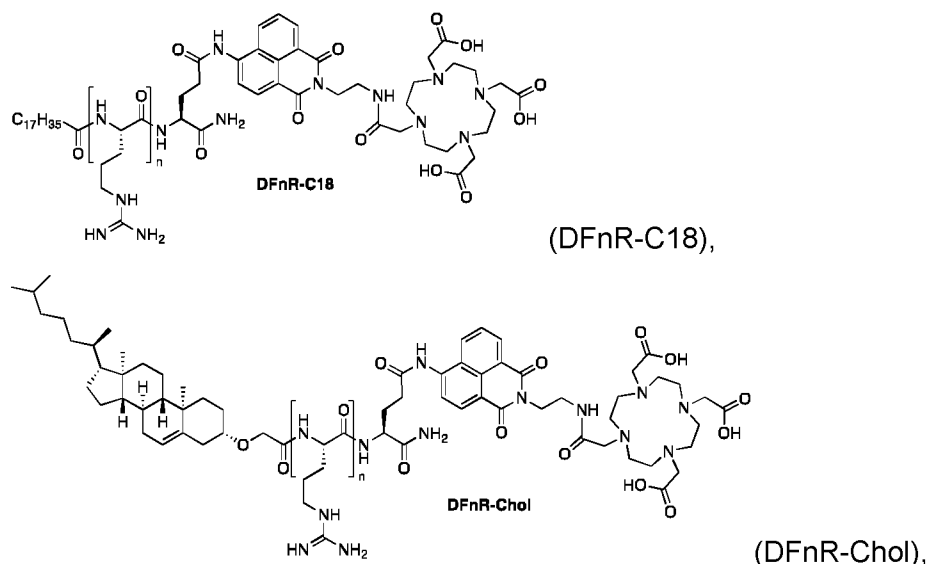
Non-cleavable fluorescent linkers

- 5 In some embodiments of the disclosure, a fluorophore (F_1) acts as a non-cleavable linker, which provides the advantage of monitoring cell uptake using non-radioactive micelles via fluorescence microscopy, spectroscopy and FACS analysis.

- 10 In one embodiment, the compound comprising a non-cleavable fluorescent linker is provided according to formula DF3R-C18,



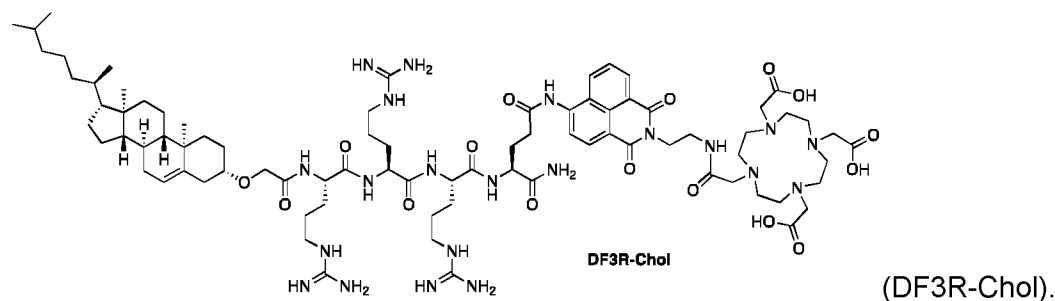
In one embodiment, the compound is provided according to formula DF n R-C18 or formula DF n R-Chol,



wherein n is 2, 3, 4, 5, 6, 7, 8, 9, or 10. In one embodiment, the compound is provided according to any of formulas DFnR-C18 or DFnR-Chol, wherein n is 3.

5

In one embodiment, the compound is provided according to DF3R-Chol,



Stabilizing buffers

- 10 In order to stabilize and not to induce premature activation of the construct presented in the current disclosure, the redox potential and pH of the buffer solution should be set properly. Therefore, buffer constituents that may induce reduction of the D3R constructs, such as HEPES or reducing sugars are avoided. pH and tonicity of the buffers in which the D3R constructs are dissolved are set to be in the range pH 4-10
- 15 and 200-400 mOsm/kg to provide optimal conditions when incubated with cells. Weakly metal chelating/coordinating buffer constituents such as ammonium acetate (NH_4OAc) may be included in the buffer to enhance the solubility of cations in solution, which aids transfer of the radionuclide into the D3R-analogue.

Radionuclides

The primary image modalities considered in the current disclosure are positron emission tomography (PET), single photon emission computed tomography (SPECT) and gamma camera imaging. To cover these modalities, the radionuclides Cu-64 (beta+, 12.7h), Zr-89 (beta+ 78.4h), In-111 (Electron capture, 2.8d), Mn-52 (beta+, 5.6d), Ga-67 (Electron capture, 3.3d) and Ga-68 (beta+, 68min) can be utilized to span a broad range of half-lives. Utilizing these radionuclides, tracking of cells may be conducted for up to 10-15 days using PET scans or organ well counting.

- 10 In one embodiment, the compound as defined herein is provided, further comprising a radionuclide, optionally chelated to the chelator group (Z_1).

- 15 In one embodiment, the radionuclide decays by emission of particles or photons. In one embodiment, the radionuclide is selected from the group consisting of alpha emitters, beta emitters, X-ray emitters, auger emitters and gamma emitters.

In one embodiment, the radionuclide is a beta emitter.

- 20 In one embodiment, the radionuclide is selected from the group consisting of: P-32, Y-90, Sm-153, Er-169, Lu-177, Cu-67, Sc-47, As-76, Te-161, At-211, Ac-225, Bi-212, Bi-213, Ra-223, Pd-212, Te-149, Ra-224, Pd-103, La-135, Er-165, I-125, I-123, Rh-103m, Co-58m, In-111, Au-198, Co-60, Cs-137, and Ir-192, I-125 and Cf-252, Am-241, Pd-103, Yb-169, Se-75 and Sm-145.

- 25 In one embodiment, the radionuclide is selected from the group consisting of: Cu-64, Mn-52, Ga-67, and Lu-177.

Gd-complexes for MRI contrast

- 30 The D3R analogues may be loaded with Gadolinium for improved magnetic resonance imaging (MRI) contrast. In this embodiment, Gd^{3+} ions are chelated by the D3R-analogues and following loaded into the target cell. The Gd-D3R constructs may be used for *in vitro* analysis of cells loaded with the construct using NMR or for *in vivo* tracking of cells using MRI.

Labeling procedures

An exemplary labeling procedure of the present disclosure may be as follows. The cells intended for labeling are isolated according to preferred methodology for the specific type. Depending on the number off cells to be labeled the procedure is optimally
5 undertaken in container that allows for a cell density that secures optimal labeling and survival of cells (e.g. $>10 \times 10^6$ cells/ml for murine T lymphocytes). The intended cell type to be labeled is re-suspended in suitable media e.g. serum-free RPMI. The D3R-analogue to be used for the labeling of cells is added at the concentration determined optimal for the specific cell type and the labeling performed at 37°C/5% CO₂ for a
10 period e.g. 60 minutes. After completion of the labeling period, cells are spun down by centrifugation e.g. 400 rcf 8 minutes and the supernatant removed. The cells are re-suspended in the appropriate media and volume. The cells are spun down by centrifugation, supernatant removed and these washing, resuspension and centrifugation steps are repeated for e.g. three times. If radiolabeling of cells is
15 performed, the radioactivity in the supernatant can be determined at each washing step to determine when non-cell associated radioactivity has been sufficiently removed. After centrifugation-based removal of non-cell associated micelles, the cells can be re-suspended in the appropriate solution for the intended in vitro or in vivo use. In case of radiolabeling all radioactive materials are handled and discarded according to national
20 and institutional guidelines.

Cell types and handling

The flexible D3R-analogue micelle based labeling is, as described above, based on electrostatic interactions and partitioning of amphipathic cationic micelles and
25 negatively charged mammalian cells. This labeling methodology is therefore not cell type specific as in the case of e.g. antibody labeling. The D3R-analogue labeling methods in this disclosure therefore provides the possibility to label multiple cell types by simple standard laboratory method and techniques. The labeling has been demonstrated both for murine and human cells and multiple cell types have been
30 labeled. The cell type unspecific labeling technology will therefore label potentially any given mammalian cell type present during the labeling procedure, which makes selection and isolation of the intended cell type(s) in the suspension vital to obtain accurate data. Isolation, sorting and purification steps must therefore be carefully applied to secure that an appropriate cell population is labeled based on the intended
35 use and study to be undertaken.

In vitro application

Labeling of cellular product by use of the D3R-analogue micelles provides the possibility to identify a labeled cell population by means of radioactivity and/or
5 fluorescence measurements. For any application, the longevity of the fluorophore must be considered in terms of photo bleaching etc. Based on specific aims of the specific study, behavior of the specific cell population labeled can be followed and evaluated in suspensions, cultures etc. of interest for the specific investigation. The possibility to
10 identify specific cellular products that have been labeled using the D3R-analogues furthermore provides the ability to study their specific behavior, biodistribution, cellular interactions etc. This can be done by harvesting the e.g. cells, specific organs and tissues from a subject to which the labeled cell product has been administered in vivo.

In one embodiment, a method for labelling cells is provided comprising the steps of:

- 15 a. providing a compound as defined herein,
- b. providing cells from a subject, and
- c. contacting the compound with the cells in vitro.

In one embodiment, the method for labelling cells as defined herein is provided, further
20 comprising a step of providing a radionuclide, and subsequently contacting the radionuclide with the compound as defined herein.

Experimental in vivo use

The possibility to perform noninvasive in vivo cell tracking by nuclear medicine
25 technologies (PET, SPECT, gamma camera) and fluorescence imaging is central for revealing the mechanisms and functions of adoptive cell transfer in real time in preclinical and clinical studies. The cell tracking possibilities provided by the D3R-analogue micelles radiolabeling technology can provide central information in the development of effective T cell therapeutic strategies and steering decision-making
30 process in clinical trials. Furthermore, they may provide crucial information to accelerate the regulatory approval process on the T cell therapy.

In the experimental animal models applied in preclinical research, the ability to label
and track a specific cell population provides the possibility to study not only therapeutic
35 cellular products but also trafficking and behavior of immune cells, cancer cells and

stem cell products to further provide information on their e.g. trafficking and engraftment. These possibilities will provide important tools to decipher clinical, physiological and immunologic questions. The D3R-analogue micelles can therefore serve as tools for optimizing in vivo diagnostics and therapeutics and improve physiological understanding of specific cells.

Clinical application

The D3R-analogue micelles are intended for use as a diagnostic tool for molecular imaging (e.g. PET, SPECT and gamma camera based technologies) and as a technology that allows for the evaluation of therapeutic cell products. The latter may be beneficial for selection of patients for interventions using therapeutic cellular products and adjuvant therapies to be applied in combination with cellular therapies. In terms of diagnostics application the flexible system may allow for labeling of e.g. polymorph nuclear granulocytes and/or monocytes for identification and diagnosing inflammatory lesions and conditions in patients.

In one embodiment, the method for labelling cells as defined herein is provided, further comprising the steps of:

- d. administering the cells to the subject, and
- e. tracking the labelled cells using an imaging modality.

In one embodiment, the method for labelling cells as defined herein is provided, wherein a further imaging modality is used.

In one embodiment, the method for labelling cells as defined herein is provided, wherein the imaging modality and/or the further imaging modality are selected from the group consisting of: PET and SPECT.

In one embodiment, the method for labelling cells as defined herein is provided, wherein the tracking comprises the use of flow cytometry of organ cell suspensions from the subject.

In one embodiment, the method for labelling cells as defined herein is provided, wherein the cells are selected from the group consisting of: T-lymphocytes, neutrophilic granulocytes, monocytes and cancer cells.

In one embodiment, the method for labelling cells as defined herein is provided, wherein the method is used in combination with adoptive cell transfer.

- 5 In one embodiment, the method for labelling cells as defined herein is provided, wherein the method is used in combination with immunotherapy.

In one embodiment, the method for labelling cells as defined herein is provided, wherein the method is used in combination with chemotherapy.

10

In one embodiment, use of a compound as defined herein is provided for tracking cell proliferation, differentiation, and/or function.

15

In one embodiment, a kit is provided for tracking cell proliferation, differentiation, and/or function, comprising:

- a. a compound as defined herein,
- b. a solvent, and optionally
- c. instructions for use

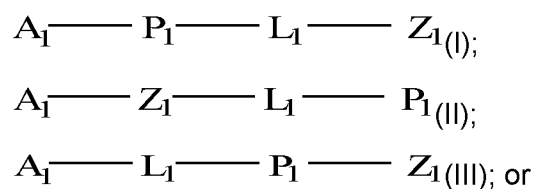
20

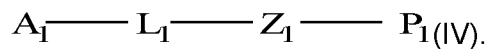
Items

25

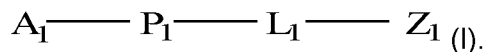
1. A compound comprising:
 - a. a chelator group (Z_1),
 - b. a cationic peptide sequence (P_1) comprising amide-bonded amino acids, and
 - c. a lipophilic aliphatic group (A_1).
2. The compound according to item 1, wherein the chelator group (Z_1), the cationic peptide sequence (P_1), and the lipophilic aliphatic group (A_1), are covalently connected via a linker (L_1) according to any one of formulas (I) to (IV):

30





3. The compound according to item 2, wherein the chelator group (Z_1) is bound via a linker (L_1) to the N-terminus or the C-terminus of the cationic peptide sequence (P_1), and the compound is represented by formula (I):



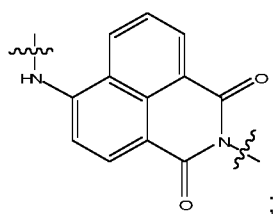
4. The compound according to any one of the preceding items, wherein the lipophilic aliphatic group (A_1) is bound via a functional group to the N-terminus or C-terminus of the cationic peptide sequence (P_1).
5. The compound according to any one of the preceding items, wherein the lipophilic aliphatic group (A_1) is bound via a carbonyl group to the N-terminus of the cationic peptide sequence (P_1), wherein the carbonyl group and the amine of the N-terminus together forms an amide.
6. The compound according to any one of the preceding items, wherein the chelator group (Z_1) is a polydentate hydrophilic chelator group.
7. The compound according to any one of the preceding items, wherein the chelator group (Z_1) is linear or cyclic.
8. The compound according to any one of the preceding items, wherein the chelator group (Z_1) comprises ethylene diamine.
9. The compound according to any one of the preceding items, wherein the chelator group (Z_1) is selected from the group consisting of: 1,4,7,10-tetraazacyclododecane-1,4,7,10-tetraacetic acid (DOTA), 1,4,7,10-tetraazacyclododecane (Cyclen), 1,4,8,11-tetraazacyclotetradecane (cyclam), 1,4-ethano-1,4,8,11-tetraazacyclotetradecane (et-cyclam), 1,4,7,11-tetraazacyclotetradecane (isocyclam), 1,4,7,10-tetraazacyclotridecane ([13]aneN₄), 1,4,7,10-tetraazacyclododecane-1,7-diacetic acid (DO2A), 1,4,7,10-tetraazacyclododecane-1,4,7-triacetic acid (DO3A), 1,4,7,10-


- 5 tetraazacyclododecane-1,7-di(methanephosphonic acid) (DO2P), 1,4,7,10-tetraazacyclododecane-1,4,7-tri(methanephosphonic acid) (DO3P), 1,4,7,10-tetraazacyclododecane-1,4,7,10-tetra(methanephosphonic acid) (DOTP), diethylenetriaminepentaacetic acid (DTPA), 1,4,8,11-tetraazacyclotetradecane-1,4,8,11-tetraacetic acid (TETA), and ethylenediaminetetraacetic acid (EDTA).
- 10 10. The compound according to any one of the preceding items, wherein the cationic peptide sequence (P_1) comprises an amino acid selected from the group consisting of: L-arginine (R), L-homoarginine (hArg), L-histidine (H), L-homohistidine (hHis), L-lysine (K), L-homolysine (hLys), L-ornithine (Orn), D-ornithine (orn), D-arginine (r), D-homoarginine (harg), D-histidine (h), D-homohistidine (hhis), D-Lysine (k), and D-homolysine (hlys).
- 15 11. The compound according to any one of the preceding items, wherein the cationic peptide sequence (P_1) comprises an amino acid selected from the group consisting of: L-arginine (R), and D-arginine (r).
- 20 12. The compound according to any one of the preceding items, wherein the cationic peptide sequence (P_1) comprises at least two amide bonded amino acids, such as at least three amino acids, such as at least four amino acids, such as at least five amino acids, such as at least six amino acids, such as at least seven amino acids, such as at least eight amino acids, such as at least nine amino acids, such as at least ten amino acids.
- 25 13. The compound according to any one of the preceding items, wherein the cationic peptide sequence (P_1) comprises from two amino acids to five amino acids, such as three amino acids.
- 30 14. The compound according to any one of the preceding items, wherein the cationic peptide sequence (P_1) is selected from the group consisting of: RR, rr, RRR, rrr, RRRR, rrrr, RRRRR, rrrrr, RRRRRR, rrrrrr, RRRRRRR, rrrrrrr, RRRRRRRR, rrrrrrrr, RRRRRRRRR, rrrrrrrrr, RRRRRRRRRR, and rrrrrrrrrr.
- 35 15. The compound according to any one of the preceding items, wherein the lipophilic aliphatic group (A_1) comprises at least 8 carbon atoms, such as at

- least 9 carbon atoms, such as at least 10 carbon atoms, such as at least 11 carbon atoms, such as at least 12 carbon atoms, such as at least 13 carbon atoms, such as at least 14 carbon atoms, such as at least 15 carbon atoms, such as at least 16 carbon atoms, such as at least 17 carbon atoms, such as at least 18 carbon atoms, such as at least 19 carbon atoms, such as at least 20 carbon atoms, such as at least 21 carbon atoms, such as at least 22 carbon atoms, such as at least 23 carbon atoms, such as at least 24 carbon atoms, such as at least 25 carbon atoms, such as at least 26 carbon atoms, such as at least 27 carbon atoms, such as at least 28 carbon atoms, such as at least 29 carbon atoms, such as at least 30 carbon atoms, such as at least 31 carbon atoms, such as at least 32 carbon atoms, such as at least 33 carbon atoms, such as at least 34 carbon atoms, such as at least 35 carbon atoms.
16. The compound according to any one of the preceding items, wherein the lipophilic aliphatic group (A_1) is an aliphatic chain or an aliphatic cycle.
17. The compound according to any one of the preceding items, wherein the lipophilic aliphatic group (A_1) is an aliphatic branched or non-branched chain.
18. The compound according to any one of the preceding items, wherein the lipophilic aliphatic group (A_1) is an aliphatic cycle comprising a gonane structure.
19. The compound according to any one of the preceding items, wherein the lipophilic aliphatic group (A_1) is an aliphatic cycle comprising a steroid, such as cholesterol.
20. The compound according to any one of the preceding items, wherein the lipophilic aliphatic group (A_1) comprises two adjacent carbon atoms connected by a double bond.
21. The compound according to any one of the preceding items, wherein the lipophilic aliphatic group (A_1) is a non-branched C15, C16, C17, C18, C19 or C20 alkyl.

22. The compound according to any one of the preceding items, wherein the lipophilic aliphatic group (A_1) is a non-branched C17 alkyl.
23. The compound according to any one of the preceding items, wherein the linker (L_1) consists of one or more linking units (U_1) to (U_4), connecting the chelator group (Z_1) with the cationic peptide sequence (P_1), according to formula (Ia), (Ib), (Ic), or (Id):
- 5
- $$A_1 - P_1 - U_1 - Z_1 \text{ (Ia);}$$
- $$A_1 - P_1 - U_1 - U_2 - Z_1 \text{ (Ib);}$$
- $$A_1 - P_1 - U_1 - U_2 - U_3 - Z_1 \text{ (Ic); or}$$
- $$A_1 - P_1 - U_1 - U_2 - U_3 - U_4 - Z_1 \text{ (Id);}$$
- 10
- wherein (A_1), (P_1) and (Z_1) are defined as in any one of the preceding items.
24. The compound according to any one of the preceding items, wherein at least one of the linking units (U_1) to (U_4) is a proteinogenic or non-proteinogenic amino acid.
- 15
25. The compound according to any one of the preceding items, wherein the proteinogenic amino acid is selected from: L-cysteine (C), D-cysteine (d), L-lysine (K), and D-lysine (d).
- 20
26. The compound according to any one of the preceding items, wherein the linker (L_1) of formula (I) is cleavable, covalently disconnecting any one of the linking units (U_1) to (U_4) by reduction, a change in pH and/or an enzymatic process.
- 25
27. The compound according to any one of the preceding items, wherein the compound of formula (Ib) is cleavable between linking units (U_1) and (U_2).
- 30
28. The compound according to any one of the preceding items, wherein the compound of formula (Ic) is cleavable between linking units (U_1) and (U_2).

29. The compound according to any one of the preceding items, wherein the compound of formula (Id) is cleavable between linking units (U_1) and (U_2).
30. The compound according to any one of the preceding items, wherein the bond between any one of (U_1) and (U_2), (U_2) and (U_3), (U_3) and (U_4), is a disulfide bond.
31. The compound according to any one of the preceding items, wherein at least one of the linking units (U_1) to (U_4) is a fluorophore (F_1).
32. The compound according to any one of the preceding items, wherein the fluorophore (F_1) emits light at a wavelength between 400 and 2600 nm.
33. The compound according to any one of the preceding items, wherein the fluorophore (F_1) is selected from the group consisting of: a naphthalene derivative, a squaraine derivative, a xanthene derivative, a cyanine derivative, a coumarine derivative, an oxadiazole derivative, an anthracene derivative, a pyrene derivative, an oxazine derivative, an acridine derivative, an arylmethine derivative, and a tetrapyrrole derivative.
34. The compound according to any one of the preceding items, wherein the fluorophore (F_1) is:

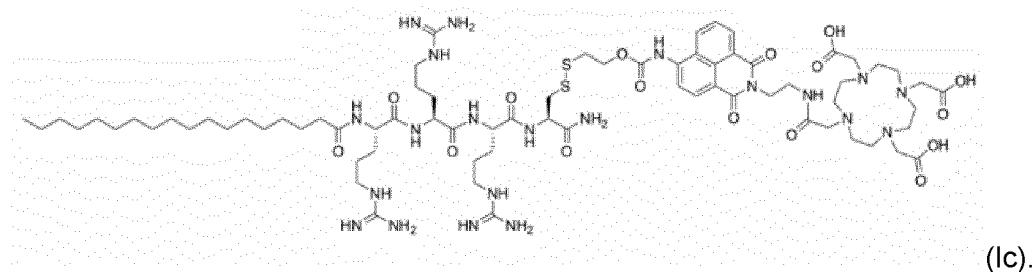
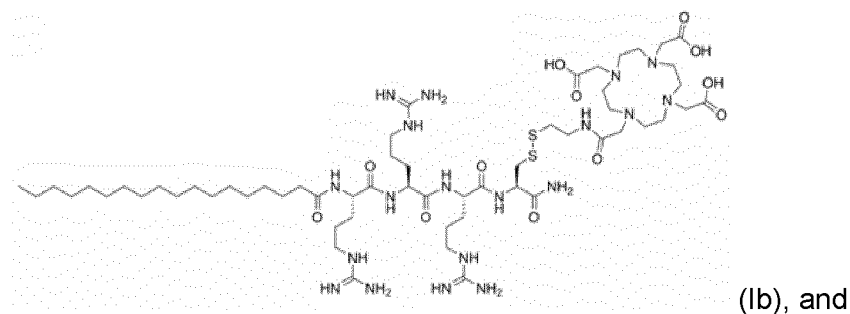
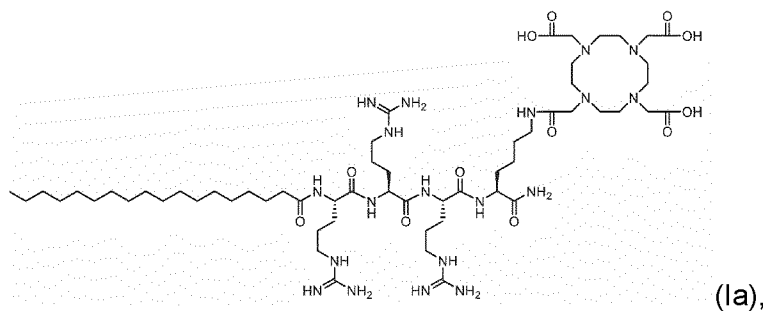


- wherein a wavy bond “” indicates by intersection the bond connected to L_1 or Z_1 of the compound as represented by formula (I).

35. The compound according to any one of the preceding items, wherein:
- the chelator group (Z_1) is DOTA,
 - the cationic peptide sequence (P_1) is RRR, and

c. the lipophilic aliphatic group (A₁) is a non-branched C17 alkyl.

36. The compound according to any one of the preceding items, wherein the compound is selected from the group consisting of:



10 37. The compound according to any one of the preceding items, further comprising a radionuclide, optionally chelated to the chelator group (Z₁).

38. The compound according to any one of the preceding items, wherein the radionuclide decays by emission of particles or photons.

15 39. The compound according to any one of the preceding items, wherein the radionuclide is selected from the group consisting of alpha emitters, beta emitters, X-ray emitters, auger emitters and gamma emitters.

40. The compound according to any one of the preceding items, wherein the radionuclide is a beta emitter.
- 5 41. The compound according to any one of the preceding items, wherein the radionuclide is selected from the group consisting of: P-32, Y-90, Sm-153, Er-169, Lu-177, Cu-67, Sc-47, As-76, Te-161, At-211, Ac-225, Bi-212, Bi-213, Ra-223, Pd-212, Te-149, Ra-224, Pd-103, La-135, Er-165, I-125, I-123, Rh-103m, Co-58m, In-111, Au-198, Co-60, Cs-137, and Ir-192, I-125 and Cf-252, Am-241, Pd-103, Yb-169, Se-75 and Sm-145.
- 10 42. The compound according to any one of the preceding items, wherein the radionuclide is selected from the group consisting of: Cu-64, Mn-52, Ga-67, and Lu-177.
- 15 43. A method for labelling cells comprising the steps of:
- a. providing a compound as defined in any one of the preceding items,
 - b. providing cells from a subject, and
 - c. contacting the compound with the cells in vitro.
- 20 44. The method according to any one of the preceding items, further comprising a step of providing a radionuclide, and subsequently contacting the radionuclide with the compound as defined in any one of the preceding items.
- 25 45. The method according to any one of the preceding items, further comprising the steps of:
- a. administering the cells to the subject, and
 - b. tracking the labelled cells using an imaging modality.
- 30 46. The method according to any one of the preceding items, wherein a further imaging modality is used.
- 35 47. The method according to any one of the preceding items, wherein the imaging modality and/or the further imaging modality are selected from the group consisting of: PET and SPECT.

48. The method according to any one of the preceding items, wherein the tracking comprises the use of flow cytometry of organ cell suspensions from the subject.
- 5 49. The method according to any one of the preceding items, wherein the cells are selected from the group consisting of: T-lymphocytes, neutrophilic granulocytes, monocytes and cancer cells.
- 10 50. The method according to any one of the preceding items, wherein the method is used in combination with adoptive cell transfer.
51. The method according to any one of the preceding items, wherein the method is used in combination with immunotherapy.
- 15 52. The method according to any one of the preceding items, wherein the method is used in combination with chemotherapy.
53. Use of a compound as defined in any one of the preceding items for tracking cell proliferation, differentiation, and/or function.
- 20 54. A micelle comprising a plurality of compounds as defined in any one of the preceding items.
55. The composition according to any one of the preceding items, wherein the compound is saturated by one or more cations, optionally chelating to the chelator.
- 25 56. The composition according to any one of the preceding items, wherein the one or more cations are radioactive or stable isotopes.
- 30 57. The composition according to any one of the preceding items, wherein the stable isotopes are Cu-63 and/or Cu-65.
58. A kit for tracking cell proliferation, differentiation, and/or function, comprising:
- 35 a. a compound as defined in any one of the preceding items,
- b. a solvent, and optionally

c. instructions for use

ExamplesMaterials

5 Buffers:

ISO-TRIS-NaCl (10 mM:150 mM, pH 7.8)

ISO-HEPES-Glucose buffer (10 mM:5 w%, pH 7.8)

ISO-HEPES-Sucrose buffer (10 mM:10w%, pH 7.4)

ISO-TRIS-Sucrose buffer (10 mM:10 w%, pH 7.4)

10 PBS-Sucrose buffer (60 mM:30 w%, pH 7.4, 1525 mOsm/kg)

NaOAc solution (10 mM, pH 5.5, 20 mOsm/kg)

NH₄OAc solution (10 mM, pH 5.5, 22 mOsm/kg)NH₄OAc solution (28 mM, pH 5.5)NH₄OAc solution (100 mM, pH 5.5)

15

TLC eluents:

5% NH₄OAc in H₂O:CH₃OH (25:75) "Chelator eluent weak"5% NH₄OAc in H₂O:CH₃OH (50:50) "Chelator eluent"5% NH₄OAc in H₂O:CH₃OH (75:25) "Chelator eluent strong"

20

Example 1: Synthesis of D3R-C16, D3R-C18, DSS3R-C18 and DFSS3R-C18Chemicals

All chemicals were purchased from Sigma-Aldrich Inc. (Broendby, Denmark) unless otherwise stated. 9-Fluorenylmethoxycarbonyl (Fmoc) amino acids and O-(7-azabenzotriazol-1-yl)-1,1,3,3-tetramethyluronium hexafluorophosphate (HATU) used for the solid phase peptide synthesis were purchased from GL Biochem (Shanghai, China) or Iris Biotech GmbH (Marktredwitz, Germany). Novasyn TGR resin was purchased from Merck Chemicals GmbH (Darmstadt, Germany). DOTA(tBu)₃-OH was purchased from Chematech (Dijon, France) or Bachem. All chemicals and reagents were of analytical grade and used without further purification.

30

Instrumentation

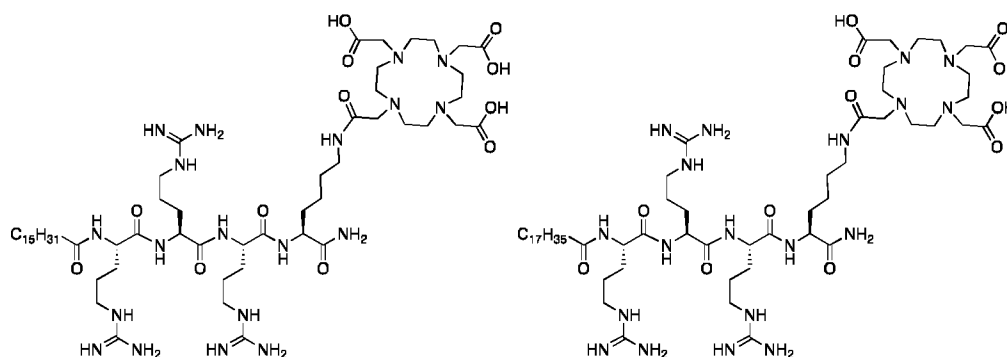
Reactions were monitored by TLC; visualization was carried out by UV-light exposure (254 and 365 nm), Cemol and KMnO₄-stain. FCC refers to column chromatography using nitrogen for continuous pressure on silica gel (60 Å, 63-200 µm). Dry flash column

35

chromatography (DFCC) refers to column chromatography using vacuum on silica gel (60 Å, 15-40 µm). Automated flash column chromatography both reverse- and normal-phase is done on a Büchi Reveleris autoflash. NMR spectra were recorded on a Varian Mercury 400 MHz Spectrometer. ¹H and ¹³C NMR were recorded at 400 and 100 MHz, respectively. Chemical shifts (δ) are reported in ppm relative to the solvents signal peak.

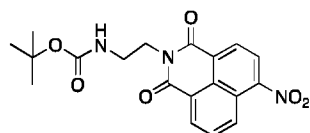
Mass spectra were recorded on a Bruker Autoflex™ MALDI-TOF MS Spectrometer using DHB spiked with sodium trifluoroacetate in CH₃OH as matrix or Waters UPLC ESI-MS (Acquity UPCL system with a TUV detector and a QDa single quadrupole MS with ESI detector by employing a Waters Acquity UPLC® BEH C₄ (1.7 µm, 2.1 × 50 mm), BEH C₈ (1.7 µm, 2.1 × 50 mm) or BEH C₁₈ (1.7 µm, 2.1 × 50 mm) column. RP-UPLC Eluent A consisted of 0.1 % FA in water; Eluent B consisted of 0.1 % FA in CH₃CN. Analytical reversed-phase high-performance liquid chromatography (RP-HPLC) was performed on a Gilson HPLC (Gilson Valvemate, UV/VIS-155, 321 Pump, 234 Auto injector) using a Waters XBridge™ C₈ or C₁₈ (5 µm, 4.6×150 mm) or Waters XTerra® C₈ or C₁₈ (5 µm, 4.6×150 mm). Semi-preparative HPLC was performed on a Waters Semi-preparative HPLC equipped with a Waters 600 Pump & Controller and a Waters 2489 UV/VIS Detector using a Waters XTerra® C₈ or C₁₈ (5 µm, 19 × 150 mm) column or a Knauer Eurosphere 100-5 C₁₈ (5 µm, 250 x 20 mm) column. HPLC Eluent A consisted of a 5 % CH₃CN aqueous solution with 0.1 % TFA; HPLC Eluent B consisted of 0.1 % TFA in CH₃CN. Preparative HPLC analysis was monitored using UV/VIS detection at 220/280 nm. FT-IR was recorded neat on a PerkinElmer Instruments Spectra One FT-IR Spectrometer. DLS and ζ-potential measurements were performed on a Brookhaven Instruments Corporation ZetaPALS ζ-potential analyzer. A Biotage® Initiator+ Alstra™ automated peptide synthesizer has been used to synthesize the peptides.

Synthesis



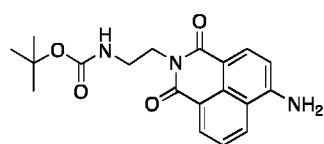
Synthesis of D3R-C16 and D3R-C18.

The tetrapeptide H-Arg(Pbf)-Arg(Pbf)-Arg(Pbf)-Lys(Mtt) was synthesized on an Initiator Alstra peptide synthesizer (Biotage, Uppsala, Sweden) using a novasyn TGR resin (loading 0.2 mmol/g). The resin was swelled in dichloromethane (DCM) for 1 hour. Each residue was coupled 30 minutes at room temperature (r.t.) using 4 eq. amino acid, 3.92 eq. HATU and 8 eq. 2,4,6-collidine in *N,N*-dimethylformamide (DMF). Fmoc deprotection was done using 20% piperidine in DMF for 3 plus 10 minutes. Afterwards, either stearic acid or palmitic acid was coupled using 4 eq. of fatty acid, 3.92 eq. HATU and 8 eq. 2,4,6-collidine in DCM:DMF (1:1) for 60 min. Mtt-deprotection was obtained using 2 % trifluoroacetic acid (TFA) in DCM. 25 washes of 10 ml for 5 min each were used. DOTA was coupled using 4 eq. of DOTA-tris-tBu, 3.92 eq. HATU and 8 eq. 2,4,6-collidine in DMF for 1 hour. The peptides were cleaved for 3 hours using 95:2.5:2.5 TFA/water/triisopropyl silane after which the cleavage solvent was removed under reduced pressure and the peptide precipitated in diethyl ether. The cleaved peptide was dissolved in 5 % DMSO in water and purified using semi-preparative HPLC (Waters 600 Pump & Controller and a Waters 2489 UV/Visible Detector). The C18 peptide was purified employing a Waters XTerra® C₁₈ 5 µm (30 x 250 mm) column. Eluent: (A) 5 % CH₃CN, 0.1 % triethylamine (TEA) in water, (B) 0.1 % TEA in acetonitrile. Gradient profile; linear gradient from 25 % B to 45 % B over 40 min. Flow rate; 40 mL/min. The product was collected from 18-30 min. The C16 peptide was purified employing a Waters XTerra® C₁₈ 5 µm (19 x 150 mm) column. Eluent: (A) 5 % CH₃CN, 0.1 % TEA (TFA) in water, (B) 0.1 % TEA in CH₃CN. Gradient profile; linear gradient from 20 % B to 40 % B over 20 min. Flow rate; 17 mL/min. The product was collected from 12-15 min. The products were lyophilized to obtain a white powder. The purity of the products was monitored by analytical HPLC using a Waters XBridge® C₁₈ 5 µm (4.6 x 150 mm) column. Eluent: (A) 5 % CH₃CN, 0.1 % TFA in water, (B) 0.1 % TFA in CH₃CN. Gradient profile; linear gradient from 0 % B to 100 % B over 15 min. Flow rate; 1 ml/min. Purity >95 %. R_f: 11.0 min (C16) and 11.1 (C18). MALDI-TOF MS (Matrix: DHB Na.TFA in CH₃OH) (*m/z*): Calc. mass C₅₆H₁₀₇N₁₉O₁₂ (D3R-C16) 1237.8; found mass [M+H]⁺ 1238.8. Calc. mass C₅₈H₁₁₁N₁₉O₁₂ (D3R-C18) 1265.9; found mass [M+H]⁺ 1266.9

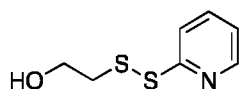


Synthesis of MB207.¹ 4-Nitro-1,8-naphthalic anhydride (984 mg, 4.05 mmol) and *N*-Boc-1,2-diaminoethane (648 mg, 4.05 mmol) was mixed in a round bottom flask. The

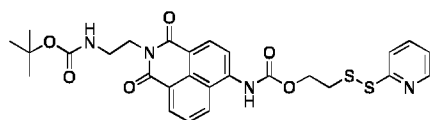
mixture was refluxed in ethanol (20 mL) for 1 h, after which the reaction was let to reach room temperature. The yellow precipitate was filtered, washed with cold ethanol and dried under vacuum at room temperature. The pure compound was isolated as a yellow crystalline solid (1.18 mg, 3.06 mmol, 75 % yield). ESI-MS (m/z): Calc. mass $C_{19}H_{19}N_3O_6$ 385.4; found mass $[M+Na]^+$ 408.1. 1H NMR (800 MHz, $CDCl_3$), δ (ppm): 8.84 (d, J = 8.6 Hz, 1H), 8.74 (d, J = 7.2 Hz, 1H), 8.70 (d, J = 7.9 Hz, 1H), 8.40 (d, J = 7.9 Hz, 1H), 7.98 (t, J = 7.9 Hz, 1H), 4.87 (bs, 1H), 4.37 (t, J = 5.2 Hz, 2H), 3.55 (s, 2H), 1.23 (s, 9H).



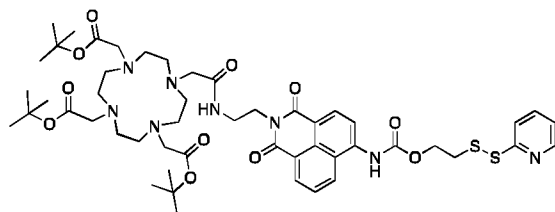
Synthesis of MB213.¹ MB207 (575 mg, 1.49 mmol) and Pd/C (10 mol%) was mixed in a flame dried round bottom flask fitted with a septum. The flask was put under vacuum and then added THF (6 mL) and then flushed with N_2 . A H_2 -balloon was bubbled through the solution followed by a second balloon added to the septum for o/n reaction. The reaction was filtered through Celite to remove the Pd/C with subsequent concentration in vacuum yielding a yellow solid (487 mg, 1.37 mmol, 92 % yield). ESI-MS (m/z): Calc. mass $C_{19}H_{21}N_3O_4$ 355.2; found mass $[M-H]^-$ 354.2. 1H NMR (400 MHz, CD_3OD), δ (ppm): 8.73 (dd, J = 7.3, 0.9 Hz, 1H), 8.62 (dd, J = 8.4, 0.9 Hz, 1H), 8.51 (d, J = 8.4 Hz, 1H), 7.84 – 7.77 (m, 1H), 7.07 (d, J = 8.4 Hz, 1H), 4.49 (t, J = 5.9 Hz, 2H), 3.65 (t, J = 5.9 Hz, 2H), 1.50 (s, 9H).



Synthesis of MB154. A flame dried three-necked flask with N_2 -atmosphere and a stir bar, was added 2,2'-dithiodipyridine (2356 mg, 10.7 mmol) in dry CH_3OH (10 mL) purged with N_2 . 2-mercaptoethanol (278 mg, 3.56 mmol) was slowly added to the solution within 1 h. The reaction turned yellow and it was let to react o/n and finally showed full conversion by LC-MS. The solvent was removed in vacuo and the compound was precipitated thrice in cold diethyl ether, and the product was obtained as a colorless crystalline solid (558 mg, 84 % yield). ESI-MS (m/z): Calc. mass $C_7H_9NOS_2$ 187.0; found mass $[M+H]^+$ 188.1. 1H NMR (400 MHz, $CDCl_3$), δ (ppm): 8.44 (dd, J = 10.9, 3.2 Hz, 1H), 7.55 (ddd, J = 9.2, 6.5, 2.7 Hz, 1H), 7.38 (d, J = 8.1 Hz, 1H), 7.09 (ddd, J = 9.9, 4.7, 2.9 Hz, 1H), 5.33 (s, 1H), 3.81 – 3.72 (m, 2H), 2.95 – 2.85 (m, 2H).

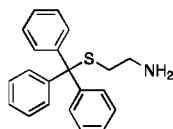


Synthesis of MB215. A dry three-necked flask was fitted a stir bar and N₂-atmosphere. **MB213** (135 mg, 0.38 mmol) was added and dissolved in dry toluene (12 mL). Phosgene (776 mg, 1.18 mmol, 15 wt. % in toluene) followed by drop wise addition of DIPEA (340 μ L, 1.95 mmol). The resulting solution was heated to reflux for 3 h. Full conversion was observed on TLC and LC-MS. The mixture was cooled to r.t., flushed with N₂ and the solvent was removed *in vacuo*. The carbanic chloride intermediate was dissolved in dry CH₂Cl₂ (15 mL) and added **MB154** (105 mg, 0.56 mmol). The reaction was stirred o/n at r.t.. The solvent was removed *in vacuo*. The residue was re-dissolved in CH₂Cl₂ (30 mL) and washed with water (3 x 50 mL). The organic phase was dried with anhydrous MgSO₄, filtered and concentrated *in vacuo*. The crude compound was purified by a Reveleris auto flash system (Büchi PrepChrom RP-C₁₈ column, 150x21 mm, 15 μ m, 5-100% CH₃CN in water with 0.1% FA over 20 min, flow: 20 mL/min, temp.: 25 °C, detection: ELSD and UV_{220/280/310 nm}). The pure fractions were isolated as a yellow powder by lyophilization (123 mg, 57 % yield). ESI-MS (*m/z*): Calc. mass C₂₇H₂₈N₄O₆S₂ 568.15; found mas [M+Na]⁺ 591.2. ¹H NMR (400 MHz, DMSO-*d*₆), δ (ppm): 10.37 (d, *J* = 19.0 Hz, 1H), 8.71 – 8.64 (m, 1H), 8.51 – 8.42 (m, 3H), 8.14-8.12 (m, 1H), 7.87 – 7.76 (m, 3H), 7.24 (ddt, *J* = 6.8, 4.7, 2.0 Hz, 1H), 6.88 (t, *J* = 6.2 Hz, 1H), 4.44 (t, *J* = 6.2 Hz, 2H), 4.21 (t, *J* = 6.0 Hz, 1H), 4.15-4.08 (m, 1H), 3.25-3.22 (m, 3H), 3.14 – 3.08 (m, 1H), 1.22 (s, 9H).

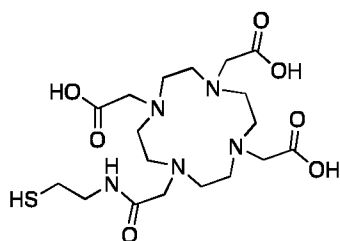


Synthesis of MB226. **MB215** (40 mg, 0.10 mmol) was dissolved in TFA:DCM (10 mL, 20:80) for 45 min. Full conversion was confirmed by LC-MS. The solvent was subsequently removed *in vacuo* leaving a yellow residual. DOTA(*t*Bu)₃-OH (85 mg, 0.14 mmol) was dissolved in anhydrous DMF (10 mL) and was activated with pyBOP (80 mg, 0.15 mmol) for 2 min. Then, a mixture of the re-dissolved deprotected **MB215** and DIPEA (166 μ L, 0.66 mmol) in anhydrous DMF (2 mL) was added. The reaction mixture was

stirred for 2h until LC MS showed full conversion. The crude compound was concentrated *in vacuo* and was purified using a Reveleris auto flash system (Büchi PrepChrom RP-C₁₈ column, 150x21 mm, 15 µm, 5-100% CH₃CN in water with 0.1% FA over 20 min, flow: 20 mL/min, temp.: 25 °C, detection: ELSD and UV_{220/280/310 nm}). The pure fractions were pooled and lyophilized to isolate a yellow powder (51 mg, 48% yield).
ESI-MS (*m/z*): Calc. mass C₅₀H₇₀N₈O₁₁S₂ 1022.46; found mass [M+H]⁺ 1022.96, [M+2H]²⁺ 512.16. ¹H NMR (600 MHz, DMSO-*d*₆), δ (ppm): 10.42 (s, 1H), 8.72 (d, *J* = 8.6 Hz, 1H), 8.62 (bs, 1H), 8.53 (d, *J* = 7.2 Hz, 1H), 8.52 – 8.45 (m, 2H), 8.13 (d, *J* = 8.2 Hz, 1H), 7.91 – 7.85 (m, 1H), 7.85 – 7.78 (m, 2H), 7.25 (ddd, *J* = 6.5, 4.8, 2.3 Hz, 1H), 4.45 (t, *J* = 6.2 Hz, 2H), 4.25 (t, *J* = 5.7 Hz, 2H), 3.85 – 2.79 (m, 28H), 1.40 (s, 27H).

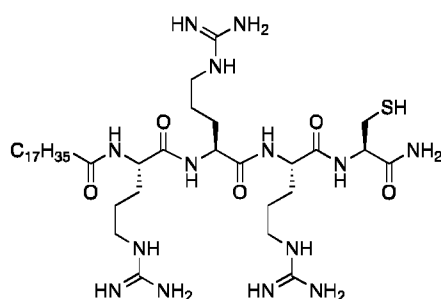


Synthesis of MB220. Cysteamine (1.39 g, 18.0 mmol) was dissolved in CH₂Cl₂:DMF (1:1, 50 mL). Trityl chloride (5.10 g, 18.3 mmol) was added, and the solution was stirred o/n at r.t.. Then, the mixture was concentrated in *vacuo* and subsequently co-concentrated with toluene (50 mL), ethanol (50 mL), and dichloromethane (50 mL). The crude product was dissolved in dichloromethane (50 mL) and washed with saturated aq. NaHCO₃ (30 mL). The organic phase was dried, filtered, and concentrated in *vacuo*. The product was purified by using a Reveleris auto flash system (Büchi FP ID HP Si 24g NP-cartridge, 1: 4CV at 0% CH₃OH in CH₂Cl₂, 2: 8CV from 0-4% CH₃OH in CH₂Cl₂, 3CV at 4% CH₃OH in CH₂Cl₂, 5CV at 20% CH₃OH in CH₂Cl₂, temp.: 25 °C, detection: UV_{220/254nm}) to yield a white pure compound (1009 g, 17 % yield). MALDI-TOF MS (*m/z*): Calc. mass C₂₁H₂₁NS 319.14; found mass [M+Na]⁺ 342.28. ¹H NMR (400 MHz, CD₃OD), δ (ppm): 7.51 – 7.19 (m, 15H), 2.51 – 2.45 (m, 2H), 2.43 – 2.36 (m, 2H).



Synthesis of MB219. tBu₃-DOTA-OH (535 mg, 0.93 mmol) dissolved in dry DMF (9 mL) was activated with pyBOP (511 mg, 0.98 mmol) in dry DMF (4 mL) for 5 min. Then, a

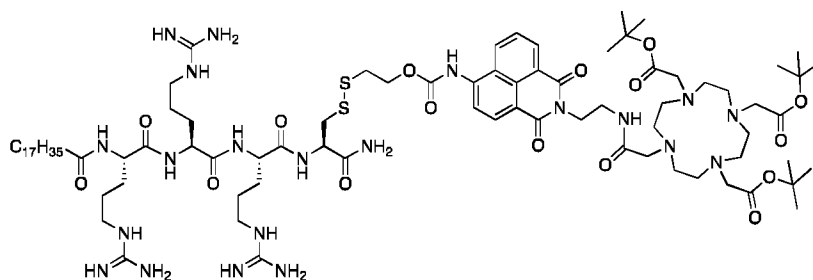
mixture of MB220A (306 mg, 0.96 mmol) and triethylamine (153 μ L, 1.10 mmol) in dry DMF (4 mL) was added and the mixture was stirred for 2 h. Ethylacetate (20 mL) and saturated aqueous sodium bicarbonate (20 mL) were added and vigorously mixed. After phase separation, the aqueous layer was extracted with additional of ethylacetate (20 mL) and the combined organic layers were washed with water, filtered over MgSO_4 and evaporated to yield a yellowish oil. This oil was mixed with 50 mL of deprotection mixture (TFA:TIPS:H₂O:thioanisole:EDT 82.5:5:5:2.5) and stirred for 2 h. The fully deprotected product was precipitated in cold diethyl ether. The white precipitated was isolated by centrifugation (3500 rpm for 15min). Residual ether was removed in vacuo and the white compound was partitioned between water (50 mL) and CHCl_3 (50 mL). The aqueous layer was collected and washed further with CHCl_3 (2x50 mL). The product was in the aqueous phase and the impurity in the CHCl_3 . The aqueous phase was lyophilized to obtain a white solid (589 mg, 85 % yield). ESI-MS (m/z): Calc. mass $\text{C}_{18}\text{H}_{33}\text{N}_5\text{O}_7\text{S}$ 463.2; found mass $[\text{M}+\text{H}]^+$ 464.2.



Synthesis of MB209. The tetrapeptide H-Arg(Pbf)₃-Cys(Trt) was synthesized on an Initiator Alstra peptide synthesizer (Biotage, Uppsala, Sweden) using a Nova Tentagel resin (loading 0.25 mmol/g, scale 0.5 mmol). The resin was swelled in DCM for 1 h. Fmoc-L-Cys(Trt)-OH was double coupled for 30 min at r.t. using 4 eq. amino acid, 3.92 eq. HATU and 8 eq. 2,4,6-collidine in DMF. The subsequent Fmoc-L-Arg(Pbf)-OH was coupled for 30 min at r.t. and 5 min at 50 °C using 4 eq. amino acid, 3.92 eq. HATU and 8 eq. 2,4,6-collidine in DMF. Fmoc deprotection was done using 20% piperidine in DMF for 3 plus 10 min. Afterwards stearic acid was coupled using 4 eq. of fatty acid, 3.92 eq. HATU and 8 eq. 2,4,6-collidine in DCM:DMF (1:1) for 60 min. The peptide was cleaved for 3 hours using 94:2.5:2.5:1 TFA:EDT:TIPS:H₂O after which the cleavage solvent was removed under reduced pressure and the peptide precipitated in diethyl ether. The crude peptide was purified using a Reveleris auto flash system (Büchi PrepChrom RP-C₁₈ column, 150x21 mm, 15 μ m, 5-100% CH_3CN in water with 0.1% FA over 20 min, flow:

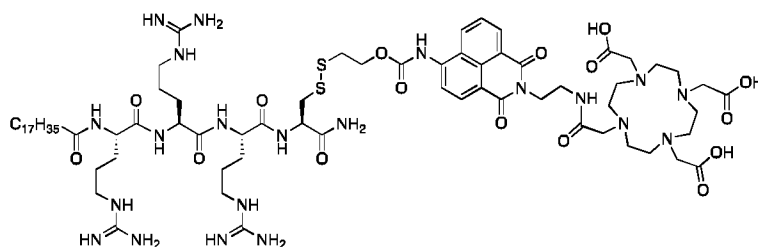
20 mL/min, temp.: 25 °C, detection: ELSD and UV_{206 nm}). The pure fractions were pooled and lyophilized to isolate a white powder (237 μmol, 47 % yield). MALDI-TOF MS (*m/z*): Calc. mass C₃₉H₇₈N₁₄O₅S 854.60, found mass [M+H]⁺ 877.96.

5



Synthesis of MB228. MB226 (40 mg, 39.1 μmol) was dissolved in DMSO (9 mL) and was added a solution of MB209 (49 mg, 57.3 μmol) in DMSO (9 mL). The reaction was left to react o/n at r.t.. Full conversion of the starting material was observed by LC MS. The compound in DMSO was diluted to <10% in water with 0.1% FA. The compound was loaded onto a RP-Waters XTerraC₁₈ column (19x150mm, 5 μm) and purified on a Waters Semi Prep. system (5-100% CH₃CN in water with 0.1% FA over 20 min, flow: 17 mL/min, temp.: 25 °C, detection: UV_{220/280 nm}, R_F-value: 8min). The pure fractions were pooled and analyzed by LC-MS (Waters Acquity RP-UPLC QDa-ESI in CH₃OH, Waters BEHC₁₈, 5-100% CH₃CN in water with 0.1% FA over 6min). The pooled fractions were lyophilized to obtain a yellow powder (14.3 μmol, 37 % yield). ESI MS (*m/z*): Calc. mass C₈₄H₁₄₃N₂₁O₁₆S₂ 1766.05; found mass [M+2H]²⁺ 883.83 and [M+3H]³⁺ 589.48.

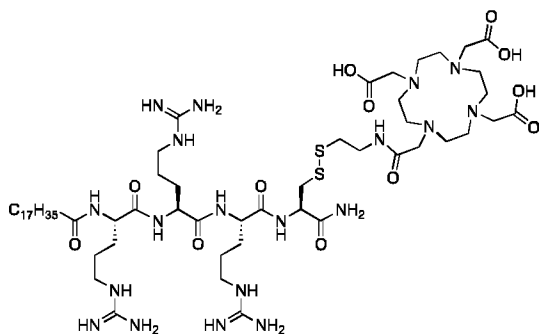
20



Synthesis of DFSSR3-C18 (MB232). MB228C (2.7 mg, 1.53 μmol) was dissolved in TFA:DCM:H₂O (48:48:4, 10 mL) for 5 h and then the solvent was removed in vacuo after full conversion on LC-MS (Waters Acquity RP-UPLC QDa-ESI in CH₃OH, Waters BEHC₁₈ (1.7 μm, 2.1 x 50 mm), 5-100% CH₃CN in water with 0.1% FA over 6min, R_f:

25

2.9 min).. The solvent was removed in vacuo resulting a film of yellow oil (1.53 μmol , quant. yield). ESI MS (m/z): Calc. mass $\text{C}_{72}\text{H}_{119}\text{N}_{21}\text{O}_{16}\text{S}_2$ 1597.86; found mass $[\text{M}+2\text{H}]^{2+}$ 800.1; $[\text{M}+3\text{H}]^{3+}$ 534.0 and $[\text{M}+4\text{H}]^{4+}$ 400.8.



5

Synthesis of DSS3R-C18 (MB224). MB219 (43.1 μmol , 20 mg) and 4-PDS (47.5 μmol , 10.5 mg) was mixed in a round bottom flask fitted a magnet. The flask was evacuated and DMSO (10 mL) was added and N_2 subsequently. The activation was let to happen for 15min before MB209 (47.5 μmol , 40.6 mg) was added dropwise in DMSO (1 mL). The reaction was let to react o/n at r.t.. The compound was purified on a Reveleris auto flash system (Büchi PrepChrom RP- C_{18} column, 150x21 mm, 15 μm , 5-60% CH_3CN in water with 0.1% FA over 20 min, flow: 20 mL/min, temp.: 25 $^\circ\text{C}$, detection: ELSD and UV_{220/280 nm}, R_f 15 min). The pure fractions were isolated and lyophilized to obtain a white powder (13.7 mg, 29 % yield). ESI MS (m/z): Calc. mass $\text{C}_{57}\text{H}_{109}\text{N}_{19}\text{O}_{12}\text{S}_2$ 1315.79; found mass $[\text{M}+2\text{H}]^{2+}$ 658.8, $[\text{M}+3\text{H}]^{3+}$ 439.7 and $[\text{M}+4\text{H}]^{4+}$ 330.2.

Example 2: CMC of D3R-C16/C18

The aim of the current analysis is to determine the critical micelle concentration (CMC) of the D3R-C16/C18 construct, i.e. the concentration at which the monomers starts aggregating into micelles. The analysis was conducted in buffers with high or low ionic strength in order to access the effect of charge screening on the CMC of the D3R constructs.

25 Methods:

D3R-C16 or D3R-C18 was dispersed in ISO-HEPES-NaCl or ISO-HEPES-Sucrose for a final concentration of 250 μM as stock solutions. Sample series were prepared by diluting the stock solutions with ISO-HEPES-NaCl or ISO-HEPES-Sucrose into concentrations of 125, 62.5, 31.25, 15.63, 7.81, 3.91, 1.95, 0.98 and 0.49 μM . The

surface tension of the sample was measured by the Du Noüy method with a platinum probe (Kibron EZ-Pi +). For each sample, the measurements were repeated until three consecutive measurements varied with less than 1 mN/m between them. The data is compiled in Fig. 1

5

Results and discussion:

Fig.1 shows the surface tension plotted against the concentration of D3R-C16 (A) and D3R-C18 (B). The results are presented as mean \pm SEM, $n = 3$. The CMC is the intersection between the regression straight line (grey dashed lines) and the straight line passing through the plateau (black dashed lines). CMC values of 35 μ M and 10 μ M was identified for D3R-C16 and D3R-C18 in ISO-HEPES-NaCl respectively, whereas no CMC was obtained in ISO-HEPES-Sucrose.

10

15

The CMC values show the expected reduction from 35 μ M to 10 μ M upon extension of the hydrophobic acyl-chain moiety from C16 to C18. Similar CMC values for lysolipids and non-ionic detergent are reported in the literature. A lower propensity for forming micelles is observed in the lower ionic strength media (ISO-HEPES-Sucrose), which is expected due to the reduction in charge screening of the arginine sequence leading to increased electrostatic repulsion and higher CMC values.

20

Conclusion

In conclusion, the D3R-C16 and D3R-C18 analogues form micelles in ISO-HEPES-NaCl media (high ionic strength) with CMC values in the micromolar range. No CMC was detected in ISO-HEPES-Sucrose (low ionic strength media) in the investigated concentration range.

25

Example 3: Fluorescence characterization of DFSS3R-C18

The aim of the current example is to determine the excitation and emission spectra of the fluorescent D3R analogues when in monomeric or micellar form, and upon activation by reduction. A conceptual drawing of the mode of action of the redox-induced cleavage of the disulphide-bridge of the DFSS3R-C18 compound is seen on Fig 2.

30

Dithiothreitol (DTT) or Cysteine (Cys) is used to induce a change in the redox potential leading to activation of the disulphide-bridge (-SS-) of the DFSS3R-C18 compound, and following a spectral shift in the fluorescent characteristics as shown in Fig 2.

35

Methods:

Micelle preparation: All the micelles were made by dissolving the fluorescent D3R analogues in ISO-TRIS-NaCl (10mM TRIS, 150mM NaCl, pH 7.8), adding CuCl₂ (2.5 mg/mL, 1 eq.), and heating the sample at 55 °C for 30 min. One sample of DFSS3R-C18 (100 µL, 25 µM) was dissolved in ISO-TRIS-NaCl (10mM TRIS, 150mM NaCl, pH 7.8). A second sample of DFSS3R-C18 (100 µL, 25 µM) was dissolved in ISO-TRIS-NaCl (10 mM TRIS, 150 mM NaCl, pH 7.8):DMSO (1:1). A third sample of DFSS3R-C18 (50 µL, 50 µM) was dissolved in ISO-TRIS-NaCl (10mM TRIS, 150mM NaCl, pH 7.8) and post-inserted into liposomes (50 µL, 5 mM in ISO-TRIS-NaCl (10 mM TRIS, 150 mM NaCl, pH 7.8) at 45 °C for 30 min.

Emission and Excitation spectra: The fluorescent characterization was performed on a Tecan platereader (Spark® Multimode Microplate Reader) in a black flat-bottom 96-well plate. All measurements were conducted as duplicates.

Fluorescent D3R analogues were dissolved in ISO-TRIS-NaCl (10mM TRIS, 150mM NaCl, pH 7.8) in a 100 µM concentration, i.e. above the CMC of the compound. The dissolved D3R-analogue (100 µL, 100 µM) was added to a black flat-bottom 96-well plate, and ISO-TRIS-NaCl (100 µL, 10mM TRIS, 150 mM NaCl, pH 7.8) was used as blank control. The samples were analysed by scanning of the emission spectrum (Em_{420-700nm} by Ex_{350nm}, bandwidth: 20 nm, Em step size: 2 nm) and excitation spectrum (Ex_{350-500nm} by Em_{600nm}, bandwidth: 20 nm, Ex step size: 2 nm). The fluorescent characteristics of DFSS3R-C18 are presented in Fig 3.

Activation by DDT: DTT (100 eq., C_{final} 10 mM) was added to the sample to cleave the disulfide-bridge and activate the compound. The samples were shaken for 1 h at 37 °C, and the emission and excitation spectrum were following recorded (Fig 2B). The emission profile was shifted from 405 to 488 nm to visualize potential fluorescence-interference from the non-cleaved compound, which is seen in Fig 3C-E.

Activation kinetics: The cleaving kinetics of the DFSS3R-C18 (50 µM, 100µL) disulphide-bridge is tested in ISO-TRIS-NaCl (10mM TRIS, 150mM NaCl, pH 7.8) in a black flat-bottom 96-well plate with ISO-TRIS-NaCl (100 µL, 10mM TRIS, 150mM NaCl, pH 7.8) used as blank. CuCl₂ (1 eq. to DOTA) was added to one of the samples to visualize the effect of Cu chelated to DOTA as well non-chelated DOTA. DTT or Cys was added (C_{final}

10 mM) and let to react at 37 °C. The cleaving kinetics was analysed in the Tecan platereader (t = 0-125 min, Ex_{485nm} and Em_{545nm}, bandwidth: 20 nm). The fluorescent reaction kinetics is seen in Fig. 5.

5 *pH-dependency of the fluorescence emission:* D3R analogues were measured in a black flat-bottom 96-well plate on a Tecan platereader at 22 °C. Both the intact and fully cleaved analogue of DFSS3R-C18 was dissolved in ISO-TRIS-NaCl (10mM TRIS, 150mM NaCl, pH 2, 3, 4, 5, 6, 7, 7.8, 8, 9, 10 and 11, adjusted with HCl/NaOH) and analysed on the Tecan instrument (Ex_{488nm} and Em_{545nm}, bandwidth: 20nm, Temp.: 22
10 °C).

Results:

Spectral properties of DFSS3R-C18 was investigated and the results are presented in Fig. 3. Fig. 3A shows emission and excitation scanning of the intact DFSS3R-C18
15 construct giving an excitation / emission maximum of 382 nm / 466 nm. B: Emission and excitation scanning of the cleaved DFSS3R-C18 construct giving an excitation / emission maximum of 438 nm / 536 nm. C: Emission profile with an excitation of 405 nm. D: Emission profile with an excitation of 438 nm. E: Emission profile with an excitation of 488 nm. In this experiment, DFSS3R-C18 was dissolved in ISO-TRIS-NaCl (10mM TRIS,
20 150mM NaCl, pH 7.8).

A fluorescence response/standard curve of the intact DFSSR3-C18 (100 µL, 37 °C) dissolved in ISO-TRIS-NaCl (10mM TRIS, 150mM NaCl, pH 7.8) was constructed and is presented in Fig. 4. Fig. 4 shows a fluorescence response/standard curve of the intact
25 DFSSR3-C18 analogue in ISO-TRIS-NaCl buffer (10 mM / 150 mM, pH 7.8) (black flat 96-well plate, 80 µL per well, Conc. 50, 25, 10, 5, 2.5, 1, 0.5, 0.25, 0.1 µM). A: Ex382 nm and Em466 nm, B: Ex438 nm and Em545 nm with a bandwidth of 10 nm.

The activation kinetics of the redox sensitive DFSS3R-C18 construct was tested using
30 Cysteine and DDT, and the results are presented in Fig. 5. Fig. 5 shows the activation kinetics of DFSSR3-C18 studied via fluorescence emission. DTT or Cys was added (C_{final} 10 mM) to DFSSR3-C18 (50 µM, 100µL) in ISO-TRIS-NaCl (10mM TRIS, 150mM NaCl, pH 7.8, 37 °C) with and without one equivalent of CuCl₂.

The fluorescent D3R analogues are amphipathic and may pack into secondary structures that might affect the fluorescent properties of the constructs. This was investigated by recording the fluorescence emission of the cleaved construct when exposed to different dissolution factors. The results are presented in Fig. 6. Fig. 6 shows the solvent effect on the fluorescence emission. DFSSR3-C18 (25 μ M, 100 μ L) in either TRIS, TRIS:DMSO or TRIS liposomes (Lipoid Stealth formulation) at 37 °C with CuCl₂ (2.5 mg/mL, 1 eq.) added DTT (100 eq., 10 mM) (n = 2).

The impact of solvent pH was further investigated for the intact and cleaved DFSS3R-C18 construct, and the result are presented in Fig. 7. Fig. 7 shows the pH dependency of the fluorescence emission of the cleaved and intact DFSS3R-C18 compound. A: The intact DFSSR3-C18 (5 μ L, 50 μ M) with Cu (1 eq., 2.5 mg/mL) was diluted in ISO-TRIS-NaCl (95 μ L, 10mM TRIS, 150mM NaCl, pH 2, 3, 4, 5, 6, 7, 7.8, 8, 9, 10 and 11 (HCl/NaOH)). Ex488nm and Em545nm, bandwidth: 20nm, Temp.: 22 °C (n = 1). B: The fully cleaved DFSSR3-C18 (5 μ L, 50 μ M) with Cu (1 eq., 2.5 mg/mL), and DTT (100 eq., 10 mM) was diluted in ISO-TRIS-NaCl (95 μ L, 10mM TRIS, 150mM NaCl, pH 2, 3, 4, 5, 6, 7, 7.8, 8, 9, 10 and 11 (HCl/NaOH)). Ex488nm and Em545nm, bandwidth: 20nm, Temp.: 22 °C (Std., n = 2).

Discussion:

Analysis of the excitation and emission properties of DFSS3R-C18 shows (Fig. 2A-E) that the construct functions as intended with a clear shift in the fluorescent emission to higher wavelength as the compound is activated/cleaved by DTT (Fig. 3). The fluorescence intensity is also found to increase upon activation of the construct. If the excitation wavelength is increased to more than 438 nm, the interference from the non-cleaved compound is found to be minimal. The linearity of the fluorescence standard curve is sufficient for both [Ex_{382 nm} and Em_{466 nm}] and [Ex_{438 nm} and Em_{545 nm}] down to 0.1 μ M on the given Tecan system. Low detection limits potentiate the detection in a post *in vivo* setting to determine bioavailability and intracellular localization of the Fluorophore-DOTA-chelators (DFS- and DFSS3R-C18, Fig. 4)).

The increase in fluorescence of the DFSS3R-C18 construct upon activation with either Cys or DTT was found to level off after 120min of incubation, indicating complete activation of the compound at this stage (Fig. 5). DTT was found to be more effective than Cys in activating DFSS3R-C18, leading to a higher conversion rate. The data (Fig.

4) further indicate that the fluorescent emission is positively affected by chelating Cu^{2+} to DFSSR3-C18.

5 Solvent polarity effects on the fluorescence emission intensity of the cleaved construct was further investigated, and fluorescence intensity was found to be unaltered in the presence of liposomes, i.e. lipid membranes does not change the emission intensity (Fig. 6). DMSO had a clear solvent induced effect leading to an increased emission intensity. As the cellular compartments have vastly differing pH values, the impact of pH was investigated for both the intact and cleaved construct. Changing the pH lead to no change in fluorescence intensity for the cleaved construct, whereas an increase in fluorescence emission intensity was observed for the intact construct above pH 8 (Fig. 7).

Conclusion:

15 The DFSS3R-C18 construct was shown to have the intended activation trigger, which led to increased fluorescence emission intensity upon activation.

Example 4: Radioactive labelling and EDTA challenge of D3R-C18 and DSS3R-C18

20 The aim of the current analysis was to quantify the radiolabelling efficiency of the ^{64}Cu -D3R analogues using radio-TLC and following determine the labelling stability of the D3R analogues by an EDTA challenge.

Method:

25 *TLC development and readout:* All TLCs were conducted on silica gel 60 F254 plates (Merck) using 5% NH_4OAc in $\text{H}_2\text{O}:\text{CH}_3\text{OH}$ (25:75) as eluent of ^{64}Cu -D3R-C18, ^{64}Cu -DSS3R-C18 and ^{64}Cu -EDTA. The radio-TLCs were measured using a phosphor imager (Cyclone Plus, PerkinElmer). The retention factors were found to be $\text{Rf}_{\text{Cu-D3R-C18}} = 0.4$, $\text{Rf}_{\text{Cu-DSS3R-C18}} = 0.3$ and $\text{Rf}_{\text{Cu-EDTA}} = 0.7$.

30 *Radiolabelling of D3R-C18 analogues:* The D3R analogues were prepared as 200 μM stock solution in ISO-TRIS-Sucrose buffer, and 1000 μL were following added to 164 MBq dry $^{64}\text{CuCl}_2$. The sample was heated and magnetically stirred at 55°C for 15-60 min. TLC samples were spotted as function of time. A 100 μL aliquot was following taken from each sample at 15 and 30 min, and the transferability (activity in solution) was

determined using a dose-calibrator (VDC-505, Comecer). The transferability in the ISO-TRIS-Sucrose buffer is seen in Table 1.

Further optimization of the radiolabelling of the DSS3R-C18. The analogue was prepared as 300 or 500 μ M stock solution in NH_4OAc solution (10 mM, pH 5.5) or (28 mM, pH 5.5), and 667 or 500 μ L respectively was following added to 116 MBq dry $^{64}\text{CuCl}_2$. The samples were heated and magnetically stirred at 55°C for 15-30 min or 30-80 min. Aliquots of 100 μ L were following taken from each sample at 15 and 30 min and the transferability (activity in solution) was determined using a dose-calibrator. A NaOAc solution (10 mM, pH 5.5) was also tested with 300 μ M stock solution of DSS3R-C18 with similar setup as previously mentioned. The transferability data of the NH_4OAc and NaOAc solutions are seen in table 2.

EDTA challenge: Aliquots of the radiolabelled micelles (100 μ L, 200 μ M) were transferred into a 1.5 mL HPLC vial, and 1.6 μ L EDTA (25 mM, pH 5.5) was spiked into the solution resulting in a final EDTA concentration of 0.39 mM. The samples were heated and magnetically stirred at 55°C for 5, 15 and 30 min, and following spotted on a TLC plate also containing a ^{64}Cu -EDTA reference and a no-EDTA reference.

20 Results:

The radiochemical purity and transferability were determined using TLC and dose-calibrator, and the results are compiled in table 1.

25 Table 1: Radiochemical purity (TLC) and transferability of ^{64}Cu -D3R analogues in ISO-TRIS-Sucrose buffer.

Entry	Buffer	Time [min]	TLC	Transferability	Overall radiolabelling efficiency
D3R-C18	ISO-TRIS- Sucrose	0	93%	-	-
		5	96%	-	-
		15	96%	-	-
		35	-	88%	-
		69	91%	98%	89%

DSS3R-C18	ISO-TRIS-Sucrose	0	9%	-	-
		5	88%	-	-
		15	88%	-	-
		20	-	78%	-
		33	88%	81%	71%
		35	-	86%	-
		69	78%	91%	71%

Radiolabelling of DSS3R-C18 was further optimized using OAc containing buffers to enhance the solubility Cu. The results are compiled in table 2.

5

Table 2: Radiochemical purity (TLC) and transferability of ^{64}Cu -DSS3R-C18 for various OAc containing buffers.

Entry	Buffer	Time [min]		TLC	Transferability	Overall radiolabelling efficiency
DSS3R-C18	NaOAc (10 mM)	18		93%	83%	77%
		33		93%	91%	85%
	NH ₄ OAc (10 mM)	18		92%	94%	87%
		33		92%	95%	87%
	NH ₄ OAc (28 mM)	30		94%	> 100%	> 94%
	ISO-TRIS-Sucrose	20		80%	78%	62%
		33		81%	81%	66%

10 The ^{64}Cu binding affinity of D3R-C18 and DSS3R-C18 was investigated by an EDTA challenge assay. In this assay, ^{64}Cu -D3R-C18 and ^{64}Cu -DSS3R-C18 were challenged by 1 equivalent of EDTA and changes in radiochemical purity was analysed using TLC. The results are compiled in table 3.

Table 3: TLC results from EDTA challenge Assay. The results are presented as the fraction of activity in TLC peaks corresponding to free ^{64}Cu , compound bound ^{64}Cu -D3R and ^{64}Cu chelated by EDTA.

Entry	Time [min]	^{64}Cu	^{64}Cu -D3R	^{64}Cu -EDTA
D3R-C18	5	1%	91%	8%
	15	1%	90%	9%
	30	1%	88%	11%
	-EDTA	9%	91%	-
DSS3R-C18	5	8%	77%	15%
	15	4%	76%	20%
	30	4%	76%	20%
	-EDTA	21%	79%	-

5

Discussion:

Radiolabelling of D3R-C18 and DSS3R-C18 in ISO-TRIS-Sucrose resulted in the highest radiochemical purity and transferability for ^{64}Cu -D3R-C18, with a maximum transfer of 98% and 96% in radiochemical purity (table 1). Optimization of the DSS3R-C18 radiolabelling procedure using OAc containing buffers increased the transferability to 100%, and the radiochemical purity increased to 94%. Highest transfer and radiochemical purity were obtained for the buffers with the highest content of OAc (table 2). The radiolabelling stability was investigated using an EDTA challenge assay, which demonstrated great stability for both the D3R-C18 and DSS3R-C18 compound, with a maximum of 3% change in radiochemical purity (table 3).

15

Conclusion:

D3R-C18 and DSS3R-C18 were effectively radiolabelled with ^{64}Cu and displayed great stability towards loss of ^{64}Cu in an EDTA challenge assay. The presence of OAc in the buffers increased the labelling efficiency.

20

Example 5: Membrane partitioning of D3R-C16/C18

The aim of the current analysis was to determine the lipid membrane partitioning properties of D3R-C16 and D3R-C18. The partitioning was evaluated for neutral, negatively charged and pegylated liposomal membranes for both constructs when chelating ^{64}Cu or ^{177}Lu as examples of di- and tri-valent cations.

Methods:

^{64}Cu production: ^{64}Cu was produced by proton irradiation of an electroplated ^{64}Ni target, and purified by anion exchange chromatography in aqueous HCl media. The ^{64}Cu was ultimately obtained in aq. HCl (1.0 M), and dried under argon flow for use in radiolabelling, as previously described.

Radiolabelling of D3R-C16 or D3R-C18: A micellar dispersion of D3R-C16 or D3R-C18 in ISO-HEPES-NaCl (2.0 mL, 200 μM) was added to dried $^{64}\text{CuCl}_2$ (about 300 MBq) or dried $^{177}\text{LuCl}_3$ (about 140 MBq). The resulting mixtures were magnetically stirred at 55 °C (with $^{64}\text{CuCl}_2$) or 90 °C (with $^{177}\text{LuCl}_3$) for 30 minutes. The formation of the ^{64}Cu -D3R-C16 and ^{64}Cu -D3R-C18 complexes was confirmed by comparing the obtained retention factor ($R_f = 0.30 - 0.40$, and $R_f = 0.40 - 0.50$, respectively) with that of a non-radioactive chemically identical reference compound. All radio-TLC analyses were performed on silica gel 60 F254 plates (Merck). 5% (w/v) ammonium acetate (NH_4OAc) in water-methanol (1:3) was used as eluent for ^{64}Cu -D3R-C16 and ^{64}Cu -D3R-C18, and 5% (w/v) ammonium acetate (NH_4OAc) in water-methanol (1:1) was used as eluent for ^{64}Cu -DOTA, ^{64}Cu -EDTA, ^{177}Lu -D3R-C16 and ^{177}Lu -D3R-C18. The radiochemical purity (RCP) was > 95%, for all samples.

Preparation of liposomes for membrane partitioning studies: Three different liposomes types were prepared: 1) POPC only, 2) POPC-POPG (9:1, w/w), 3) commercially available stealth lipid mixture. POPC or the POPC-POPG mixture was freeze-dried from tert-butanol:water (9:1). The resulting lyophilizates or the stealth lipid mixture (187.5 mg) was then hydrated with ISO-HEPES-NaCl (5.0 mL) at 65 °C for 60 minutes by magnetically stirring. Liposomes were prepared using a mini-extruder (Avanti Polar Lipids) or a LIPEX Thermobarrel Pressure Extruder (10 mL, Northern Lipids). The hydrodynamic size and zeta potential of liposomes were measured by dynamic light scattering (DLS) on a Zetasizer (Malvern) based on intensity with normal size distribution. The size was measured by dynamic light scattering (DLS) in ISO-HEPES-

NaCl and the zeta potential was measured in ISO-HEPES-Sucrose. Lipid concentration was measured by ICP-MS (Thermo Scientific, iCAP Q). The phosphorous concentration of each liposome sample was measured by ICP-MS (Thermo scientific) with an internal standard of Gallium (10 ppb). This was followed by sizing through a mini-extruder with a cut-off size of 100 nm. Size, polydispersity index (PDI) and zeta potential of all three preparations were POPC (size 120.6 ± 0.3 nm, PDI 0.040, zeta potential 2.3 ± 0.6 mV), POPC+10%POPG (size 129.6 ± 0.9 nm, PDI 0.07, zeta potential 49.1 ± 0.6 mV) and stealth (size 134.2 ± 0.8 nm, PDI 0.05, zeta potential 2.7 ± 0.3 mV). The liposomes were diluted to lipid concentrations of 0.4, 1.0 and 4.0 mM for partitioning studies.

Partitioning of D3R-C16 and D3R-C18 radiolabelled with ^{64}Cu or ^{177}Lu into liposomes

The kinetics of partitioning ^{64}Cu -D3R-C16 or ^{64}Cu -D3R-C16 into liposomes were studied in order to assess the equilibrium time of the process. A dispersion of ^{64}Cu -D3R-C16 (200 μM) in ISO-HEPES- NaCl (100 μL) was added to POPC liposomes (900 μL , 0.4 mM). The resulting mixture was magnetically stirred at 37 °C. Aliquots were analyzed by size-exclusion chromatography (SEC) at 10, 30, 60, 120 and 180 minutes after addition. The mixture (100 μL) was applied to a PD-10 cartridge and eluted with ISO-HEPES-NaCl. Two consecutive fractions of 5.5 and 4.5 mL were collected. The radioactivity of the two collected fractions and the column were measured by dose calibrator (VDC-505 Comecer). The liposome fraction eluted in the first 5.5 mL, whereas free ^{64}Cu -D3R-C16 and ^{64}Cu -D3R-C18 were retained by the column. The partitioning of the radiolabeled constructs into liposomes was calculated as the ratio of the radioactivity of the liposomes fraction to the total radioactivity of the fraction of liposomes and the column.

Next, the partitioning of ^{64}Cu -D3R-C16 and ^{64}Cu -D3R-C18 into liposomes with different lipid compositions and different concentrations was studied. A dispersion of ^{64}Cu radiolabeled D3R-C16 or D3R-C18 (200 mM, about 6 MBq) in ISO-HEPES-NaCl (30 μL) was added to POPC, POPC-POPG (9:1) or stealth liposomes (270 μL , 0.4 mM, 1.0 mM or 4.0 mM) respectively. The resulting mixtures were magnetically stirred at 37 °C for 60 minutes. The mixtures were analyzed by SEC by applying 200 μL to a PD-10 cartridge (see above). The liposome fraction eluted in the first 5.5 mL, whereas free ^{64}Cu -D3R-C16 and ^{64}Cu -D3R-C18 were retained on the column.

An ISO-HEPES-NaCl dispersion containing the ^{177}Lu -D3R-C16 (30 μL , 200 μM) or ^{177}Lu -D3R-C18 (30 μL , 200 μM) was added to stealth liposomes (270 μL , 0.4 mM, 1.0 mM or 4.0 mM). The resulting mixtures were magnetically stirred at 37 °C for 60 minutes. The

mixtures were analyzed by SEC by applying 200 µL to a PD-10 cartridge using similar collection principle as for the ^{64}Cu radiolabelled analogues.

Results and discussion

5 The kinetics of the partitioning were initially assessed in order to elucidate the incubation time needed for reaching partitioning equilibrium. ^{64}Cu -D3R-C16 was incubated at 37 °C with POPC liposomes at a relatively low lipid concentration of 0.36 mM. The partitioning equilibrium was reached within 10-30 minutes. Consequently, the total incubation time in subsequent studies was set to 60 minutes to ensure equilibrium.

10

Fig. 8 shows the partitioning into liposomes of ^{64}Cu -D3R-C16 (A) and ^{64}Cu -D3R-C18 (B). Comparison of liposome partitioning of D3R-C16 (C) and D3R-C18 (D) labelled with $^{64}\text{Cu}^{2+}$ or $^{177}\text{Lu}^{3+}$. The results are presented as mean \pm SEM, n = 3.

15

Cu-64 labelled D3R-C16 and D3R-C18 were found to partition into POPC, POPC+POPG and stealth liposomes in a concentration dependent manor, i.e. higher lipid concentration led to higher degree of partitioning as a response to increase of the oil like phase. The D3R-C18 analogue exhibited the highest degree of partitioning as expected due to the longer and more hydrophobic acyl chain. Both analogues displayed higher degree of partitioning into negatively charged membranes (POPC+POPG and stealth) having negative zeta potentials, which is expected to be governed by electrostatic interactions of the membrane and arginine sequence on the D3R analogues. Similar degree of partitioning was observed for ^{64}Cu and ^{177}Lu labelled D3R-C16, whereas slightly higher degree of partitioning was observed for ^{177}Lu -D3R-C18 compared to ^{64}Cu -D3R-C18.

20

Conclusion

25 In conclusion, both D3R analogues partition into lipid membranes in a concentration dependent manor and thereby interact similarly with membranes as detergents. The D3R analogues display higher affinity for negatively charged membranes and also partition
30 into pegylated membranes. Higher degree of partitioning is obtained by increasing the acyl-chain from C16 to C18.

Example 6: Murine lymphocytes and human leukocytes tolerate incubation with high concentrations of cationic micelles

The aim of this example was to investigate micelle concentrations of DFSS3R-C18 that are tolerated by murine lymphocytes and human leukocytes during incubation.

5

Methods:

Micelle preparation: The micelles were made by dissolving the fluorescent DFSS3R-C18 analogue (200 μ M) in ISO-HEPES-Glucose buffer (10 mM:5 w%, pH 7.8), adding CuCl_2 (2.5 mg/mL, 1 eq.), and heating the sample at 55 °C for 30 min with magnetic stirring.

10

In a 96-well plate murine T lymphocytes (50×10^6 cells/mL) in serum free RPMI media were added DFSS3R-C18 at increasing concentrations (0 – 100 μ M) for a total well volume of 100 μ L. Cells were incubated with micelles for 1 hour at 37 °C/5% CO_2 . After the incubation period cells were washed 3 times with 100-150 μ L FACS buffer (PBS, 10 % bovine serum albumin, 0.1% NaN_3 , 0.5M EDTA). For washing steps cells were centrifuged at 600xg (4°C, 3 minutes) and supernatant was decanted. Cell concentration of the samples was determined using MUSE® Cell Count and Viability Assay on a MUSE® Cell Analyzer (MERCK Millipore) according to the manufacturer's guidelines. Fixable Viability Dye eFluor™780 from eBioscience™ was used to assess viability and stained in FACS buffer 15 minutes at RT. Samples was run on a 4-laser LSR II Fortessa x-20. After completion of washing steps cell viability, percentage of cells positive for DFSS3R-C18 and mean fluorescence intensity (MFI).

15

20

Results:

25

Both human leukocytes and murine T lymphocytes display high uptake of DFSS3R-C18 micelles with increasing percentage of positive cells with increasing micelle concentrations in the incubation step. Both murine T lymphocytes and human leukocytes displayed decreasing viability when incubated with increasing micelle concentration during incubation (Fig. 9A-B). Fig. 9 shows the flow cytometric characteristics of murine T lymphocytes (A) and human leukocytes (B) displaying loading efficiency in terms of mean fluorescence intensity (MFI) and percent positively labelled cells (% DFSS3R-C18+) and fraction of viable cells (% Viability) after incubation with DFSS3R-C18 at increasing concentrations.

30

35

Discussion:

Cationic micelles composed of DFSS3R-C18 were demonstrated to be loaded efficiently into both murine T lymphocytes and human leukocytes with increasing number of DFSS3R-C18 positive cells and increased mean fluorescence intensity (MFI) with increasing micelle concentration during incubation. The observed decrease in viability with increasing micelle concentrations during incubation indicates that micelle incubation concentrations must be adjusted to provide an optimal trade of between loading efficiency, imaging possibilities and cell viability.

Conclusion:

The DFSS3R-C18 micelle formulation is an effective methodology to label murine T lymphocytes and human leukocytes *in vitro*. Concentration of micelles during incubation is preferably adjusted to achieve optimal loading efficiency and fluorescence properties.

Example 7: Shorter incubation periods can improve murine T lymphocyte survival without influencing cell uptake and labelling

The aim of the current example was to investigate the influence of incubation period on T lymphocyte DFSS3R-C18 labelling.

Methods:

Micelles were prepared as described in example 6.

In a 96-well plate murine T lymphocytes (50×10^6 cells/mL) in serum free RPMI media were added DFSS3R-C18 at increasing concentrations (0 – 100 μ M) for a total well volume of 100 μ L. Cells were incubated with micelles for different timepoints at 37 °C/5% CO₂. After the incubation period cells were washed 3 times with 100-150 μ l FACS buffer (PBS, 10 % bovine serum albumin, 0.1% NaN₃, 0.5M EDTA). For the washing steps cells were centrifuged at 600xg (4°C, 3 minutes) and supernatant was decanted. Cell concentration of the samples was determined using MUSE® Cell Count and Viability Assay on a MUSE® Cell Analyzer (MERCK Millipore) according to the manufacturer's guidelines. Fixable Viability Dye eFluor™780 from eBioscience™ was used to assess viability and stained in FACS buffer 15 minutes at RT. Samples was run on a 4-laser LSR II Fortessa x-20. After completion of the washing steps, the cell viability, percentage of cells positive for DFSS3R-C18 and mean fluorescence intensity (MFI) was recorded.

Results:

Murine T lymphocytes displayed increased viability with decreased incubation period without a compromised labelling efficiency or decreased fluorescence properties (Fig. 10A-C). Fig. 10 shows that murine T lymphocytes display increased viability at shorter incubation periods for all DFSS3R-C18 micelle concentrations investigated (A). The percentage of murine T lymphocytes positive for DFSS3R-C18 fluorescent signal is comparable between incubation periods of 20 minutes and 60 minutes across the investigated micelle concentrations (B). Mean fluorescence intensity is comparable between murine T lymphocytes incubated for 20 minutes, 40 minutes and 60 minutes (C).

Conclusion:

Murine T lymphocytes display increased viability with shorter incubation periods and the shorter incubation period displays no negative influence on cellular uptake efficiency and uptake levels. The shorter incubation period provides improved labelling of murine T lymphocytes.

Example 8: Saturation of DOTA-chelator with copper improved viability of cells during cell labelling

The aim of this examples was to investigate the influence of D3R-C18 and D3R-C16 on the viability of murine T lymphocytes during labelling with and without copper present in the DOTA chelator of the constructs.

Methods:

D3R-C16 and D3R-C18 micelles were prepared by dispersion in ISO-HEPES-NaCl at 100 μ M concentration with and without 1 equivalent of copper (CuCl_2). The copper chelate formation was facilitated by heating and stirring at 55°C for 30 min.

Murine T lymphocytes (10×10^6 cells/500 μ L) in serum free RPMI media were incubated with D3R-C18 or D3R-C16 at micelle concentrations ranging from 5 μ M – 50 μ M for 1 hour at 37 °C/5% CO_2 . After the incubation period cells were washed 3 times with 100-150 μ l FACS buffer (PBS, 10 % bovine serum albumin, 0.1% NaN_3 , 0.5M EDTA). For washing steps cells were centrifuged at 600xg (4°C, 3 minutes) and supernatant was decanted. Cell concentration of the samples was determined using MUSE® Cell Count and Viability Assay on a MUSE® Cell Analyzer (MERCK Millipore) according to the

manufacturer's guidelines. Fixable Viability Dye eFluor™780 from eBioscience™ was used to assess viability and stained in FACS buffer 15 minutes at RT. Samples was run on a 4-laser LSR II Fortessa x-20. After completion of washing steps cell viability, percentage of cells positive for DFSS3R-C18 and mean fluorescence intensity (MFI).

5

Results:

DOTA-chelator saturation with copper is important to maintain viability of the cells to be labelled using with D3R-C18 and D3R-C16 micelles. Cellular viability was stable for micelle formulations having saturated DOTA-chelators whereas micelles with empty DOTA-chelator displayed increased cytotoxicity with increasing micelle concentrations (Fig. 10). Fig. 11 shows the viability of murine T lymphocytes incubated for 1 hour with D3R-C18 or D3R-C16 micelles with saturated (+Cu) DOTA-chelator and unsaturated chelator.

10

Discussion:

Copper saturation of DOTA-chelators on micelles has been demonstrated to be central for viability of the cell population being labelled. Saturation of chelators must be secured during the radiolabelling steps of micelle formulation before any cellular labelling procedures are performed.

15

Conclusion:

DOTA-chelator saturation with copper is central for maintaining cellular viability during micelle labelling procedures.

20

Example 9: Murine T lymphocytes display increasing viability with increasing cellular concentrations during incubation

The aim of this example was to determine optimal cellular concentrations during labelling of murine T lymphocytes with DFSS3R-C18.

25

Methods:

Murine T lymphocytes were labelled with DFSS3R-C18 (40 µM) at increasing cellular density (0.1×10^6 – 50×10^6 cells/mL) in 96 well plates with a volume 100µL/well in serum free RPMI media and an incubation period of 1 hour at 37 °C/5% CO₂. After the incubation period cells were washed 3 times with 100-150 µl FACS buffer (PBS, 10 % bovine serum albumin, 0.1% NaN₃, 0.5M EDTA). For washing steps cells were

30

centrifuged at 600xg (4°C, 3 minutes) and supernatant was decanted. Cell concentration of the samples was determined using MUSE® Cell Count and Viability Assay on a MUSE® Cell Analyzer (MERCK Millipore) according to the manufacturer's guidelines. Fixable Viability Dye eFluor™780 from eBioscience™ was used to assess viability and stained in FACS buffer 15 minutes at RT. Samples was run on a 4-laser LSR II Fortessa x-20. After completion of washing steps cell viability, percentage of cells positive for DFSS3R-C18 and mean fluorescence intensity (MFI).

Results:

Murine T lymphocytes demonstrated an increased viability with increasing cellular concentration. Increasing cellular concentrations display low influence percentage of cells positive for fluorescence signal whereas mean fluorescence intensity decreased with increasing cell density during incubation (Fig. 12). Fig. 12 shows the influence of cellular density of murine T lymphocytes during incubation with DFSS3R-C18 at a micelle concentration of 40 µM on cellular viability (% viability), percentage cells positive for fluorescent signal (% DFSS3R-C18 +) and mean fluorescence intensity (MFI). The viability of unloaded control was 81.5%. 0% viability was obtained at a cell density of 0.1×10^6 and 10^6 cells/mL.

Discussion:

Increased cellular density/concentration seems to improve cell survival during the incubation period without negatively affecting the percentage of cells successfully labelled. Labelling intensity seems to be reduced slightly with increased cellular concentrations.

Conclusion:

Murine T lymphocytes are optimally loaded at high cellular densities as this secures a high viability and maintains high percentage of cells positively labelled.

Example 10: Radiolabelling murine cytotoxic T lymphocytes with ^{64}Cu -D3R-C18 or ^{64}Cu -DSS3R-C18

The aim of the current example is to investigate the loading efficiency of ^{64}Cu -D3R-C18 or ^{64}Cu -DSS3R-C18 in murine T lymphocytes.

Methods:

Murine T lymphocytes (50×10^6 cells/mL) in serum free RPMI media were incubated with ^{64}Cu -D3R-C18 (200 μM , 5.60 MBq/mL) or ^{64}Cu -DSS3R-C18 (200 μM , 5.65 MBq/mL) at micelle concentrations 20, 40, 60 μM and on average 56, 112 and 169 kBq ^{64}Cu in 2 ml eppendorf tubes for 30 minutes at 37 °C/5% CO_2 . After incubation cells were washed 3 times with 1.5-2 ml RPMI without serum. For washing steps cells were centrifuged at 600xg (4°C, 3 minutes) and supernatant was decanted. Specific radioactivity was determined for T lymphocytes by gamma counting (Wizard2, Perkin Elmer, Branford, CT, USA) using an isotope specific and decay corrected counting protocol. Cell concentration of the samples was determined using MUSE® Cell Count and Viability Assay on a MUSE® Cell Analyzer (MERCK Millipore) according to the manufacturer's guidelines. The loading efficiency was then determined as the activity of the T lymphocyte fraction divided by the total activity applied to the cells.

Results:

Table 4: Loading efficiency in the T lymphocytes following incubation for 30 min with three different concentrations of the micelle formulations listed. The loading efficiency was determined following 30 min loading and three subsequent washes of the T lymphocytes. Mean and SD are listed (n = 3).

D3R-analogue	Micelle concentration		
	20 μM	40 μM	60 μM
^{64}Cu -D3R-C18	$38.7 \pm 4.4\%$	$30.7 \pm 1.2\%$	$26.3 \pm 2.1\%$
^{64}Cu -DSS3R-C18	$37.3 \pm 2.5\%$	$32.9 \pm 5.5\%$	$32.5 \pm 0.6\%$

Discussion:

The loading efficiency was comparable between the D3R analogues with a tendency of higher loading efficiency at 20 μM compared to 40 and 60 μM concentrations for both micelle formulations. The largest drop in cell labelling efficiency of 12% was obtained for the D3R-C18, whereas DSS3R-C18 only decreased 5% upon increasing the micelle concentration from 20 μM to 60 μM .

Conclusion:

In conclusion, both ^{64}Cu -D3R-C18 and ^{64}Cu -DSS3R-C18 were taken up by T lymphocytes to a similar extent. On average, more than 1/3 of the activity was taken up by the cell for the lowest micelle concentration.

5

Example 11: Murine T lymphocytes radiolabelled using ^{64}Cu -D3R-C18 displays high retention of their radiolabel during co-culture with murine splenocytes

Aim: Investigate the retention stability of murine T lymphocytes radiolabelled using ^{64}Cu -D3R-C18.

10

Methods:

50 x 10⁶ cells/mL murine T lymphocytes were radiolabelled using 50 μM ^{64}Cu -D3R-C18 micelles in 50 ml Falcon tubes incubation period of 1 hour at 37 °C/5% CO₂. Spleens were isolated from an autologous donor mouse and passed through 70 μm filters (Corning and Sigma-Aldrich, Søborg, Denmark) to achieve single cell solution of splenocytes and washed with 40 ml PBS 400xg (4°C, 8 minutes). Erythrolysis was performed with versalyse (Beckman Coulter, Denmark) according to protocol and passaged through a 70 μm filter with a subsequent wash 400xg (4°C, 8 minutes). Splenocytes were then stained with CellTrace™ Violet Cell proliferation Kit according to protocol. Flow cytometry analysis confirmed >99% cell-trace⁺ splenocytes (data not shown). The radiolabelled murine T lymphocytes were co-incubated with autologous splenocytes at a ratio of 1:1 at 37 °C/5% CO₂ for 2 hours in RPMI media with 10% serum (FCS). The combined cell population of the co-culture was divided into cell trace positive (splenocyte fraction) and cell trace negative (micelle labelled murine T lymphocytes) by FACS using BD FACSmelody (BD Bioscience). Cell concentration of the samples was determined using MUSE® Cell Count and Viability Assay on a MUSE® Cell Analyzer (MERCK Millipore) according to the manufacturer's guidelines. Specific radioactivity was then determined for T lymphocytes and splenocytes by gamma counting (Wizard2, Perkin Elmer, Branford, CT, USA) using an isotope specific and decay corrected counting protocol.

30

Results:

The splenocyte fraction (cell trace positive) displayed more than 10 times lower specific radioactivity in comparison to the original radiolabelled murine T lymphocyte fraction (cell trace negative) (Fig. 13). Fig. 13 shows murine T lymphocytes that were radiolabelled

35

using ^{64}Cu -D3R-C18 micelles and co-incubated with cell trace stained splenocytes for 2 hours. After co-incubation cell population were sorted by FACS based on cell trace staining. The sorted population were gamma counted to determine specific radioactivity in each population.

5

Discussion:

Retention of transferred radioactivity by the radiolabelled micelles is central for the *in vivo* applicability of the technology. It has been demonstrated that even during a two-hour co-incubation with a mixed cell population (splenocytes) containing multiple cell populations with a high phagocytic potential only very low amounts of radioactivity are observed in this population in comparison to the originally labelled T lymphocytes. Considering that T lymphocytes are continually dying, and that cellular debris or micelles in the media can be taken up by splenocyte populations, only extremely limited transfer can occur directly indicating that high retention in originally labelled cells.

15

Conclusion:

T lymphocytes display high retention of ^{64}Cu transferred by labelling with ^{64}Cu -D3R-C18 micelles.

20 **Example 12: Radiolabelled ^{64}Cu -D3R-C18 micelles murine T lymphocytes homes to the thymus in lymphodepleted mice**

The aim of this example was to demonstrate that murine T lymphocytes radiolabelled with ^{64}Cu -D3R-C18 micelles *in vitro* locate to the thymus when adoptively transferred into mice that have been lymphodepleted by whole body irradiation.

25

Methods:

Murine T cells (C57BL/6) were radiolabelled with ^{64}Cu -D3R-C18 micelles as described in example 10.

Female C57BL/6 mice were divided into two groups (N=3). Mice in group 1 were whole body irradiated with 5 Gy using a small animal dedicated irradiator (320kV/12.5mAs, 1Gy/min, Xrad, pXi Inc, CT, USA). Mice in group 2 served as unirradiated controls. Mice were injected with 5×10^6 radiolabelled murine T lymphocytes 24 hours after irradiation. PET/CT scans were performed at 1, 16, and 40 hours after injection of radiolabelled T lymphocytes using a dedicated small animal PET/CT scanner (Inveon, Siemens Medical Systems, Erlangen, Germany). Image analysis was performed using commercially

35

available Inveon software (Siemens Medical Systems, Malvern, PA, USA). Regions of interest (ROIs) were manually drawn based on the co-registered PET/ CT images.

Results:

5 In whole body irradiated lymphodepleted mice high ^{64}Cu activity was observed in the thymus whereas corresponding control mice displayed significantly lower activity (Fig. 14). Fig. 14 shows ^{64}Cu -D3R-C18 micelle labelled T cells (5×10^6 Murine T lymphocytes) that were injected intravenously in mice 24 hours after 5Gy whole body irradiation and compared to untreated controls by PET/CT scanning 16 and 40 hours after injection of
10 T cells. Mice having received whole body irradiation displayed activity in thymus (5Gy TBI, dashed ellipse) whereas un-irradiated controls did not display accumulation in the thymus (Control, dashed ellipse). Whole body irradiated mice displayed significantly higher ($p < 0.05$) compared to un-irradiated mice at PET scans performed 16 and 40 hours after injection of ^{64}Cu -D3R-C18 micelle labelled T cells (C), un-paired t-test.

15

Discussion:

In lymphodepleted mice, it has been demonstrated that adoptively transferred T lymphocytes locates to the thymus. The observed activity in the thymus of lymphodepleted mice therefore demonstrates that T lymphocytes radiolabelled using the
20 ^{64}Cu -D3R-C18 micelles displays a T lymphocyte specific behaviour which demonstrates that; the radiolabel is retained and the T lymphocytes maintain cell line specific characteristics/activity.

Conclusion:

25 The observed homing indicates that the technology enables T lymphocytes without compromising their functionality in terms of homing to the thymus in lymphodepleted animals.

Example 13: In vitro uptake and accumulation of DFSS3R-C18 in HT1080 cells evaluated by live cell microscopy

30

The aim of the current example was to visualize the uptake of the fluorescent DFSS3R-C18 analogues in HT1080 cancer cells using confocal spinning disc microscopy. The cellular uptake was investigated for DFSS3R-C18 with and without complexation of copper.

35

Method:

DFSS3R-C18 was dissolved in ISO-HEPES-Glucose buffer (10 mM:5w%, pH 7.4) at a concentration of 200 μ M. A batch of copper labelled DFSS3R-C18 was prepared by incubation of DFSS3R-C18 (5.32 mL, 200 μ M) mixed with CuCl₂ (58 μ L, 2.5 mg/mL in Millipore H₂O) at 55 °C for 30 min.

15.000 HT1080 cells was seeded in 300 μ L full growth medium in each well of an Ibidi 8 well microscopy chamber and incubated for 24 hours (37 °C, 5 % CO₂). To 300 μ L fresh medium 37.5 μ L of either 1) DFSS3R-C18, 2) Cu-DFSS3R-C18 or 3) medium was added for a final concentration of 12.5 μ M. After 1 hour incubation the cells were washed 2x with Fluorobrite DMEM Medium and imaged using 405nm excitation and a quad band emission filter on an inverted Nikon Ti2 spinning disc confocal microscope equipped with a sCMOS camera. Z-stacks of whole cells were acquired and maximum intensity projection (MIP) were produced for visualization.

Results:

Fig. 15 shows the bright field and MIP (maximum intensity projection) images of HT1080 cells in the presence of no micelles, DFSS3R-C18 or Cu-DFSS3R-C18.

Discussion:

A strong cellular uptake was detected for both DFSS3R-C18 and Cu-DFSS3R-C18. Both systems showed minimal plasma membrane labelling, but a clear localization in puncta like structures inside cells. This indicates that the micelles are taken up through an endocytic pathway and resides in intracellular organelles, potentially endo- and/or lysosomes.

Conclusion:

After 1 hour of incubation both DFSS3R-C18 and Cu-DFSS3R-C18 show a strong intracellular signal from puncta like structures, indicating endocytic uptake.

Example 14: Study on the in vitro uptake and retention kinetics of DFSS3R-C18 in HT1080 cells evaluated using spinning disc microscopy of fixed cells

The aim of the current example was to quantify the uptake and retention kinetics of the fluorescent DFSS3R-C18 analogue in fixed HT1080 cancer cells using confocal spinning disc microscopy.

Methods:

Micelles were prepared as in example 6.

15.000 HT1080 cells was seeded in 300 μ L full growth medium in each well of an Ibidi 8 well microscopy chamber and incubated for 24 hours (37 °C, 5 % CO₂). To 300 μ L fresh
5 medium, 6 μ L of D3RF-SS-C18 or blank medium was added for a final micelle concentration of 4 μ M. For the kinetic uptake study cells were incubated for 3, 6, 12, 24 or 48 hours before they were fixed using 4 % paraformaldehyde and following standard protocols. For the retention study cells were incubated with DFSS3R-C18 for 24 hours, before exchanging to non-micelle containing medium and fixing cells after additional 24
10 hours (denoted 24 h + 24 h in the Fig. below). Cell were imaged using bright field and 488 nm laser excitation and a quad band emission filter on an inverted Nikon Ti2 spinning disc confocal microscope equipped with a sCMOS camera. Z-stacks of whole cells were acquired and summed intensity projection micrographs were produced. To quantify the DFSS3R-C18 uptake and retention, bright field images were used for outlining cells and
15 the intracellular average pixel (Int_{AvrPix}) intensity for the DFSS3R-C18 channel was calculated for each individual cell. The mean Int_{AvrPix} was found by fitting a gaussian function to the histogram of the cellular Int_{AvrPix} values. Next the mean Int_{AvrPix} was plotted for the various incubation and retention time points.

Results:

20 Fig. 16 shows in A: Summed intensity projection images of HT1080 cells after incubation with either no micelles, DFSS3R-C18 for 12 and 48 hours or DFSS3R-C18 for 24 hours and then 24 hours in non-micelle medium; and in B: Histogram depicting the Int_{AvrPix} histogram for 114 individual cells and the mean Int_{AvrPix} quantified using the gaussian fit.
25 C: Mean Int_{AvrPix} for the no micelle control, various incubation times and the retention after 24 hour incubation with and without micelles.

Discussion:

The kinetic uptake study revealed increased uptake for increasing incubation time, with
30 a 1.6 fold higher mean Int_{AvrPix} for 48 hours versus 3 hour incubation. Interestingly, even at 48 hours the uptake did not seem to have reached saturation. For the 24 h + 24 h retention study, a significant reduction in the intracellular level of DFSS3R-C18 could be detected as compared to the 24 h measurement, however micelles were still clearly visible with an Int_{AvrPix} value comparable to the one quantified for the 6 hour incubation.

Conclusion:

DFSS3R-C18 displays an incubation time dependent uptake in HT1080 cells, even for incubation periods up to 48 hours. Also, the DFSS3R-C18 is retained inside HT1080 cells at significant levels even after 24 hours incubation in medium without micelles.

5

Example 15: Labeling of T cells does not change their phenotype

The aim of the current example was to investigate the effect of labeling T cells using D3R-C18 cationic micelles. For this purpose, the phenotype of CD8⁺ T cells was investigated using flow cytometry.

10

Methods:

D3R-C18 micelles (200µM) were prepared in ISO-TRIS-Sucrose buffer.

15

CD8⁺ T cells were isolated from spleens of a C57BL/6 -Tg(TcraTcrb)100Mjb/J (OT.1) mice using a negative selection kit (CD8⁺ T Cell Isolation Kit, Milteny). T cells were then loaded in serum free RPMI media for 2 hours at 37°C with 40 µM D3R-C18 micelles. Subsequently the T cells were washed with PBS and cultured in complete RPMI medium for three days (n=6). The T cells were harvested and analyzed with an LSR Fortessa X20 and compared to an unloaded T cell population (n=6). The panel used for analysis is shown in table 4.

20

Table 4: Fluorochromes and targets used to characterize T cell phenotypes.

Fluorochrome	Target
BV421	PD1
BV480	CD44
BV650	CD4
BV786	CD11c
BB515	CD8
PE	CD3
PE-Cy7	CD62L
eFluor 780	Dead cells

25

Results

The D3R-C18 micelles did not change the composition of T cell population following IL-2 and CD3/CD28 activation (central memory, effector memory). The findings are shown in fig. 17 as % positive and MFI of PD1 expression. Furthermore, the viability of the T cells did not change following D3R-C18 loading.

Conclusion:

D3R-C18 labeling does not change viability or activation phenotype of T cells following 72 hrs incubation.

Example 16: Proportionality between radioactivity and T-cell numbers

The aim of the current example was to investigate the correlation between the number of infused radiolabeled T cells in a mouse, and the organ specific radioactivity acquired by well counting and PET imaging.

Methods:

Murine CD8+ T cells were collected as described in Example 15.

Radioactive D3R-C18 micelles were prepared in ISO-TRIS-Sucrose buffer as described in Example 4.

Murine CD8+ T cells were labeled with 40 μ M of the D3R-C18 construct in serum free media for 20 min at 37°C and then washed 3 times. Mice were injected intravenously with the loaded T cells either 1, 5 or 10 million cells in 100 μ L. After 24 hours, mice were PET/CT scanned as described in example 12. After scanning the mice were culled and thymus, spleen and tumor were harvested and their radioactivity measured with a well counter (Wizard2, Perkin Elmer).

Results:

The activity in the thymus, spleen and tumor was quantified by whole-organ well counting and the results are presented as function of the number of infused T cells in Figure 18A-E. PET scans were acquired 24 hours post infusion of radiolabeled T cells, and the activity per organ ROI is reported as the activity ratio obtained for 5 and 10 million cells in Figure 18D.

Conclusion

The radioactivity recorded by well counting the thymus, spleen and tumor increases proportionally with the number of injected radiolabeled T cells. This indicate that radioactivity and injected T cells display linearity between the accumulated number of T cells and organ radioactivity, i.e. the radioactivity provides a relative measure of the T cell distribution *in vivo*.

Example 17: PET imaging of the in vivo biodistribution of ⁶⁴Cu-D3R-C18 radiolabeled murine T-cells

The aim of the current example was to investigate the biodistribution of murine T cells in mice using copper-64 radiolabeled D3R-C18 cationic micelles for tracking. The biodistribution of free ⁶⁴Cu-D3R-C18 micelles were compared to T cells radiolabeled with ⁶⁴Cu-D3R-C18.

Methods

Murine CD8+ T cells were collected as described in Example 15.

Radioactive D3R-C18 micelles were prepared in ISO-TRIS-Sucrose buffer as described in Example 4.

50 million/mL murine CD8+ T cells were loaded with 40 μM of the radiolabeled D3R-C18 construct in serum free media for 2 hours at 37°C and then washed 3 times before resting them in complete medium for 2 hours at 37°C. Cells were then harvested and 10 million cells injected i.v. into CT26 tumor bearing mice. The mice (n=6) were dynamically PET/CT scanned after the injection and following scans were recorded at 1 h, 3 h and 18 h post infusion of T cells or D3R-C18 control micelles. The PET/CT data were acquired and processed as described in example 12. Data are presented as percent injected dose per cm³ (Mean ± SEM). The total body radioactivity was quantified by manually constructing a large region of interest covering the complete body volume (based on CT).

Results

PET/CT data were acquired for mice injected with either T cells labeled with ⁶⁴Cu-D3R-C18 or ⁶⁴Cu-D3R-C18 micelles as control. The results are presented in Figure 19A-G.

The total whole-body radioactivity was normalized to t=0 and is presented in Figure 19G.

Conclusion

5 The D3R-C18 radiolabeled T cells provides information of in vivo biodistribution and pharmacokinetics. The difference in biodistribution and pharmacokinetics between free micelles and T cells loaded with radiolabeled micelles demonstrate that radioactivity is not lost as free micelles.

10 **Example 18: T-cell tumor infiltration in response to sustained release depot of a TLR7 agonist (immunogel) treatment**

The aim of the current example is to follow the T cell tumor infiltration in response to intratumoral sustained delivery of a TLR7 agonist stimulating intratumoral T cell recruitment. The T cell infiltration will be monitored using PET/CT scanning of T cells
15 labeled with ^{64}Cu -D3R-C18.

Methods

Murine CD8+ T cells were collected as described in Example 15.

20 Radioactive D3R-C18 micelles were prepared in ISO-TRIS-Sucrose buffer as described in Example 4.

50 million/mL CD8+ T cells were labeled for 2 hours at 37°C with ^{64}Cu -D3R-C18, and then washed 3 times with RPMI before injecting 10 million labeled cells i.v. in 100 μL
25 into tumor bearing mice. an intratumoral injection of a sustained release depot containing TLR7 agonist was performed 24 hours prior injecting the T cells. Mice were PET/CT scanned 40 hours after adoptive T cell transfer including controls not receiving intratumoral TLR7 agonist depot. The PET/CT data were acquired and processed as described in example 12. Data are presented as percent injected dose per cm^3 (Mean \pm
30 SEM).

Results:

The increased tumor recruitment of T cells following intratumoral TLR7 agonist administration is demonstrated by PET/CT imaging of radiolabeled T cells. Figure 20

demonstrate the increased tumor activity (mean and maximum activity) after TLR7 agonist treatment compared to non-injected tumor.

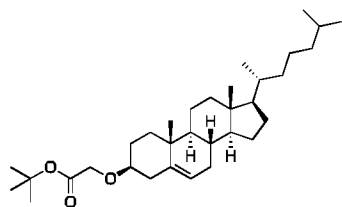
Conclusion

5 T cells accumulation can be used to demonstrate adjuvant therapy influence on radiolabeled T cell homing and accumulation. The radiolabeled T cells provide a theranostic tool for evaluating immunotherapies including adoptive cell transfers and therapies aiming at improving T cell infiltration in cancerous tissues.

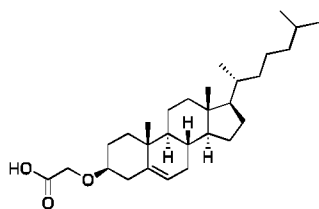
10 **Example 19: Synthesis of D3R-Chol**

The aim of the current example was to synthesize the DOTA triarginine cholesterol derivate, D3R-Chol.

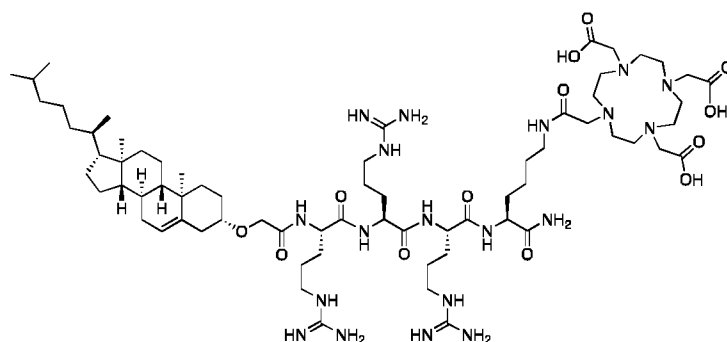
Synthesis



15 Tert-butyl cholesteroxy-acetate. NaH (33.4 mmol, 1.34 g, 60% oil disp.) and dry THF (20 mL) were added to a flame-dried flask fitted with a magnetic stir bar, septum and N₂-atmosphere. The flask was cooled to 0 °C before adding cholesterol (25.1 mmol, 9.70 g) dissolved in dry THF (5 mL) and let to react for 15min. *Tert*-butyl-bromoacetate (63.0 mmol, 9.30 mL) was added dropwise followed by addition of 18-Crown-6 ether (3.9 mmol, 1.04 g). The reaction was let to reach r.t. o/n. The reaction was quenched by slowly adding CH₃OH. The solvent is removed in vacuo. The crude compound was dissolved in EtOAc and washed twice with Brine. The aqueous phase was subsequently washed with EtOAc twice. The combined organic phase was dried with MgSO₄, filtered and concentrated in vacuo. The compound was purified by normal FCC (Eluent: EtOAc:Hexane (1:9), Cemol stain) and isolated as a white solid (3.53 g, 28 % yield). MALDI TOF-MS (*m/z*): Calc. mass [M+Na]⁺ 523.41; found mass [M+Na]⁺ 523.24. ¹H NMR (400 MHz, CDCl₃), δ (ppm): 5.35 (d, *J* = 5.3 Hz, 1H), 4.00 (s, 2H), 3.27 – 3.19 (m, 1H), 2.41 – 2.22 (m, 2H), 2.03-0.85 (m, 47H), 0.67 (s, 3H). ¹³C NMR (101 MHz, CDCl₃), δ (ppm): 170.27, 140.78, 121.95, 81.49, 79.91, 66.19, 56.91, 56.28, 50.28, 42.45, 39.91, 39.65, 38.89, 37.27, 36.96, 36.32, 35.92, 32.07, 32.01, 28.37, 28.27, 28.24, 28.14, 24.42, 23.96, 22.95, 22.70, 21.19, 19.48, 18.85, 11.99.



Cholesteroxy acetic acid. Tert-butyl cholesteroxy-acetate (0.053 mmol, 26.5 mg) was dissolved in TFA:DCM:H₂O (10 mL, 20:79:1) and stirred for 1 h until TLC showed full conversion. The solvent was removed in vacuo. The crude compound was purified by normal FCC (SiO₂ with EtOAc:Hexan (1:5) with 1% AcOH). The compound was isolated as a white powder (0.040 mmol, 75 % yield). MALDI TOF-MS (*m/z*): Calc. mass [M+Na]⁺ 467.35; found mass [M+Na]⁺ 467.51. ¹H NMR (400 MHz, CDCl₃), δ (ppm): 9.08 (bs, 1H), 5.36 (d, *J* = 5.3 Hz, 1H), 4.16 (s, 2H), 3.34 – 3.22 (m, 1H), 2.43 – 2.18 (m, 2H), 2.03-0.85 (m, 38H), 0.67 (s, 3H). ¹³C NMR (101 MHz, CDCl₃), δ (ppm): 174.72, 140.15, 122.48, 80.51, 65.29, 56.86, 56.28, 50.25, 42.44, 39.87, 39.65, 38.78, 37.13, 36.90, 36.32, 35.92, 32.05, 31.98, 28.36, 28.19, 28.15, 24.41, 23.96, 22.96, 22.70, 21.20, 19.47, 18.85, 11.99.

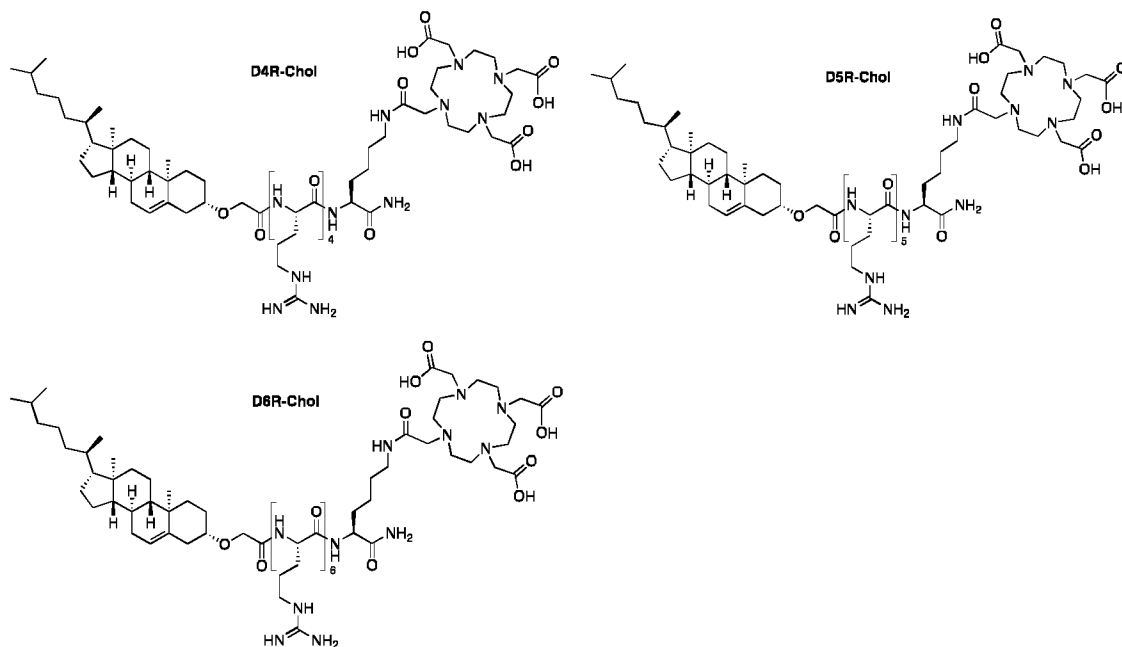


Synthesis of D3R-Chol.

The tetrapeptide Fmoc-Arg(Pbf)-Arg(Pbf)-Arg(Pbf)-Lys(Alloc) was synthesized on an Initiator Alstra peptide synthesizer (Biotage, Uppsala, Sweden) using a novasyn TGR resin (loading 0.2 mmol/g, scale 0.200 mmol). The resin was swelled in CH₂Cl₂ for 1 hour. Each coupling was performed using 4.0 eq. Fmoc protected amino acid, 3.95 eq. HATU, and 8 eq. 2,4,6-collidine in DMF. 5 min microwave was utilized to facilitate the coupling. All Fmoc-Arg(Pbf)-OH residues were double coupled. Deprotection of the Fmoc-group was carried out using 20 % piperidine in DMF for 2 x 5 min. Subsequently, removal of Alloc protection group on the lysine ϵ -amine was achieved by washing the resin with dry CH₂Cl₂ (5 x 5 mL) under N₂ flow. The resin was swelled in dry CH₂Cl₂ (3 mL) and mixed with Ph₃SiH (370 μ L, 3.0 mmol) for 1 min. Pd(0)(PPh₃)₄ (23 mg, 0.020

mmol) was added in dry CH₂Cl₂ (2 mL). The deprotection was achieved after 5 x 10 min. The reaction vial was flushed 3 times with CH₂Cl₂, 3 times with DMF and finishing off with 3 times CH₂Cl₂. Kaiser test and a test cleavage (TFA: TIPS:H₂O; 95:2.5:2.5) confirmed full conversion. DOTA was coupled using 1.30 eq. of DOTA-tris-tBu, 1.27 eq. HATU and 8 eq. 2,4,6-collidine in DMF for 1.5 hour. N-terminus was Fmoc-deprotected using 20% piperidine in DMF for 2 x 5 min. Afterwards Cholesteroxy acetic acid (114 mg, 0.256 mmol, 1.28 eq.) was coupled using 1.22 eq. HATU and 8.25 eq. 2,4,6-collidine in DCM:DMF (1:2) o/n. The peptide was cleaved for 3 hours using TFA:TIPS:H₂O (94:2.5:2.5, 10mL) after which the cleavage solvent was removed under reduced pressure and the crude compound (2 mL) was precipitated in cold diethyl ether. The crude peptide was purified using a Reveleris auto flash system (Büchi PrepChrom RP-C₁₈ column, 150x21 mm, 15 µm, 5-100% CH₃CN in water with 0.1% FA over 20 min, flow: 20 mL/min, temp.: 25 °C, detection: ELSD and UV_{206 nm}). The pure fractions were pooled and lyophilized to isolate D3R-Chol as a white powder. MALDI-TOF MS (*m/z*): Calc. mass C₆₉H₁₂₃N₁₉O₁₃ 1425.95, found mass [M+H]⁺ 1427.12.

Example 20: Synthesis of D4R-Chol, D5R-Chol, D6R-Chol and DF3R-C18 compounds



Methods:

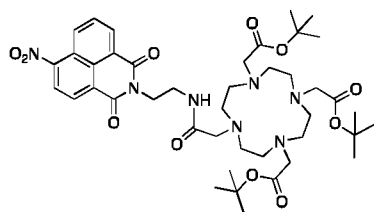
Synthesis of D4-6R-Chol (MB253): The peptides Fmoc-[Arg(Pbf)]_n-Lys(Alloc) were synthesized on an Initiator Alstra peptide synthesizer (Biotage, Uppsala, Sweden) using a novasyn TGR resin (loading 0.2 mmol/g, scale 0.100 mmol). The resin was swelled in

CH₂Cl₂ for 1 hour. Each coupling was performed using 4.0 eq. Fmoc protected amino acid, 3.95 eq. HATU, and 8 eq. 2,4,6-collidine in DMF. 5 min microwave was utilized to facilitate the coupling. All Fmoc-Arg(Pbf)-OH residues were double coupled. Deprotection of the Fmoc-group was carried out using 20 % piperidine in DMF for 2 x 5 min. Subsequently, removal of Alloc protection group on the lysine ε-amine was achieved by washing the resin with dry CH₂Cl₂ (5 x 5 mL) under N₂ flow. The resin was swelled in dry CH₂Cl₂ (3 mL) and mixed with Ph₃SiH (370 μL, 3.0 mmol) for 1 min. Pd(0)(PPh₃)₄ (23 mg, 0.020 mmol) was added in dry CH₂Cl₂ (2 mL). The deprotection was achieved after 5 x 10 min. The reaction vial was flushed 3 times with CH₂Cl₂, 3 times with DMF and finishing off with 3 times CH₂Cl₂. Kaiser test and a test cleavage (TFA: TIPS:H₂O; 95:2.5:2.5) confirmed full conversion. DOTA was coupled using 1.30 eq. of DOTA-tris-tBu, 1.27 eq. HATU and 8 eq. 2,4,6-collidine in DMF for 1.5 hour. N-terminus was Fmoc-deprotected using 20% piperidine in DMF for 2 x 5 min. Afterwards MB175 (30 mg, 0.067mmol, 0.67 eq.) was coupled using 0.66 eq. HATU and 8.00 eq. 2,4,6-collidine in DCM:DMF (1:2) o/n. The peptide was cleaved for 3 hours using TFA:H₂O:anisole:TIPS (85:5:5:5, 10 mL) after which the cleavage solvent was removed under reduced pressure and the crude compound (2 mL) was precipitated in cold diethyl ether. The crude compounds were purified by Thermo Fisher prep. HPLC (5-50% CH₃CN with 0.1% FA in water over 20min, flow: 20 mL/min, detection: UV_{214/280 nm}, Phenomenex C18 (5 μm, 110 Å, 250 x 30 mm)).

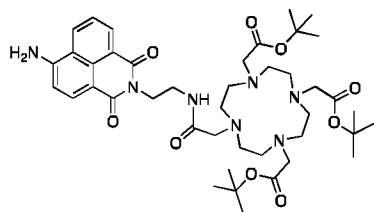
D4R-Chol: The pure fractions were pooled and lyophilized to isolate a white powder. (6.9 mg, 6 % yield, purity >98%). MALDI-TOF MS (*m/z*): Calc. mass (C₇₅H₁₃₅N₂₃O₁₄): 1582.1, found mass, [M+H]⁺: 1583.3.

D5R-Chol: The pure fractions were pooled and lyophilized to isolate a white powder. (2.6 mg, 2 % yield, purity >98%). MALDI-TOF MS (*m/z*): Calc. mass (C₈₁H₁₄₇N₂₇O₁₅): 1738.2, found mass, [Mr]: 1738.4.

D6R-Chol: The pure fractions were pooled and lyophilized to isolate a white powder. (2.6 mg, 2 % yield, purity >98%). MALDI-TOF MS (*m/z*): Calc. mass (C₈₇H₁₅₉N₃₁O₁₆): 1894.3, found mass, [Mr]: 1894.5.

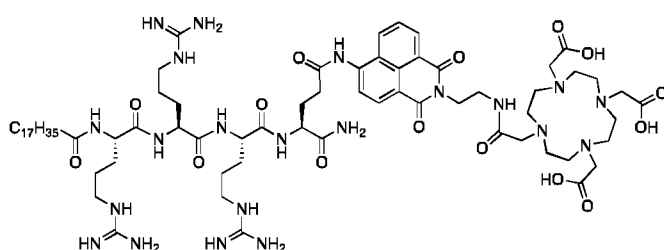


Synthesis of MB222: MB207 (401 mg, 1.04 mmol) was dissolved in TFA:DCM (1:1, 40 mL) for 1h. The solvent was subsequently removed in vacuo leaving a yellow residual. In a separate vial, the tBu₃-DOTA-OH (389 mg, 0.68 mmol) was dissolved in anhydrous DMF (7 mL) and was activated with pyBOP (371 mg, 0.71 mmol) for 2min. Then, a mixture of the re-dissolved Boc-deprotected MB207 and triethylamine (870 mg, 8.60 mmol) in DMF (6 mL) was added to the activated tBu₃-DOTA-OH. The reaction was let to react with stirring o/n at room temperature. The solvent was removed in vacuo. The yellow oil was redissolved in CH₂Cl₂ (50 mL) and washed with water (50 mL). The aqueous phase was washed with CH₂Cl₂ twice (2 x 60 mL). The organic phase was dried with MgSO₄, filtered and concentrated in vacuo. The compound was redissolved in CH₂Cl₂ (2 mL) and precipitated in cold diethyl ether twice. The residual compound was isolated as a yellow powder (368 mg, 0.44 mmol, 65 % yield). ESI-MS (*m/z*): Calc. mass C₄₂H₆₁N₇O₁₁ 839.4, found [M+H]⁺ 840.2. ¹H NMR (400 MHz, CDCl₃), δ (ppm): 8.80 (dd, J = 8.8, 0.9 Hz, 1H), 8.66 (dd, J = 7.3, 0.9 Hz, 1H), 8.62 (d, J = 8.0 Hz, 1H), 8.36 (d, J = 8.0 Hz, 1H), 7.94 (dd, J = 8.7, 7.3 Hz, 1H), 6.50 (t, J = 5.8 Hz, 1H), 3.75 – 1.92 (m, 28H), 1.46 (d, J = 4.1 Hz, 27H). ¹³C NMR (101 MHz, CDCl₃), δ (ppm): 172.63, 172.54, 164.00, 163.18, 149.52, 132.55, 129.97, 129.93, 129.47, 129.41, 127.19, 124.05, 123.74, 123.10, 81.96, 56.09, 55.87, 55.71, 39.82, 38.26, 28.15, 28.08.



Synthesis of MB223: MB222 (483 mg, 0.58 mmol) and Pd/C (10mol%, 38 mg) was added to a flame dried flask fitted a magnet. The flask was put under vacuum and then added 100% ethanol and then flushed with N₂. The flask was subsequently flushed with H₂. A new H₂ balloon was bobbed through the solution followed by a second balloon added to the septum for o/n reaction. The reaction was filtered through celite to remove Pd/C using CH₃OH with subsequent concentration in vacuo. The crude compound was redissolved in CH₂Cl₂ (1 mL) and precipitated in cold diethyl ether. The precipitate was spun down

and wash with cold diethyl ether (5 x 30 mL). The pure compound was isolated as a yellow powder (424 mg, 0.52 mmol, 91 % yield). ESI-MS (m/z): Calc. mass $C_{42}H_{63}N_7O_9$ 809.5; found mass $[M+H]^+$ 810.2. 1H NMR (400 MHz, $CDCl_3$), δ (ppm): 8.50 (dd, $J = 7.3$, 1.0 Hz, 1H), 8.31 – 8.24 (m, 2H), 7.61 (dd, $J = 8.4$, 7.3 Hz, 1H), 6.85 (d, $J = 8.3$ Hz, 1H), 6.13 (t, $J = 5.5$ Hz, 1H), 5.54 (s, 2H), 4.36 (t, $J = 5.3$ Hz, 2H), 3.34 – 1.80 (m, 26H), 1.47 – 1.41 (m, 27H). ^{13}C NMR (101 MHz, $CDCl_3$), δ (ppm): 172.66, 171.50, 165.06, 164.58, 151.36, 134.84, 132.25, 131.02, 129.87, 128.92, 128.81, 124.96, 121.98, 119.87, 109.83, 109.65, 81.90, 68.28, 56.73, 55.66, 39.00, 38.85, 38.82, 36.62, 31.56, 30.49, 30.45, 29.83, 29.05, 28.05, 28.03, 23.87, 23.12, 14.19, 11.09.



Synthesis of DF3R-C18 (MB237): The tetrapeptide Fmoc-Arg(Pbf)-Arg(Pbf)-Arg(Pbf)-Glu(All) was synthesized on an Initiator Alstra peptide synthesizer (Biotage, Uppsala, Sweden) using a novasyn TGR resin (loading 0.2 mmol/g, scale 0.055 mmol). The resin was swelled in CH_2Cl_2 for 1 hour. Each coupling was performed using 4.0 eq. Fmoc protected amino acid, 3.95 eq. HATU, and 8 eq. 2,4,6-collidine in DMF. 5 min microwave was utilized to facilitate the coupling. All Fmoc-Arg(Pbf)-OH residues were double coupled. Deprotection of the Fmoc-group was carried out using 20 % piperidine in DMF for 2 x 5 min. Afterwards stearic acid was coupled using 4 eq. of fatty acid, 3.92 eq. HATU and 8 eq. 2,4,6-collidine in DCM:DMF (1:1) for 60 min. Subsequently, removal of Allyl protection group on the glutamic acid was achieved by washing the resin with dry CH_2Cl_2 (5 x 5 mL) under N_2 flow. The resin was swelled in dry CH_2Cl_2 (3 mL) and mixed with 0.2 eq. Ph_3SiH for 1 min. 15 eq. $Pd(0)(PPh_3)_4$ was added in dry CH_2Cl_2 (2 mL). The deprotection was achieved after 5 x 10 min. The reaction vial was flushed 3 times with CH_2Cl_2 , 3 times with DMF and finishing off with 3 times CH_2Cl_2 . Kaiser test and MS analysis of a test cleavage (TFA:TIPS: H_2O ; 95:2.5:2.5) confirmed full conversion. MALDI-TOF MS (m/z): Calc. mass $C_{41}H_{80}N_{14}O_7$ 880.6, found mass $[M+2H]^{2+}$ 441.3. MB223 was coupled using 1.20 eq. MB223, 1.10 eq. HATU and 10 eq. 2,4,6-collidine in DMF o/n with an initial activation of the glutamic acid. The compound was cleaved from the resin in TFA: H_2O :anisole:TIPS (85:5:5:5) for 3h. The solvent was reduced to approx. 2mL and the cleaved compound was precipitated in cold diethyl ether. The crude

compound where purified by Thermo Fisher prep. HPLC (5-50% CH₃CN with 0.1% TFA in water over 20min, flow: 20 mL/min, detection: UV_{214/280 nm}, Phenomenex C18 (5 µm, 110 Å, 250 x 30 mm)). The pure fractions were pooled and lyophilized to isolate a pale yellow powder. (1.1 mg, 1 % yield, purity >98%). MALDI-TOF MS (*m/z*): Calc. mass (C₇₁H₁₁₇N₂₁O₁₅): 1503.9, found mass, [M+H]⁺: 1503.0.

Results and discussion:

The synthesis of D4R-Chol, D5R-Chol, D6R-Chol and DF3R-C18 was performed successfully as confirmed by the performed analyses.

Conclusion:

The compounds of the present disclosure, including D4R-Chol, D5R-Chol, D6R-Chol and DF3R-C18 can be synthesized using the described methodology.

Example 21: Fluorescence characterization of DF3R-C18

The aim of the current example is to determine the excitation and emission spectra of the fluorescent DF3R-C18 analogue.

Methods:

Micelle preparation: All the micelles were made by dissolving the fluorescent D3R analogues in ISO-TRIS-NaCl (10mM TRIS, 150mM NaCl, pH 7.8), adding CuCl₂ (2.5 mg/mL, 1 eq.), and heating the sample at 55 °C for 30 min. The sample of DF3R-C18 (759 µL, 200 µM) was dissolved in ISO-TRIS-NaCl (10mM TRIS, 150mM NaCl, pH 7.8).

Emission and Excitation spectra: The fluorescent characterization was performed on a Tecan platereader (Spark® Multimode Microplate Reader) in a black flat-bottom 96-well plate. All measurements were conducted as duplicates.

Fluorescent DF3R-C18 analogue was dissolved in ISO-TRIS-NaCl (10mM TRIS, 150mM NaCl, pH 7.8) in a 200 µM concentration, i.e. above the CMC of the compound. The dissolved DF3R-C18 analogue (100 µL, 200 µM) was added to a black flat-bottom 96-well plate, and ISO-TRIS-NaCl (100 µL, 10mM TRIS, 150 mM NaCl, pH 7.8) was used as blank control. The samples were analysed by scanning of the emission spectrum (Em_{480-600nm} by Ex_{434nm}, bandwidth: 20 nm, Em step size: 2 nm) and excitation

spectrum (Ex_{350-500nm} by Em_{550nm}, bandwidth: 20 nm, Ex step size: 2 nm). The fluorescent characteristics of DF3R-C18 are presented in Fig. 21.

Results:

5 Spectral properties of DF3R-C18 was investigated and the result is presented in Fig. 22.

Conclusion:

10 The DF3R-C18 construct was shown to have excitation maximum at 434nm and emission maximum at 546nm.

Example 22: Formulation of D4R-Chol, D5R-Chol, D6R-Chol and DF3R-C18 compounds as micelles

The aim of the current analysis was to explore micelle formulation techniques.

15

Method:

Buffers

ISO-TRIS-NaCl (20 mM:150 mM, pH 7.4)

NH₄OAc solution (28 mM, pH 5.5, 22 mOsm/kg)

20

Micelle preparation. A stock of the DnR analogues (2 mM) were prepared in NH₄OAc (28 mM, pH 5.5, 22 mOsm/kg). The stocks are stored at -20 °C until further use. The DnR analogues (50 µL, 2 mM) were aliquoted into vials with a magnet stir bar and diluted with NH₄OAc (200 µL, 28 mM, pH 5.5, 22 mOsm/kg). The micelles were heated to 55 °C with stirring. TRIS (250 µL, 20 mM, 150 mM NaCl, pH 7.4) or HEPES (250 µL, 25 mM, 150 mM NaCl, pH 7.4) was added to the stirring solution at 55 °C. CuCl₂ in miliQ water (6 µL, 2.5 mg/mL, 1.1 eq.) was added after 15 min giving a DnR analogue micelle formulation (506 µL, 198 µM).

30 *Flow micelle preparation.* The DnR analogues are solubilized in tBuOH:H₂O (9:1, 1 mL, 3.2 mM) and loaded into a 2 mL syringe. NH₄OAc (10 mL, 28 mM, pH 5.5, 22 mOsm/kg) was loaded in a 10 mL syringe. A Precision Nanosystems Nanoassembler system was loaded with the two syringes, a primed flow cassette and two 15 mL falcon tubes for collecting. The formulation was injected into the buffer using the following specifications. Total flow rate: 10 mL/min with a 1:4 ratio of DnR analogue to buffer.

35

The collected formulation volume was added to a primed Thermo Scientific Slide-A-Lyzer® Dialysis cassette (2 MWCO, 3 mL) and dialysed o/n in NH₄OAc (28 mM, pH 5.5, 22 mOsm/kg) at 2-8 °C. The concentration of the DnR analogues were determined by Shimadzu Nexera-I UHPLC-Sedere Sedex-100 LT-ELSD using a Waters Xterra C8 column. The micelle size was measured by DLS.

DLS size determination. Size measurements were performed using dynamic light scattering (DLS) measurements performed on a ZetaPALS instrument (Brookhaven, Holtsville, USA) equipped with a 35 mV solid-state laser (659 nm). Samples were run neat or diluted in milliQ water (20 x dilution) followed by equilibration to 25°C before a minimum of five measurements was made of each sample.

Results:

The DLS size and zeta potential measurements of the the different DnR analogues can be seen in table 5.

Table 5: DLS size measurements of the micelle formulations. All samples were measured neat. N.D. = not determined.

Formulation	Methodology	Buffer	DLS Z-av./Number mean/volume mean size [nm]	PDI
D3R-C16	Micelle preparation	HEPES:NaCl (25 : 150 mM, pH 7.4)	10.3 / 5.8 / 6.8	0.36
D3R-C18	Micelle preparation	HEPES:NaCl (25 : 150 mM, pH 7.4)	9.4 / 6.1 / 7.5	0.29
	Micelle preparation	TRIS:NaCl (20 : 150 mM, pH 7.4)	41.9 / 7.1 / 8.4	0.31
	Flow micelle preparation	NH ₄ OAc (28 mM, pH 5.5)	17.2 / 6.7 / 7.5	0.42
D3R-Chol	Micelle preparation	TRIS:NaCl (20 : 150 mM, pH 7.4)	149.4 / 8.8 / 10.8	0.59
D4R-Chol	Micelle preparation	TRIS:NaCl (20 : 150 mM, pH 7.4)	101.3 / 7.4 / 8.4	0.28
D5R-Chol	Micelle preparation	TRIS:NaCl (20 : 150 mM, pH 7.4)	220.7 / 7.4 / 8.4	0.40
D6R-Chol	Micelle preparation	TRIS:NaCl (20 : 150 mM, pH 7.4)	134.1 / 7.3 / 8.7	0.40
CuCl	Blank	NH ₄ OAc	N.D.	N.D.

Discussion:

The DLS size data in table 5 show that all construct form micelle aggregates upon dispersion in buffered solution. The C16 and C18 based analogues display lower DLS Z-av. values than the Chol based analogues. The number mean and volume mean micelle size is approximately 5-11nm for all constructs.

Conclusion:

All DnR analogues form micelles in buffered media with a diameters of 5-11nm.

Example 23: Radiolabelling of D4R-Chol, D5R-Chol and D6R-Chol compounds

The aim of the current analysis was to quantify the radiolabeling efficiency and transferability of the ^{64}Cu -D4-6R analogues using radio-TLC.

Method:

TLC development and readout: All TLCs were conducted on silica gel 60 F254 plates (Merck) using 5% NH_4OAc in $\text{H}_2\text{O}:\text{CH}_3\text{OH}$ (25:75) as eluent of ^{64}Cu -D3R-Chol, of ^{64}Cu -D4R-Chol, of ^{64}Cu -D5R-Chol, and of ^{64}Cu -D6R-Chol. The radio-TLCs were measured using a phosphor imager (Cyclone Plus, PerkinElmer). The retention factors were found to be $\text{Rf}_{\text{Cu-D3R-Chol}} = 0.4$, $\text{Rf}_{\text{Cu-D4R-Chol}} = 0.3$, $\text{Rf}_{\text{Cu-D5R-Chol}} = 0.3$ and $\text{Rf}_{\text{Cu-D6R-Chol}} = 0.2$.

Radiolabelling of DnR-Chol analogues: The DnR analogues were prepared as 2 mM stock solution in NH_4OAc (28 mM, pH 5.5, 22 mOsm/kg), and 50 μL were following added to $^{64}\text{CuCl}_2$ (50 μL , 1000 MBq/mL in NH_4OAc (28 mM, pH 5.5, 22 mOsm/kg)) in a 2 mL glass vial. 150 μL of NH_4OAc (28 mM, pH 5.5, 22 mOsm/kg) was added to reach the desired concentration. The sample was heated and magnetically stirred at 55°C for 15-60 min. 250 μL TRIS (20 mM, 150 mM NaCl, pH 7.4) was added after 45 min of coordination. TLC samples were spotted just prior to addition of $^{63}\text{CuCl}_2$ and 15 min after addition. 6 μL of a $^{63}\text{CuCl}_2$ stock solution (2.5 mg/mL in milliQ water) was added at 60 min. The vials entire content was transferred to a new 2 mL glass vial to determine the transferability. The transferability (activity in solution) was determined using a dose-calibrator (VDC-505, Comecer). The transferability in the TRIS:NaCl: NH_4OAc (10:75:14 mM, pH 6.5-7.0) buffer is seen in Table 6.

Results:

The radiochemical purity and transferability were determined using TLC and dose-calibrator, and the results are compiled in table 6.

5 Table 6 - Radiochemical radiolabelling efficiency and transferability of ^{64}Cu -DnR-Chol.

Entry	Buffer	TLC [*]	TLC [*]	Transferability	Overall radiolabelling efficiency
		No $^{63}\text{Cu}^{**}$	Added $^{63}\text{Cu}^{**}$		
D3R-Chol	TRIS:NaCl:NaOAc (10:75:14 mM, pH 6.5-7)	96%	88%	99%	95%
D4R-Chol	TRIS:NaCl:NaOAc (10:75:14 mM, pH 6.5-7)	92%	87%	101%	92%
D5R-Chol	TRIS:NaCl:NaOAc (10:75:14 mM, pH 6.5-7)	86%	80%	102%	86%
D6R-Chol	TRIS:NaCl:NaOAc (10:75:14 mM, pH 6.5-7)	91%	84%	102%	91%

* 5% NH_4OAc in $\text{H}_2\text{O}:\text{CH}_3\text{OH}$ (25:75)

** ^{63}Cu is added to ensure DOTA saturation.

Discussion:

10 Radiolabelling of the DnR-Chol analogues in TRIS:NaCl buffer resulted in high overall radiolabeling efficiency of 86 to 95%. The transferability was near quantitative by using a NaOAc (28 mM, pH 5.5) buffer to solubilize ^{64}Cu and coordination buffer to the DnR analogues. Addition of ^{63}Cu to the DnR-Chol micelles reduced the coordinated ^{64}Cu in the DOTA complex with a maximum change of 8%.

15

Conclusion:

DnR-Chol analogues were effectively radiolabelled with ^{64}Cu and display great transferability.

Example 24: Radiolabelling murine cytotoxic T lymphocytes with ^{64}Cu -D3R-Chol

The aim of the current example is to investigate the loading efficiency of ^{64}Cu -D3R-Chol in murine T lymphocytes when incubated with different micelle concentrations.

5 Methods:

Murine T lymphocytes (50×10^6 cells/mL) in serum free RPMI media were incubated with ^{64}Cu -D3R-Chol (198 μM , 29.8 MBq/mL) at micelle concentrations 20, 40, 60 μM and a ^{64}Cu mean activity of 298, 596 and 894 kBq in 96 well round bottom cell culture plates for 2 hours at 37 °C/5% CO_2 . After incubation cells were washed 3 times with
10 100-150 μL RPMI without serum. For washing steps cells were centrifuged at 600xg (4°C, 3 minutes) and supernatant was decanted. Specific radioactivity was determined for T lymphocytes by gamma counting (Wizard2, Perkin Elmer, Branford, CT, USA) using an isotope specific and decay corrected counting protocol. Cell concentration of the samples was determined using MUSE® Cell Count and Viability Assay on a
15 MUSE® Cell Analyzer (MERCK Millipore) according to the manufacturer's guidelines. The loading efficiency was then determined as the activity of the T lymphocyte fraction divided by the total activity applied to the cells.

Results:

20 The radiolabelled micelles are effectively transferred to the T lymphocytes during the two-hour incubation period. No statistical differences between the investigated micelle concentrations were observed ($p > 0.05$, one-way ANOVA test).

25 Table 7: Loading efficiency of the T lymphocytes following incubation for 2 hours with three different concentrations of the micelle formulations listed. The loading efficiency was determined following 2 hour loading and three subsequent washes of the T lymphocytes. Mean and SD are listed ($n = 3$).

^{64}Cu -D3R-Chol	Micelle concentration		
	20 μM	40 μM	60 μM
Loading	$35.4 \pm 2.9\%$	$44.1 \pm 2.7\%$	$38.5 \pm 8.0\%$

Discussion:

The ^{64}Cu -D3R-Chol micelles was loaded effectively into T lymphocytes at all concentrations investigated, the highest loading was observed for the 40 μM micelle concentration.

Conclusion:

In conclusion, ^{64}Cu -D3R-Chol was effectively taken and well tolerated up by T lymphocytes.

Example 25: Radiolabelling murine cytotoxic T lymphocytes with ^{64}Cu -D3R-Chol, ^{64}Cu -D4R-Chol, ^{64}Cu -D5R-Chol and ^{64}Cu -D6R-Chol

The aim of the current example is to investigate the influence of arginine residues for loading efficiency and viability of radiolabelled micelles in murine T lymphocytes.

Methods:

The following micelle formulations were included: ^{64}Cu -D3R-Chol, ^{64}Cu -D4R-Chol, ^{64}Cu -D5R-Chol and ^{64}Cu -D6R-Chol. Murine T lymphocytes (50×10^6 cells/mL) in serum free RPMI media were incubated with ^{64}Cu -D3R-Chol (198 μM , 82MBq/mL), ^{64}Cu -D4R-Chol (198 μM , 84MBq/mL), ^{64}Cu -D5R-Chol (198 μM , 86MBq/mL), and ^{64}Cu -D6R-Chol (198 μM , 86MBq/mL), at micelle concentration 40 μM and on average 1.69 MBq ^{64}Cu in 96 well round bottom cell culture plates for 2 hours at 37 °C/5% CO_2 . After incubation cells were washed 3 times with 100-150 μL RPMI without serum. For washing steps cells were centrifuged at 600xg (4°C, 3 minutes) and supernatant was decanted. Specific radioactivity was determined for T lymphocytes by gamma counting (Wizard2, Perkin Elmer, Branford, CT, USA) using an isotope specific and decay corrected counting protocol. Cell concentration of the samples was determined using MUSE® Cell Count. Fixable Viability Dye eFluor™780 from eBioscience™ was used to assess viability and stained in FACS buffer 15 minutes at RT. Samples were run on a 4-laser LSR II Fortessa x-20. After completion of washing steps cell viability was recorded.

Results:

The loading efficiency was significantly improved for the ^{64}Cu -D4R-Chol, ^{64}Cu -D5R-Chol, ^{64}Cu -D6R-Chol formulations compared to the ^{64}Cu -D3R-Chol formulation (one-way ANOVA, Tukey's multiple comparison test, $p = 0.0001$). The viability of the T

lymphocytes was not affected by increasing the number of arginine residues in the radiolabelled micelle formulation and was not different from included unloaded controls.

5 Table 8: Loading efficiency in the T lymphocytes following incubation for 2 hours with 40 μ M of the micelle formulations listed. The loading efficiency was determined following 2 hour loading and three subsequent washes of the T lymphocytes. Mean and SD are listed (n = 3).

D3R-analogue 40 μ M	Micelle concentration	Viability
	Loading efficiency	40 μ M
^{64}Cu -D3R-Chol	$38.3 \pm 0.6\%$	92.8 %
^{64}Cu -D4R-Chol	$55.5 \pm 4.1\%$	91.6 %
^{64}Cu -D5R-Chol	$60.4 \pm 2.4\%$	94.0 %
^{64}Cu -D6R-Chol	$58.3 \pm 1.1\%$	94.0 %
Control		94.7%

10 Discussion:

The loading efficiency was significantly higher for the micelle formulations containing 4 to 6 arginine residues (^{64}Cu -D4R-Chol, ^{64}Cu -D5R-Chol and ^{64}Cu -D6R-Chol) compared to ^{64}Cu -D3R-Chol. The loading efficiency was comparable between ^{64}Cu -D4R-Chol, ^{64}Cu -D5R-Chol and ^{64}Cu -D6R-Chol. The viability was not affected by increasing
 15 number of arginine which supports that addition of increasing numbers of arginine residues may provide a method to improve transfer levels of radioactivity to the cells intended for radiolabelling.

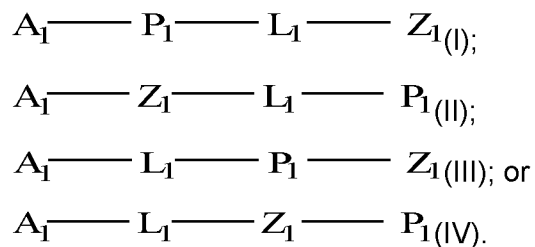
Conclusion:

20 In conclusion, all ^{64}Cu -Chol were taken up and well tolerated by T lymphocytes. Radiolabelled micelle formulations with 4 to 6 arginine residues transferred significantly more radioactivity to the T lymphocytes in comparison to the micelle formulation containing 3 arginine residues. Increasing the number of arginine residues in the radiolabelled micelle formulation from 3 to 4, 5 or 6 provides a method to improve
 25 loading without compromising cell viability.

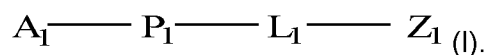
Claims

1. A compound comprising:
 - a. a chelator group (Z_1),
 - b. a cationic peptide sequence (P_1) comprising amide-bonded amino acids, and
 - c. a lipophilic aliphatic group (A_1);

wherein the chelator group (Z_1), the cationic peptide sequence (P_1), and the lipophilic aliphatic group (A_1), are covalently connected via a linker (L_1) according to any one of formulas (I) to (IV):



2. The compound according to claim 1, wherein the chelator group (Z_1) is bound via a linker (L_1) to the N-terminus or the C-terminus of the cationic peptide sequence (P_1), and the compound is represented by formula (I):



3. The compound according to any one of the preceding claims, wherein the lipophilic aliphatic group (A_1) is bound via a functional group to the N-terminus or C-terminus of the cationic peptide sequence (P_1).

4. The compound according to any one of the preceding claims, wherein the lipophilic aliphatic group (A_1) is bound via a carbonyl group to the N-terminus of the cationic peptide sequence (P_1), wherein the carbonyl group and the amine of the N-terminus together forms an amide.

5. The compound according to any one of the preceding claims, wherein the chelator group (Z_1) is a polydentate hydrophilic chelator group.

6. The compound according to any one of the preceding claims, wherein the chelator group (Z_1) is linear or cyclic.
7. The compound according to any one of the preceding claims, wherein the chelator group (Z_1) comprises ethylene diamine.
8. The compound according to any one of the preceding claims, wherein the chelator group (Z_1) is selected from the group consisting of: 1,4,7,10-tetraazacyclododecane-1,4,7,10-tetraacetic acid (DOTA), 1,4,7,10-tetraazacyclododecane (Cyclen), 1,4,8,11-tetraazacyclotetradecane (cyclam), 1,4-ethano-1,4,8,11-tetraazacyclotetradecane (et-cyclam), 1,4,7,11-tetraazacyclotetradecane (isocyclam), 1,4,7,10-tetraazacyclotridecane ([13]aneN₄), 1,4,7,10-tetraazacyclododecane-1,7-diacetic acid (DO2A), 1,4,7,10-tetraazacyclododecane-1,4,7-triacetic acid (DO3A), 1,4,7,10-tetraazacyclododecane-1,7-di(methanephosphonic acid) (DO2P), 1,4,7,10-tetraazacyclododecane-1,4,7-tri(methanephosphonic acid) (DO3P), 1,4,7,10-tetraazacyclododecane-1,4,7,10-tetra(methanephosphonic acid) (DOTP), diethylenetriaminepentaacetic acid (DTPA), 1,4,8,11-tetraazacyclotetradecane-1,4,8,11-tetraacetic acid (TETA), and ethylenediaminetetraacetic acid (EDTA).
9. The compound according to any one of the preceding claims, wherein the cationic peptide sequence (P_1) comprises an amino acid selected from the group consisting of: L-arginine (R), L-homoarginine (hArg), L-histidine (H), L-homohistidine (hHis), L-lysine (K), L-homolysine (hLys), L-ornithine (Orn), D-ornithine (orn), D-arginine (r), D-homoarginine (harg), D-histidine (h), D-homohistidine (hhis), D-Lysine (k), and D-homolysine (hlys).
10. The compound according to any one of the preceding claims, wherein the cationic peptide sequence (P_1) comprises an amino acid selected from the group consisting of: L-arginine (R), and D-arginine (r).
11. The compound according to any one of the preceding claims, wherein the cationic peptide sequence (P_1) comprises at least two amide bonded amino acids, such as at least three amino acids, such as at least four amino acids, such as at least five amino acids, such as at least six amino acids, such as at least seven amino acids,

such as at least eight amino acids, such as at least nine amino acids, such as at least ten amino acids.

5 12. The compound according to any one of the preceding claims, wherein the cationic peptide sequence (P_1) comprises from two amino acids to five amino acids, such as three amino acids.

10 13. The compound according to any one of the preceding claims, wherein the cationic peptide sequence (P_1) is selected from the group consisting of: RR, rr, RRR, rrr, RRRR, rrrr, RRRRR, rrrrr, RRRRRR, rrrrrr, RRRRRRR, rrrrrrr, RRRRRRRR, rrrrrrrr, RRRRRRRR, rrrrrrrr, RRRRRRRRR, and rrrrrrrrr.

15 14. The compound according to any one of the preceding claims, wherein the lipophilic aliphatic group (A_1) comprises at least 8 carbon atoms, such as at least 9 carbon atoms, such as at least 10 carbon atoms, such as at least 11 carbon atoms, such as at least 12 carbon atoms, such as at least 13 carbon atoms, such as at least 14 carbon atoms, such as at least 15 carbon atoms, such as at least 16 carbon atoms, such as at least 17 carbon atoms, such as at least 18 carbon atoms, such as at least 19 carbon atoms, such as at least 20 carbon atoms, such as at least 21 carbon atoms, such as at least 22 carbon atoms, such as at least 23 carbon atoms, such as at least 24 carbon atoms, such as at least 25 carbon atoms, such as at least 26 carbon atoms, such as at least 27 carbon atoms, such as at least 28 carbon atoms, such as at least 29 carbon atoms, such as at least 30 carbon atoms, such as at least 31 carbon atoms, such as at least 32 carbon atoms, such as at least 33 carbon atoms, such as at least 34 carbon atoms, such as at least 35 carbon atoms.

25 15. The compound according to any one of the preceding claims, wherein the lipophilic aliphatic group (A_1) is an aliphatic chain or an aliphatic cycle.

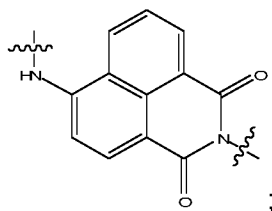
30


16. The compound according to any one of claims 1 to 15, wherein the lipophilic aliphatic group (A_1) is an aliphatic cycle comprising a gonane structure.

17. The compound according to any one of claims 1 to 15, wherein the lipophilic aliphatic group (A_1) is a sterol, such as a sterol selected from the group consisting of cholesterol, campesterol, sitosterol, stigmasterol, and ergosterol.
- 5 18. The compound according to any one of claims 1 to 15, wherein the lipophilic aliphatic group (A_1) is an aliphatic cycle comprising a steroid, such as cholesterol.
19. The compound according to any one of the preceding claims, wherein the lipophilic aliphatic group (A_1) is an aliphatic branched or non-branched chain.
- 10 20. The compound according to any one of the preceding claims, wherein the lipophilic aliphatic group (A_1) comprises two adjacent carbon atoms connected by a double bond.
- 15 21. The compound according to any one of claims 19 to 20, wherein the lipophilic aliphatic group (A_1) is a non-branched C15, C16, C17, C18, C19 or C20 alkyl.
22. The compound according to any one of the preceding claims, wherein the lipophilic aliphatic group (A_1) is a non-branched C17 alkyl.
- 20 23. The compound according to any one of the preceding claims, wherein the linker (L_1) consists of one or more linking units (U_1) to (U_4), connecting the chelator group (Z_1) with the cationic peptide sequence (P_1), according to formula (Ia), (Ib), (Ic), or (Id):
- 25
- $$A_1 - P_1 - U_1 - Z_1 \text{ (Ia);}$$
- $$A_1 - P_1 - U_1 - U_2 - Z_1 \text{ (Ib);}$$
- $$A_1 - P_1 - U_1 - U_2 - U_3 - Z_1 \text{ (Ic); or}$$
- $$A_1 - P_1 - U_1 - U_2 - U_3 - U_4 - Z_1 \text{ (Id);}$$
- 30 wherein (A_1), (P_1) and (Z_1) are defined as in any one of the preceding claims.
24. The compound according to claim 23, wherein at least one of the linking units (U_1) to (U_4) is a proteinogenic or non-proteinogenic amino acid.

25. The compound according to any one of the preceding claims, wherein the proteinogenic amino acid is selected from: L-cysteine (C), D-cysteine (d), L-lysine (K), and D-lysine (d).
- 5
26. The compound according to claim 23, wherein the linker (L_1) of formula (I) is cleavable, covalently disconnecting any one of the linking units (U_1) to (U_4) by reduction, a change in pH and/or an enzymatic process.
- 10
27. The compound according to any one of claims 23 to 26, wherein the compound of formula (Ib) is cleavable between linking units (U_1) and (U_2).
28. The compound according to any one of claims 23 to 26, wherein the compound of formula (Ic) is cleavable between linking units (U_1) and (U_2).
- 15
29. The compound according to any one of claims 23 to 26, wherein the compound of formula (Id) is cleavable between linking units (U_1) and (U_2).
30. The compound according to any one of claims 23 to 29, wherein the bond between any one of (U_1) and (U_2), (U_2) and (U_3), (U_3) and (U_4), is a disulfide bond.
- 20
31. The compound according to any one of claims 23 to 29, wherein at least one of the linking units (U_1) to (U_4) is a fluorophore (F_1).
- 25
32. The compound according to claim 31, wherein the fluorophore (F_1) emits light at a wavelength between 400 and 2600 nm.
33. The compound according to any one of claims 31 to 32, wherein the fluorophore (F_1) is selected from the group consisting of: a naphthalene derivative, a squaraine derivative, a xanthene derivative, a cyanine derivative, a coumarine derivative, an oxadiazole derivative, an anthracene derivative, a pyrene derivative, an oxazine derivative, an acridine derivative, an arylmethine derivative, and a tetrapyrrole derivative.
- 30

34. The compound according to any one of claims 31 to 33, wherein the fluorophore (F₁) is:

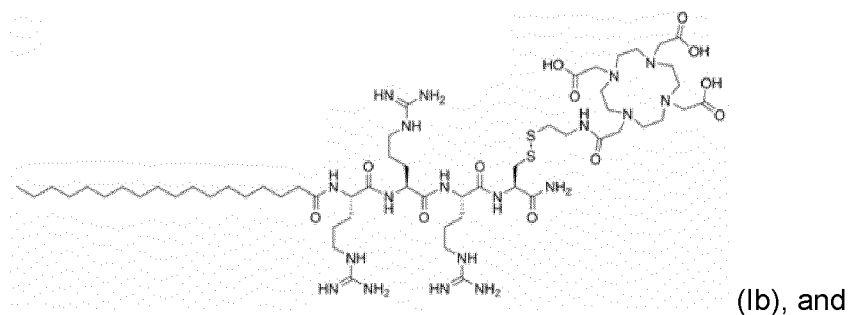
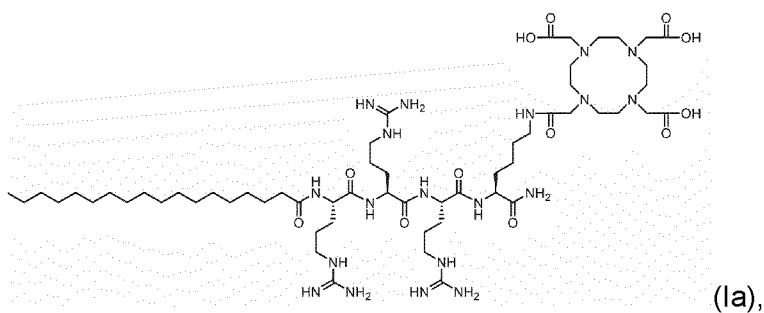


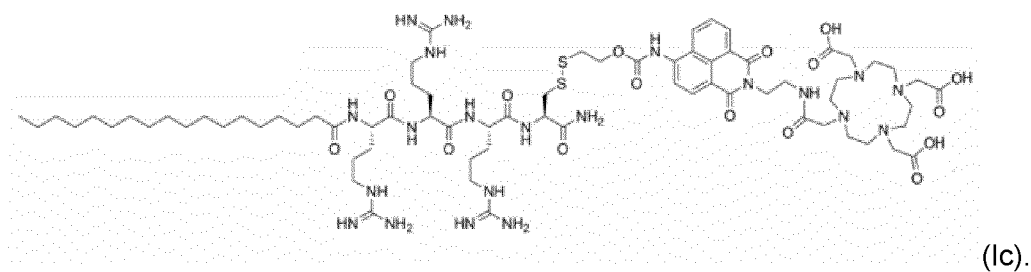
5 wherein a wavy bond “” indicates by intersection the bond connected to L₁ or Z₁ of the compound as represented by formula (I).

35. The compound according to any one of the preceding claims, wherein:

- 10
- a. the chelator group (Z₁) is DOTA,
 - b. the cationic peptide sequence (P₁) is RRR, and
 - c. the lipophilic aliphatic group (A₁) is a non-branched C17 alkyl.

15 36. The compound according to any one of the preceding claims, wherein the compound is selected from the group consisting of:

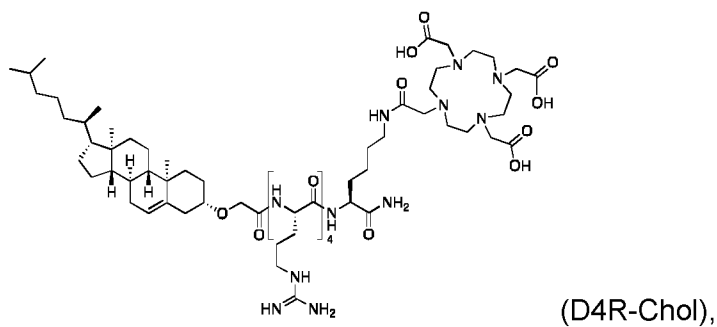
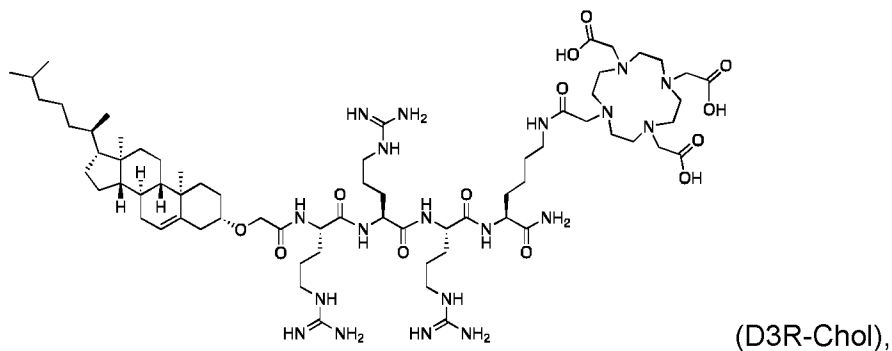


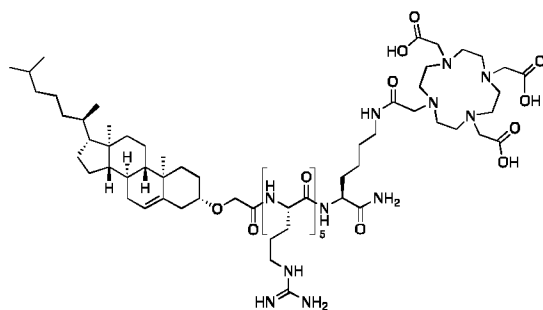


37. The compound according to any one of the preceding claims, wherein:

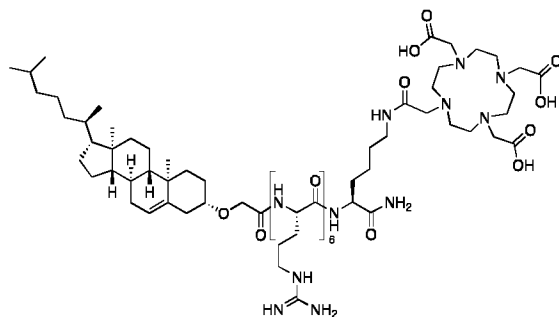
- 5
 - a. the chelator group (Z_1) is DOTA,
 - b. the cationic peptide sequence (P_1) is RRR, RRRR, RRRRR, or RRRRRR and
 - c. the lipophilic aliphatic group (A_1) is a sterol.

10 38. The compound according to any one of the preceding claims, wherein the compound is selected from the group consisting of:





(D5R-Chol), and



(D6R-Chol).

39. The compound according to any one of the preceding claims, further comprising a
5 radionuclide, optionally chelated to the chelator group (Z_1).
40. The compound according to claim 39, wherein the radionuclide decays by emission of particles or photons.
- 10 41. The compound according to any one of claims 39 to 40, wherein the radionuclide is selected from the group consisting of alpha emitters, beta emitters, X-ray emitters, auger emitters and gamma emitters.
42. The compound according to any one of claims 39 to 41, wherein the radionuclide is
15 a beta emitter.
43. The compound according to any one of claims 39 to 42, wherein the radionuclide is selected from the group consisting of: P-32, Y-90, Sm-153, Er-169, Lu-177, Cu-67, Sc-47, As-76, Te-161, At-211, Ac-225, Bi-212, Bi-213, Ra-223, Pd-212, Te-149,
20 Ra-224, Pd-103, La-135, Er-165, I-125, I-123, Rh-103m, Co-58m, In-111, Au-198, Co-60, Cs-137, and Ir-192, I-125 and Cf-252, Am-241, Pd-103, Yb-169, Se-75 and Sm-145.

44. The compound according to any one of claims 39 to 42, wherein the radionuclide is selected from the group consisting of: Cu-64, Mn-52, Ga-67, and Lu-177.
45. A method for labelling cells comprising the steps of:
- 5 a. providing a compound as defined in any one of the preceding claims,
- b. providing cells from a subject, and
- c. contacting the compound with the cells in vitro.
46. The method according to claim 45, further comprising a step of providing a
- 10 radionuclide, and subsequently contacting the radionuclide with the compound as defined in any one of the preceding claims.
47. The method according to any one of claims 45 to 46, further comprising the steps of:
- 15 d. administering the cells to the subject, and
- e. tracking the labelled cells using an imaging modality.
48. The method according to any one of claims 45 to 47, wherein a further imaging modality is used.
- 20 49. The method according to any one of claims 47 to 48, wherein the imaging modality and/or the further imaging modality are selected from the group consisting of: PET and SPECT.
- 25 50. The method according to any one of claims 47 to 49, wherein the tracking comprises the use of flow cytometry of organ cell suspensions from the subject.
- 30 51. The method according to any one of claims 45 to 50, wherein the cells are selected from the group consisting of: T-lymphocytes, neutrophilic granulocytes, monocytes and cancer cells.
52. The method according to any one of claims 45 to 51, wherein the method is used in combination with adoptive cell transfer.

53. The method according to any one of claims 45 to 51, wherein the method is used in combination with immunotherapy.
54. The method according to any one of claims 45 to 53, wherein the method is used in combination with chemotherapy.
55. Use of a compound as defined in any one of claims 1 to 44 for tracking cell proliferation, differentiation, and/or function.
56. A micelle comprising a plurality of compounds as defined in any one of claims 1 to 44.
57. The micelle according to claim 56, wherein the compound is saturated by one or more cations, optionally chelating to the chelator.
58. The micelle according to claim 57, wherein the one or more cations are radioactive or stable isotopes.
59. The micelle according to claim 58, wherein the stable isotopes are Cu-63 and/or Cu-65.
60. A kit for tracking cell proliferation, differentiation, and/or function, comprising:
- a. a compound as defined in any one of claims 1 to 44,
 - b. a solvent, and optionally
 - c. instructions for use

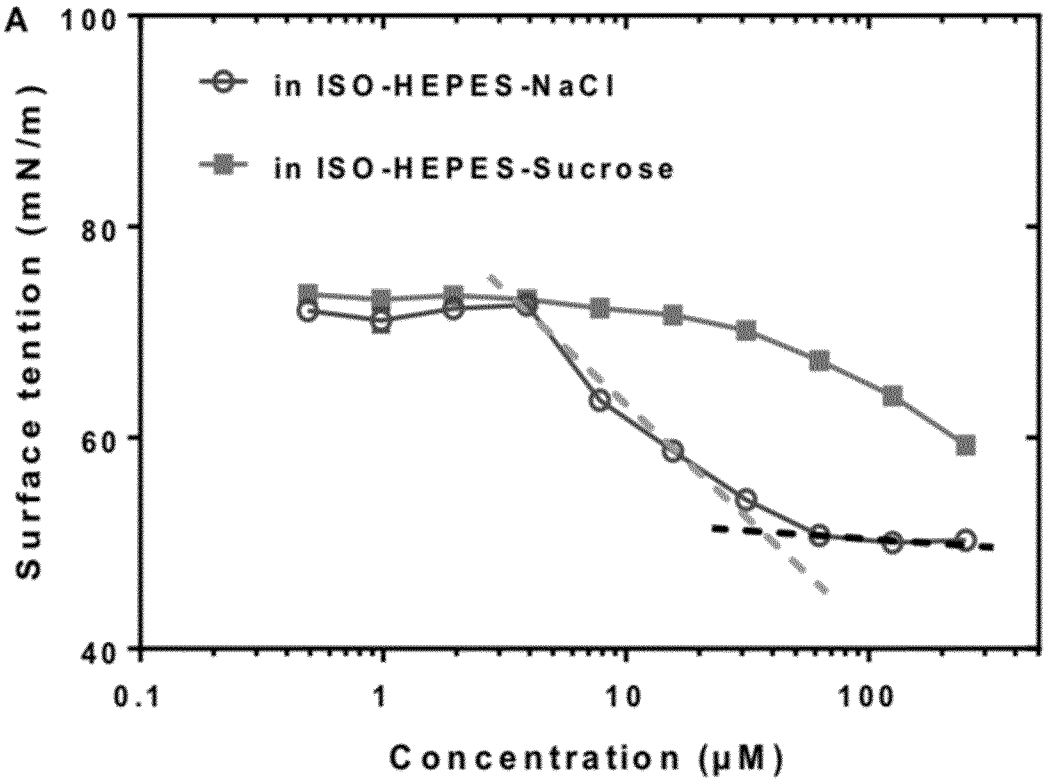


Fig. 1A

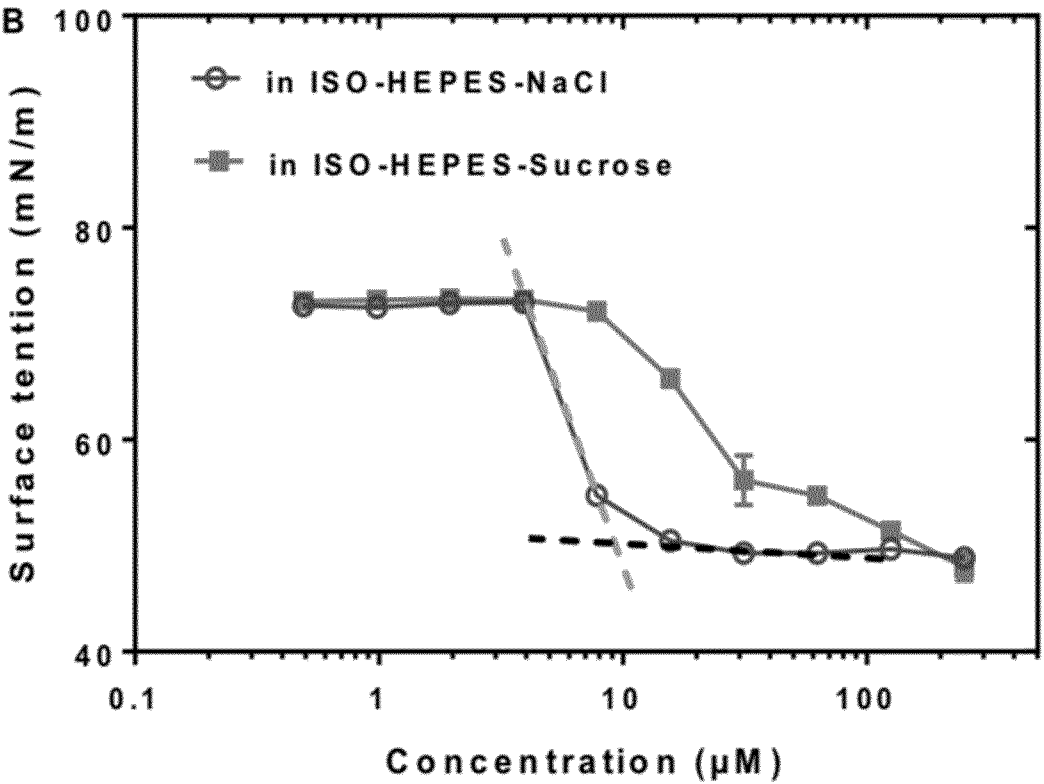


Fig. 1B

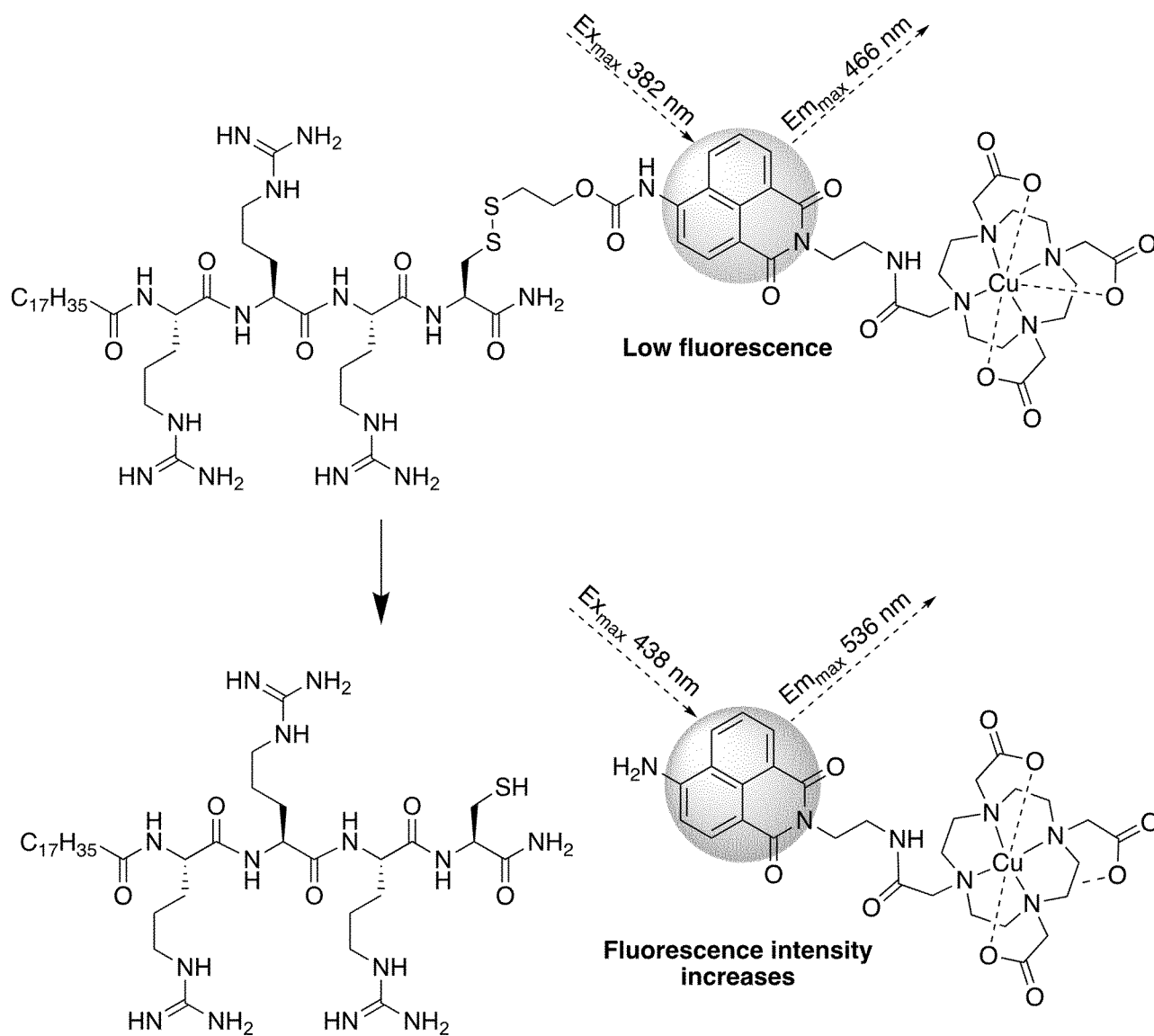


Fig. 2

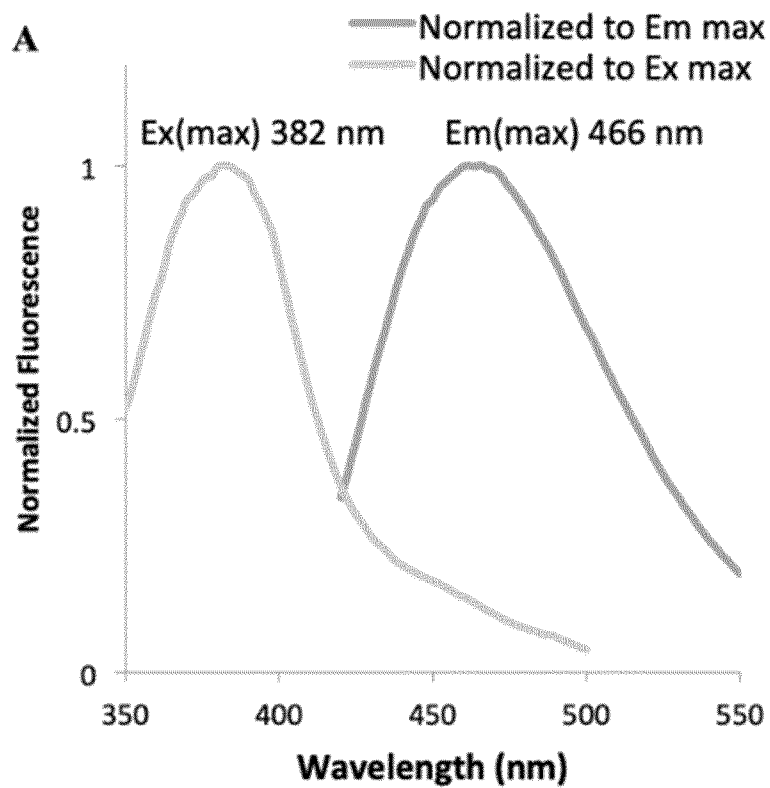


Fig. 3A

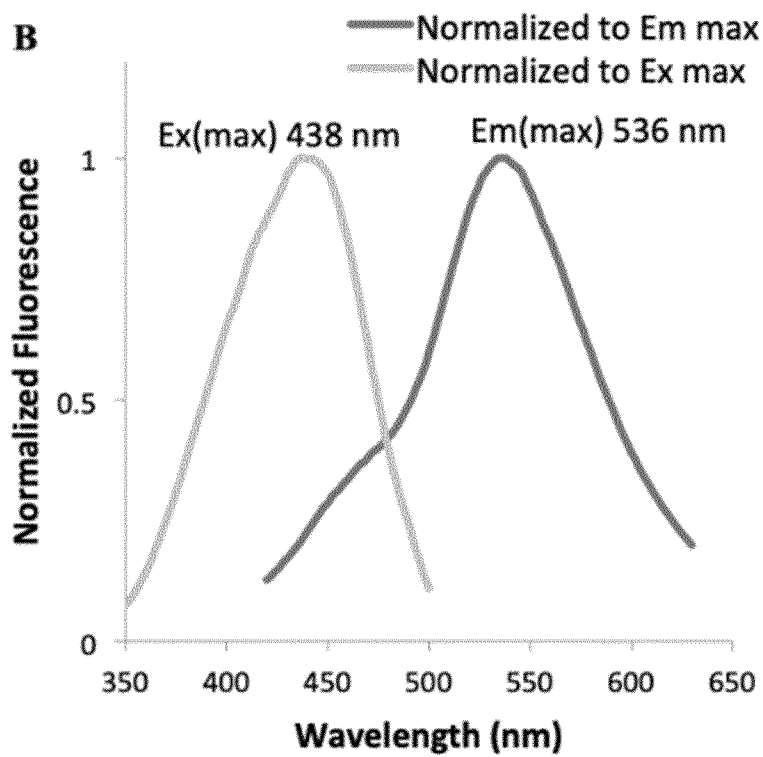


Fig. 3B

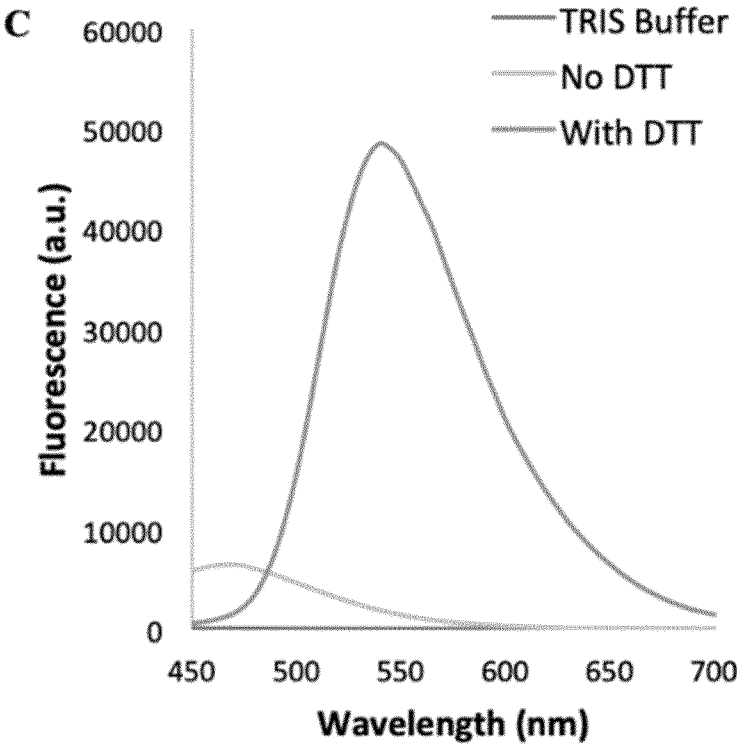


Fig. 3C

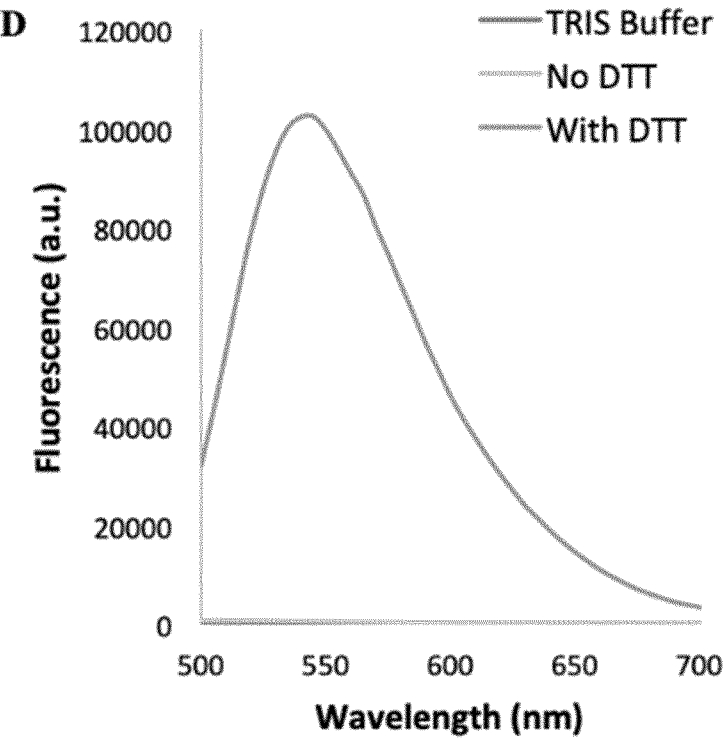


Fig. 3D

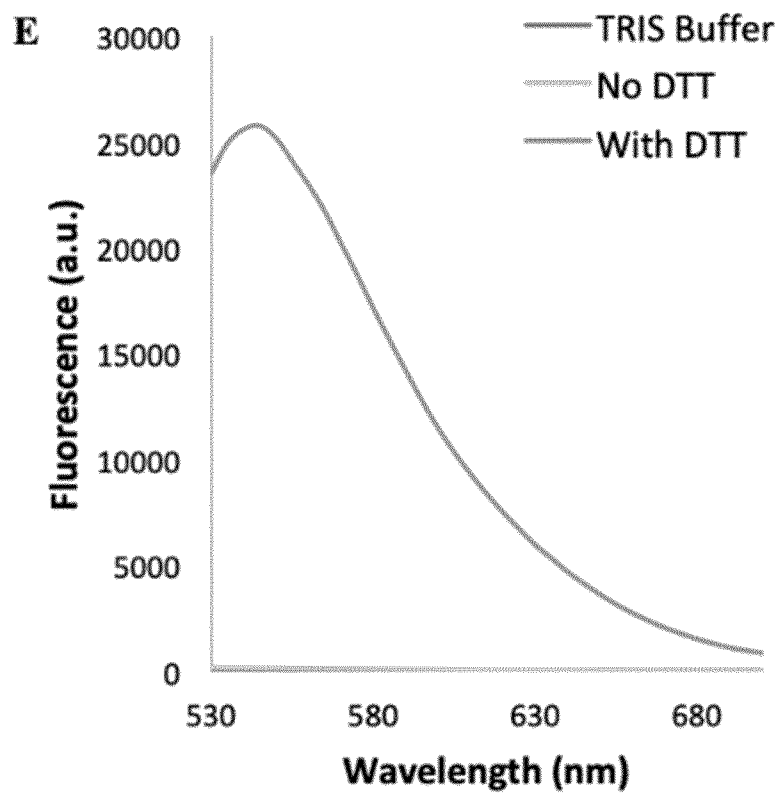


Fig. 3E

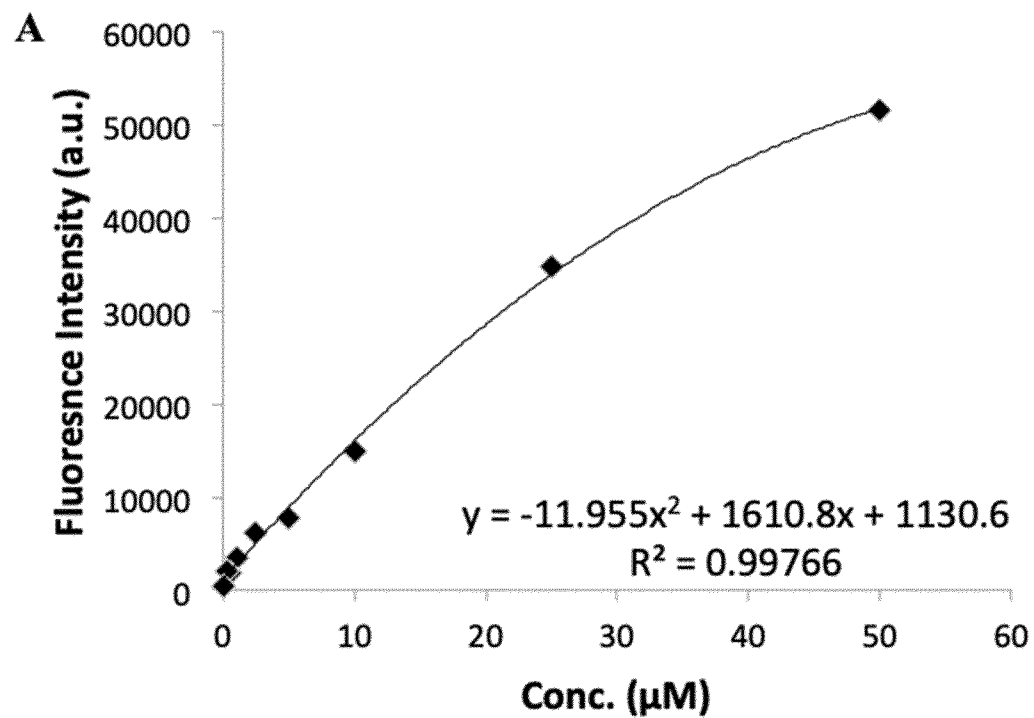


Fig. 4A

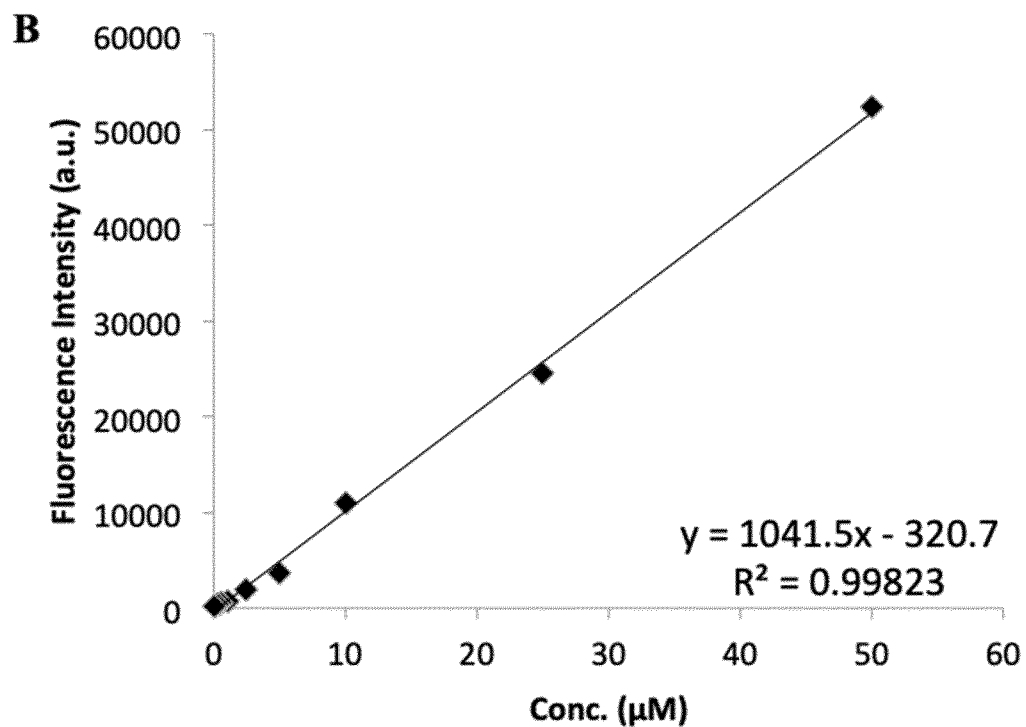


Fig. 4B

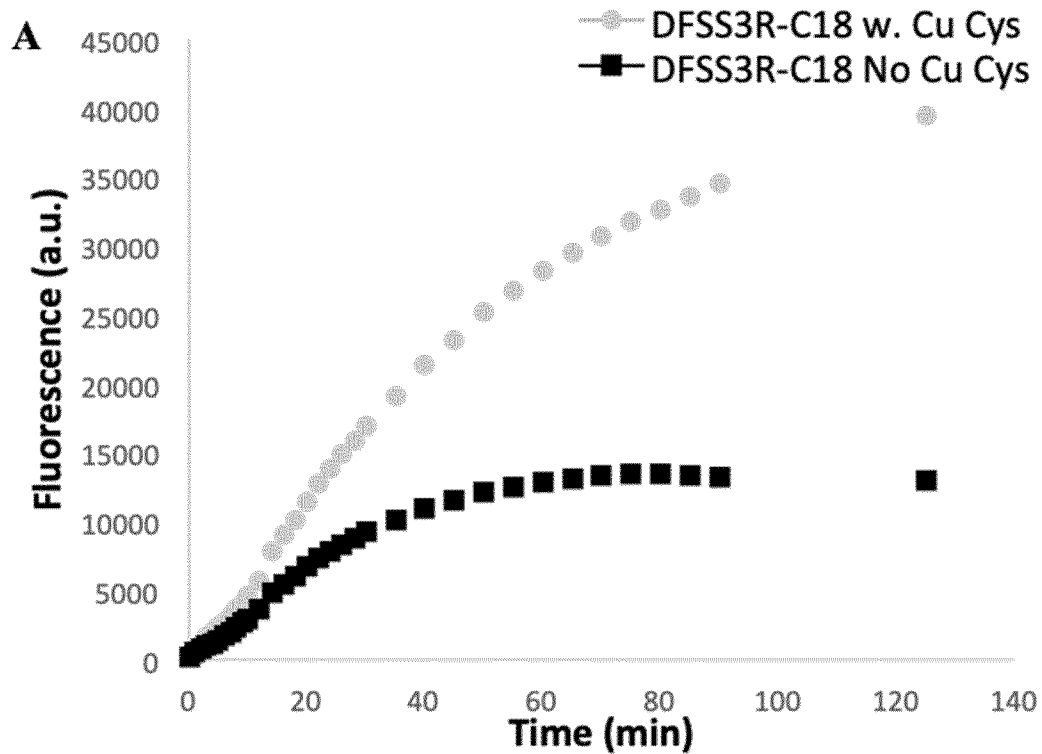


Fig. 5A

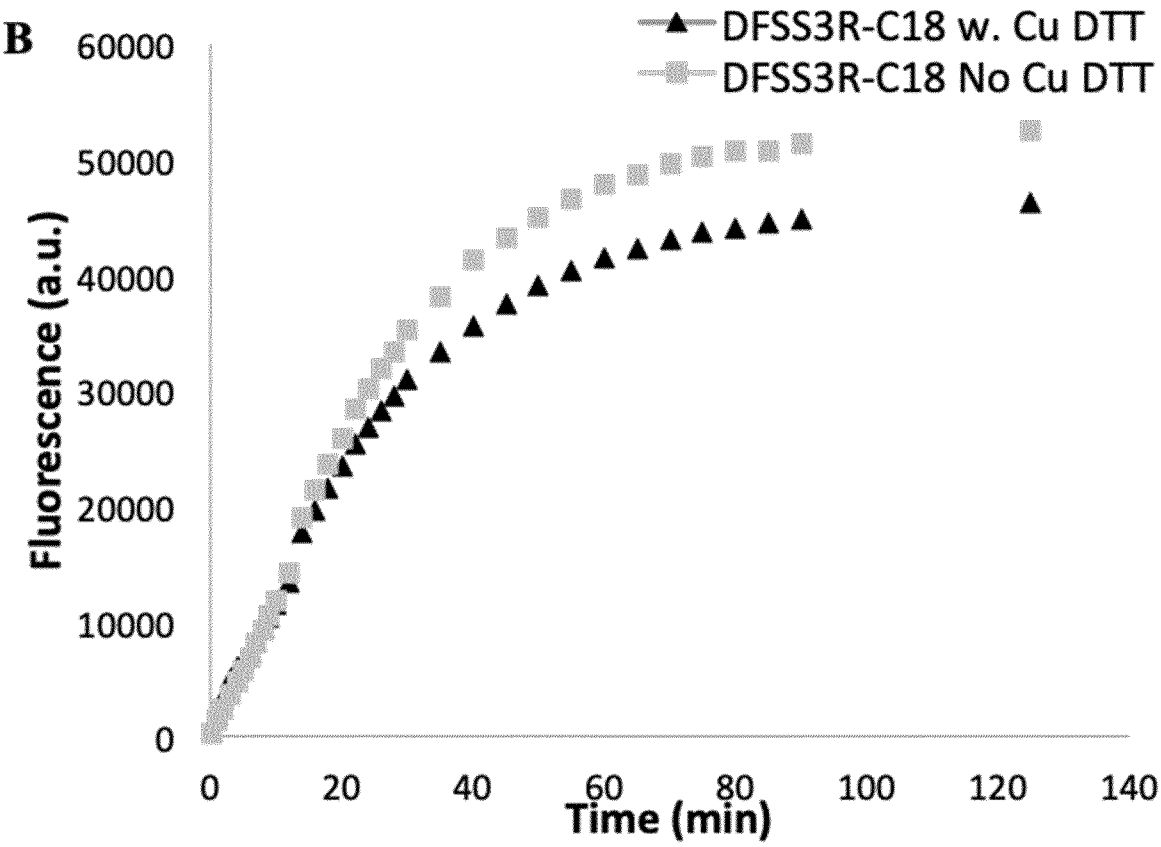


Fig. 5B

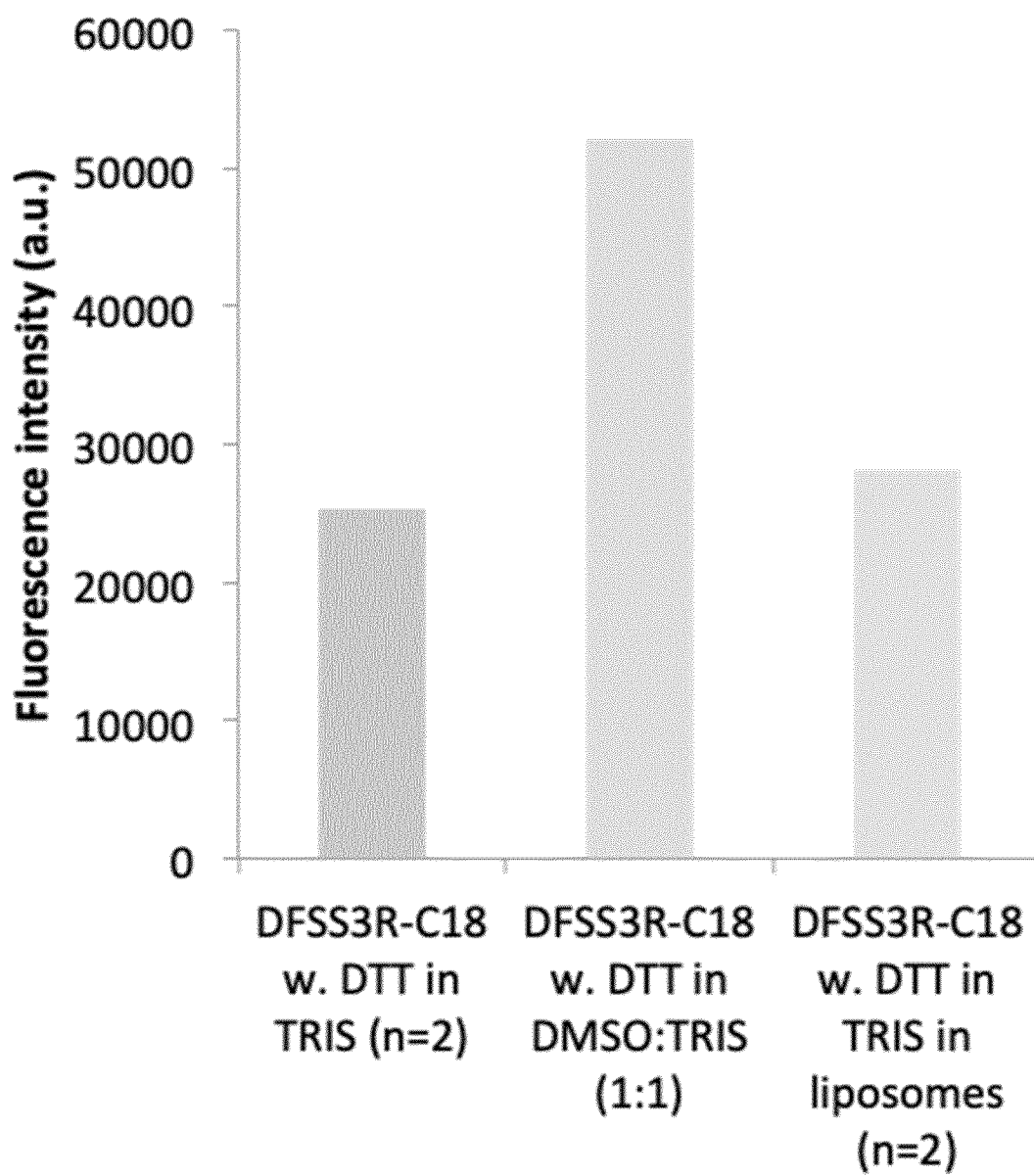


Fig. 6

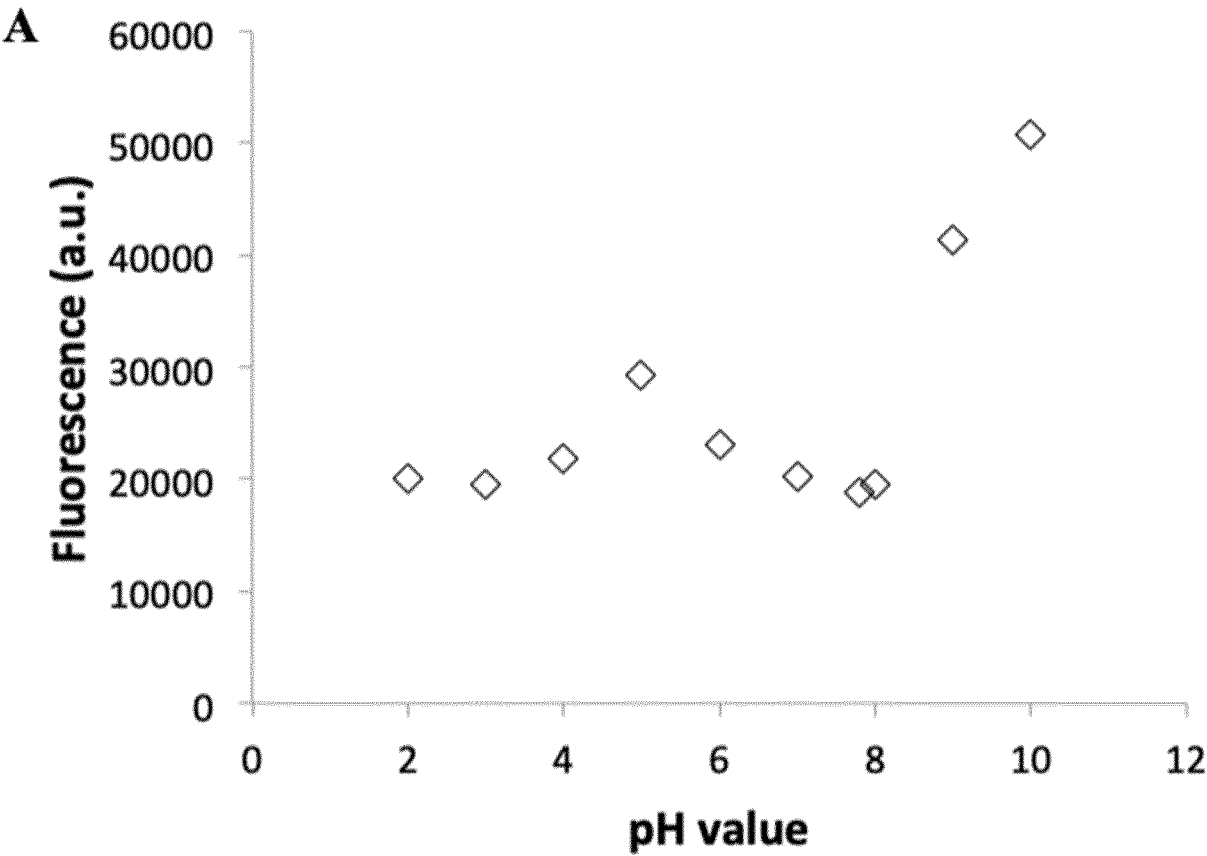


Fig. 7A

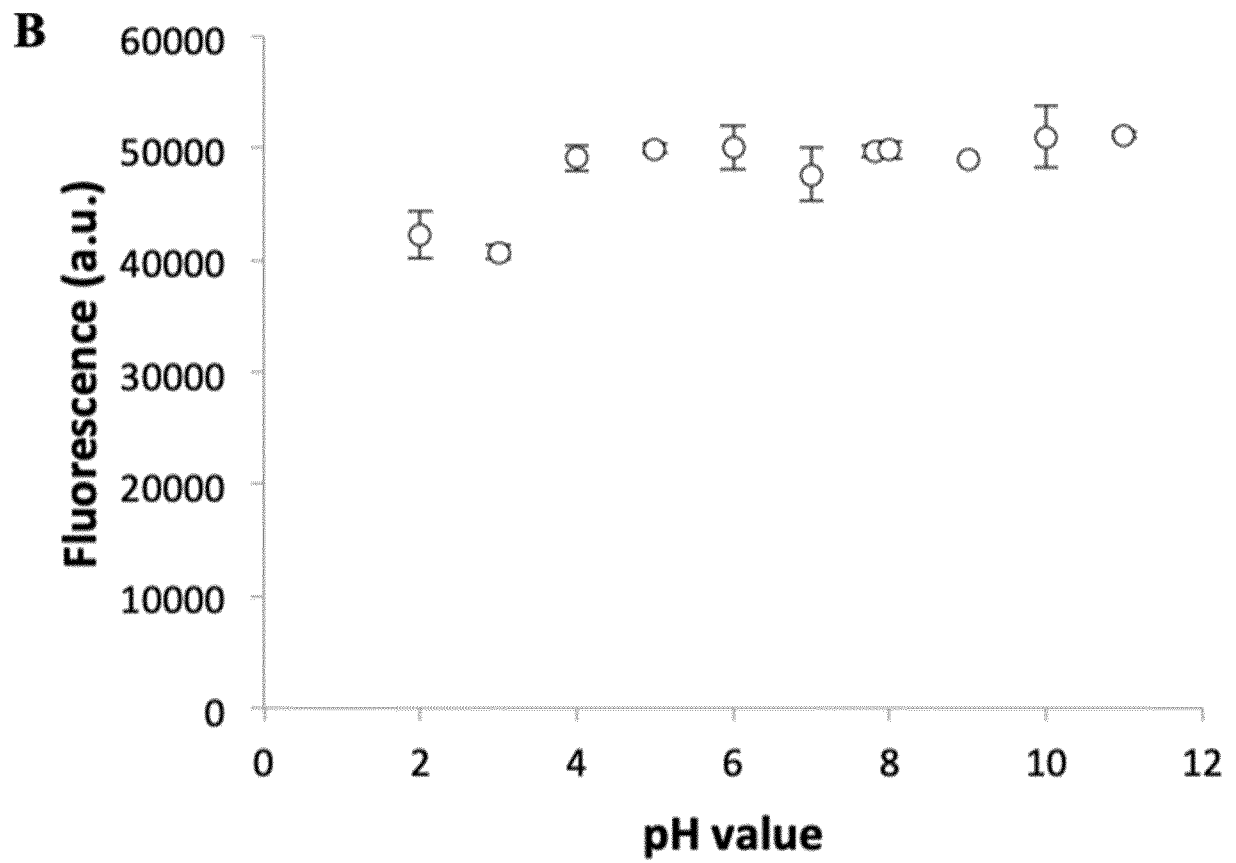


Fig. 7B

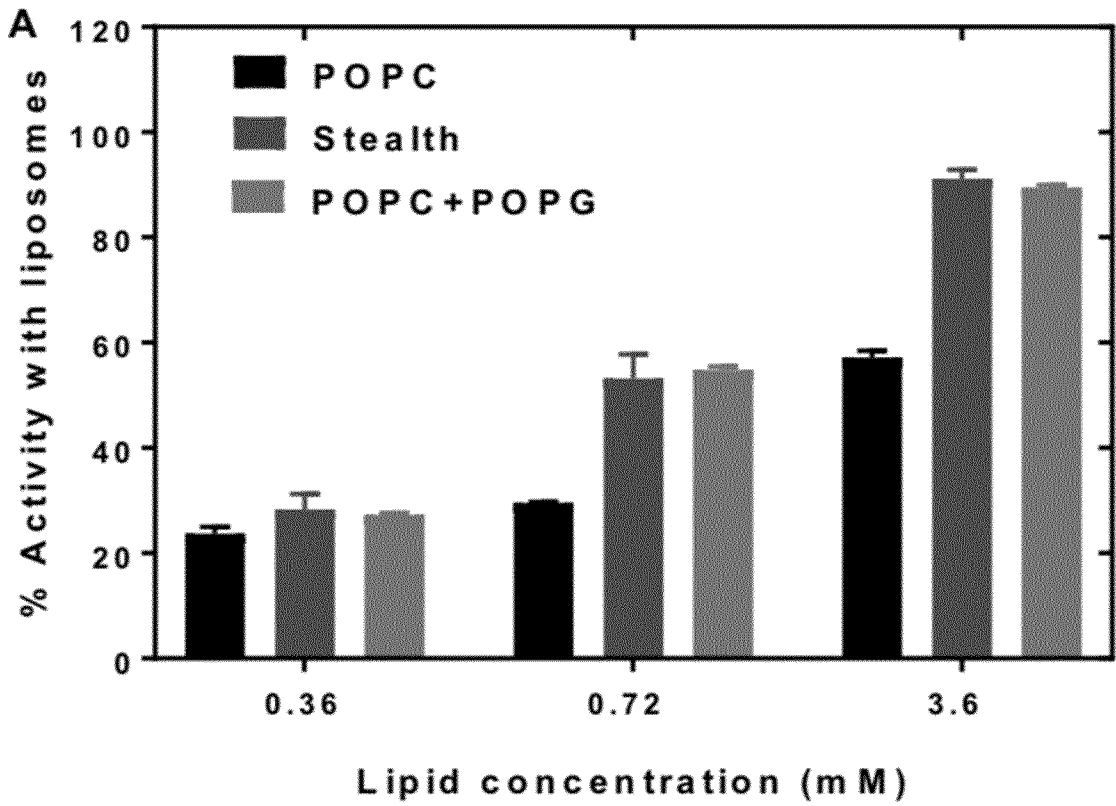


Fig. 8A

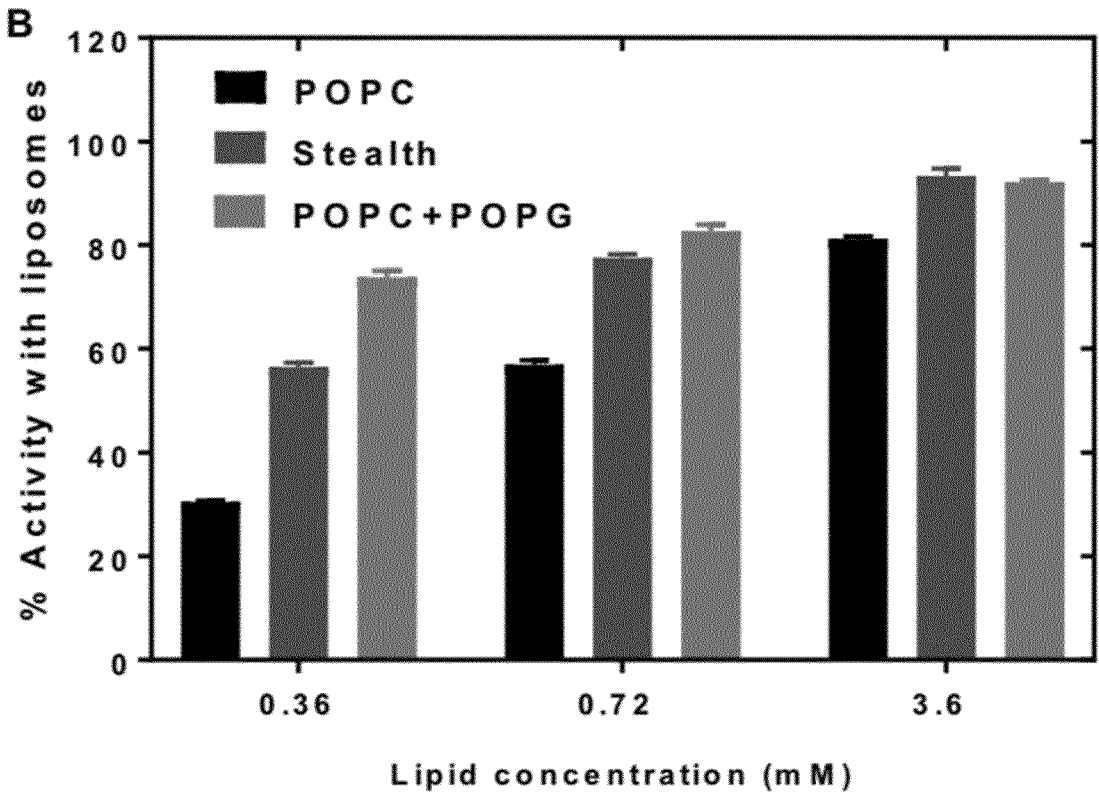


Fig. 8B

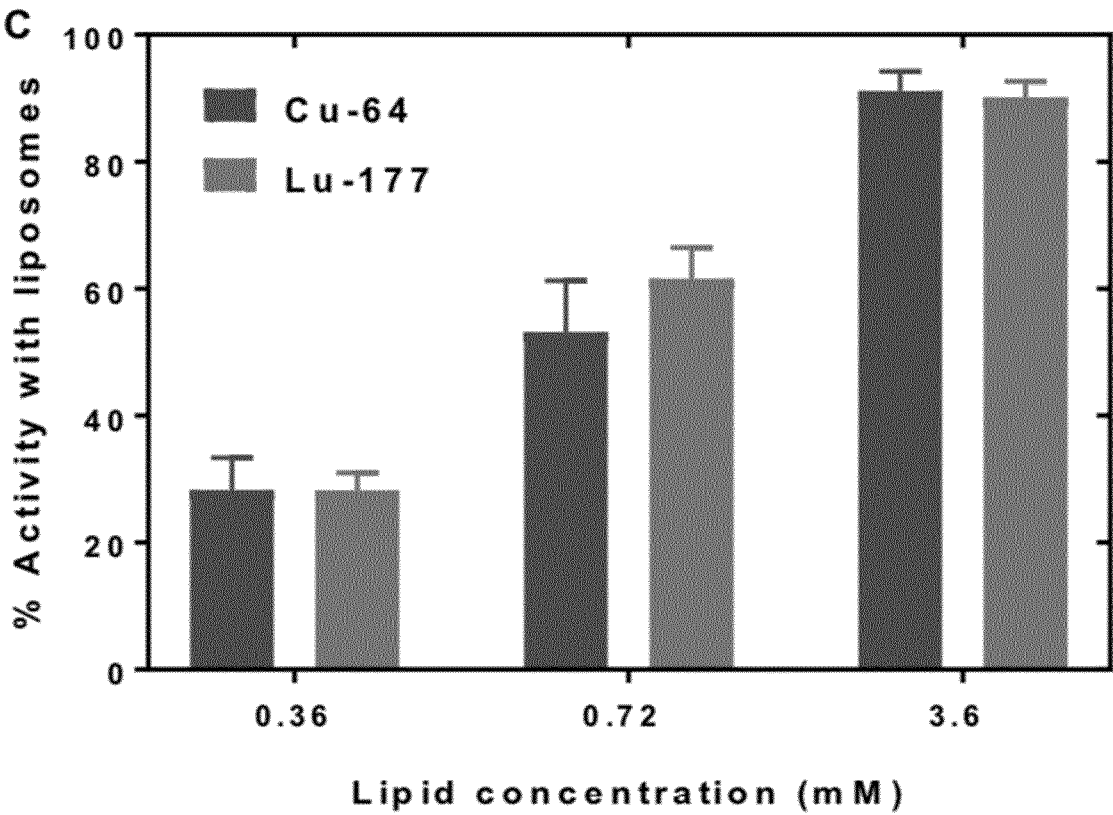


Fig. 8C

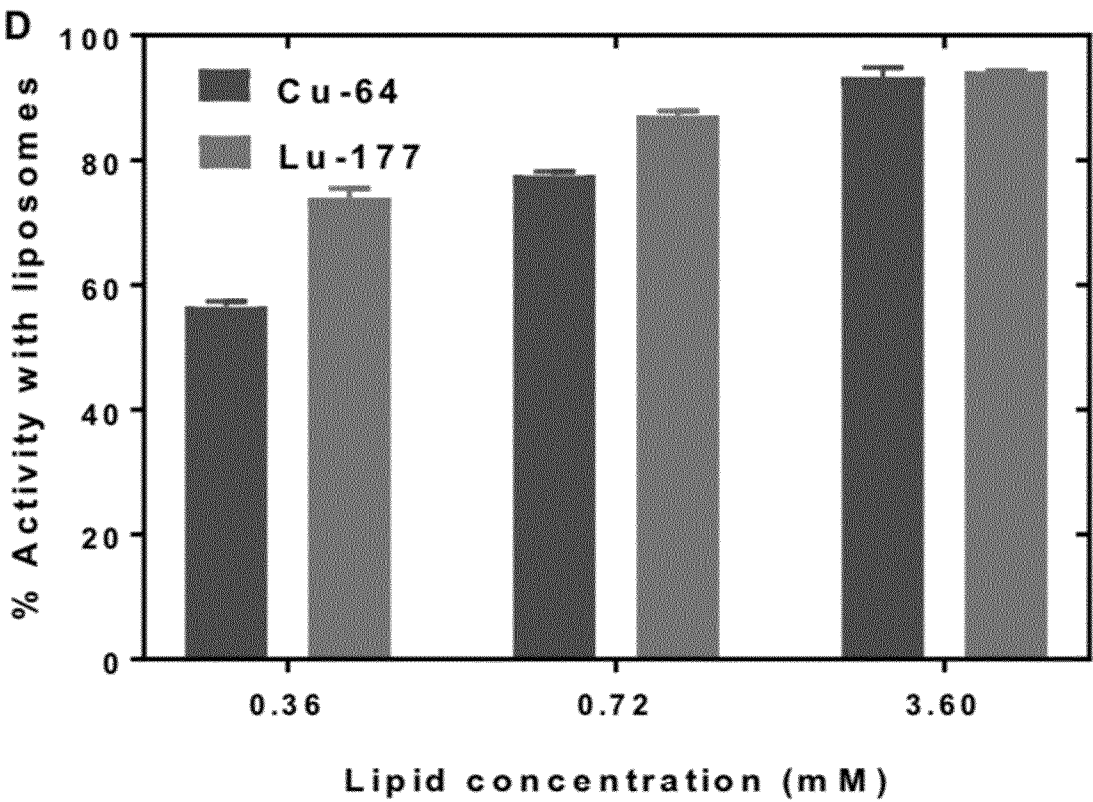


Fig. 8D

A

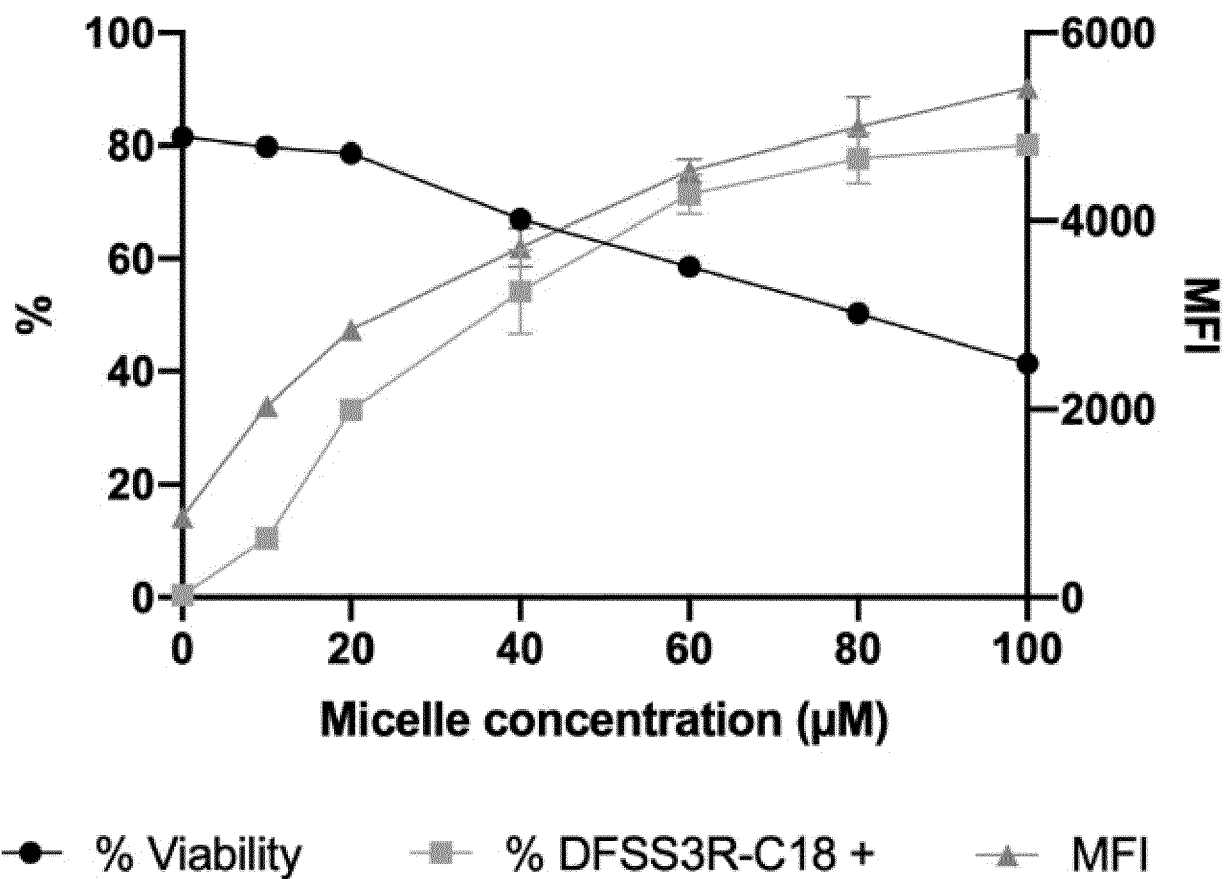
Murine T lymphocytes

Fig. 9A

B

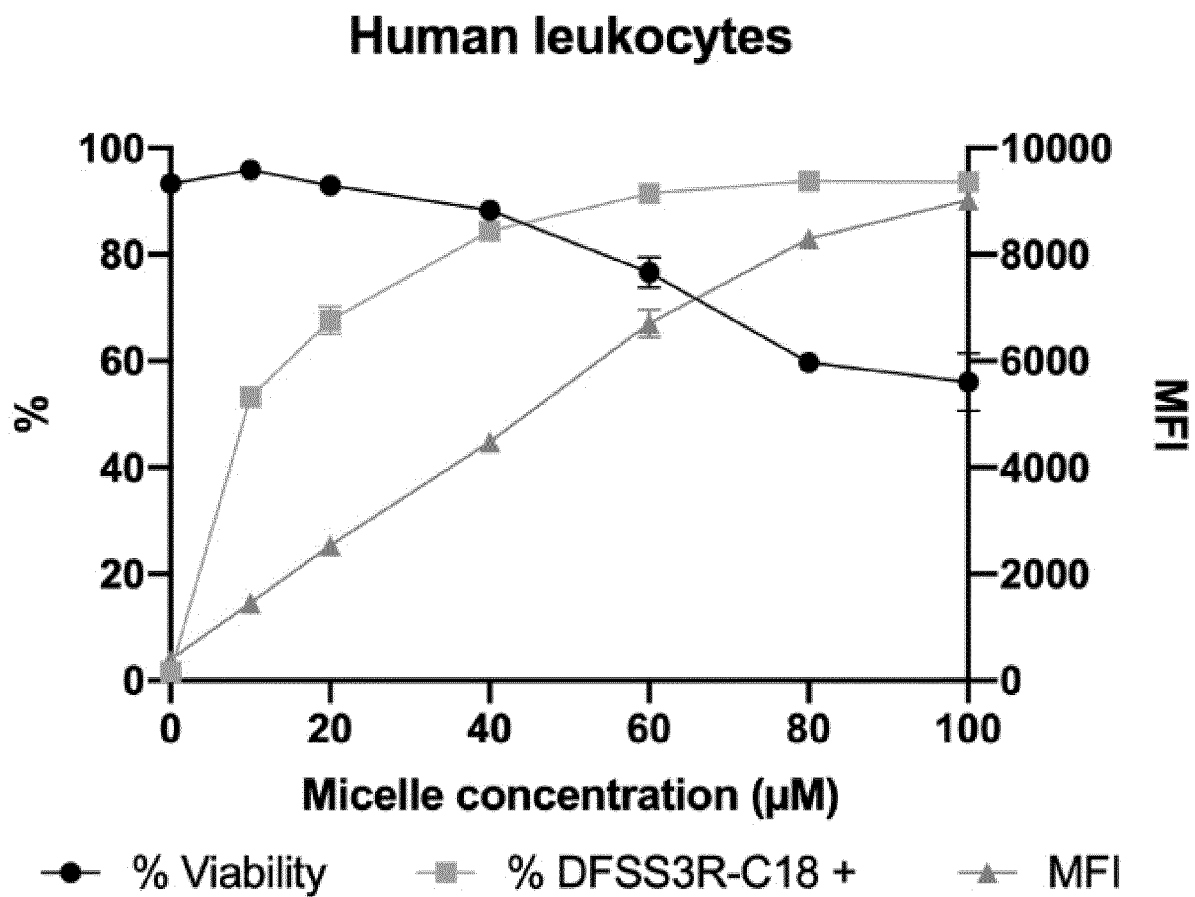


Fig. 9B

A

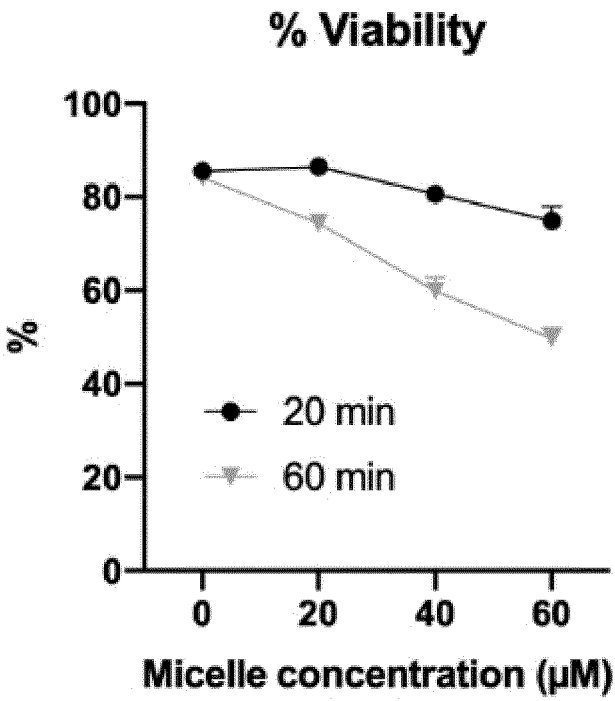


Fig. 10A

B

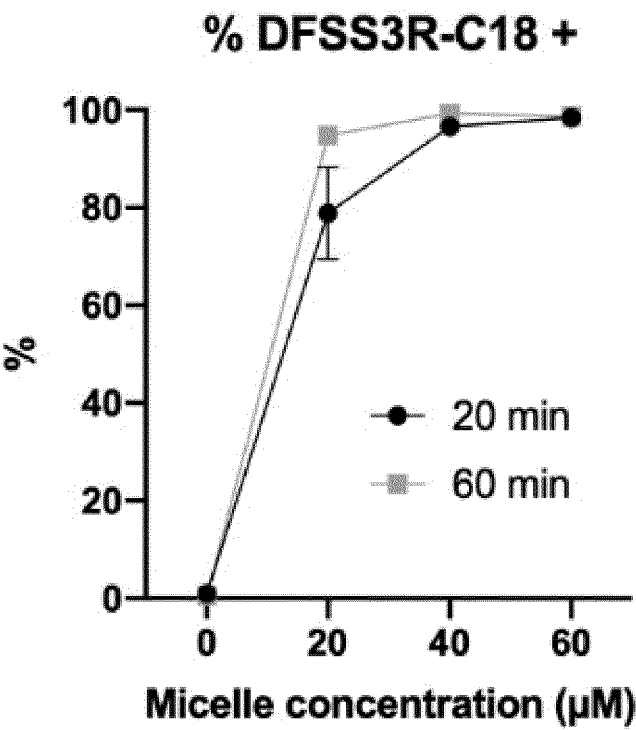


Fig. 10B

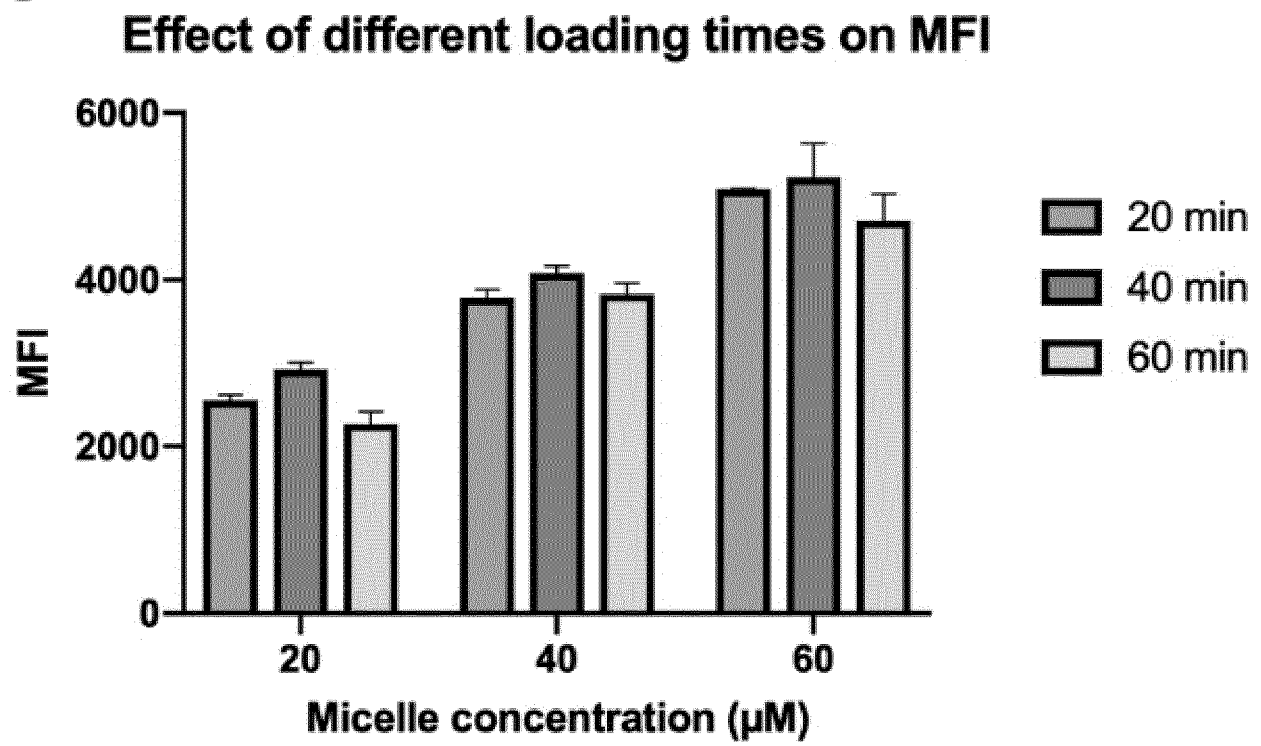
C

Fig. 10C

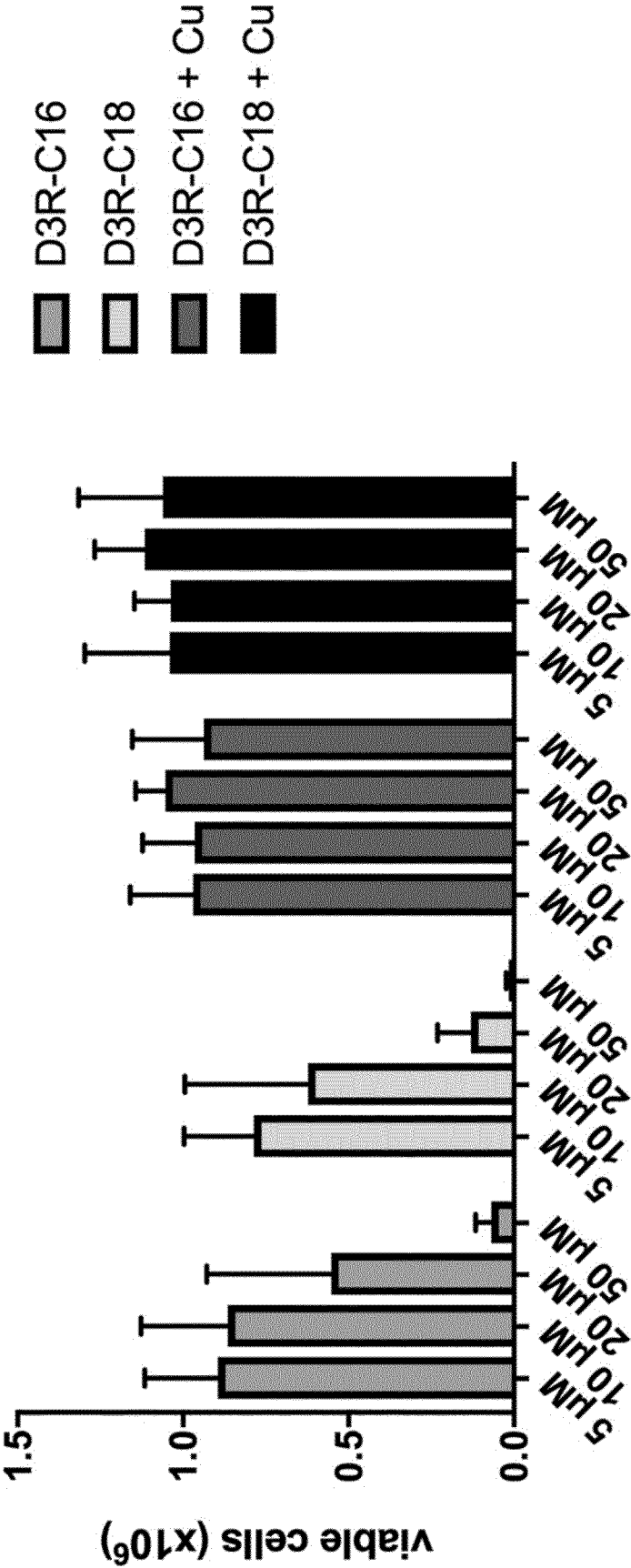


Fig. 11

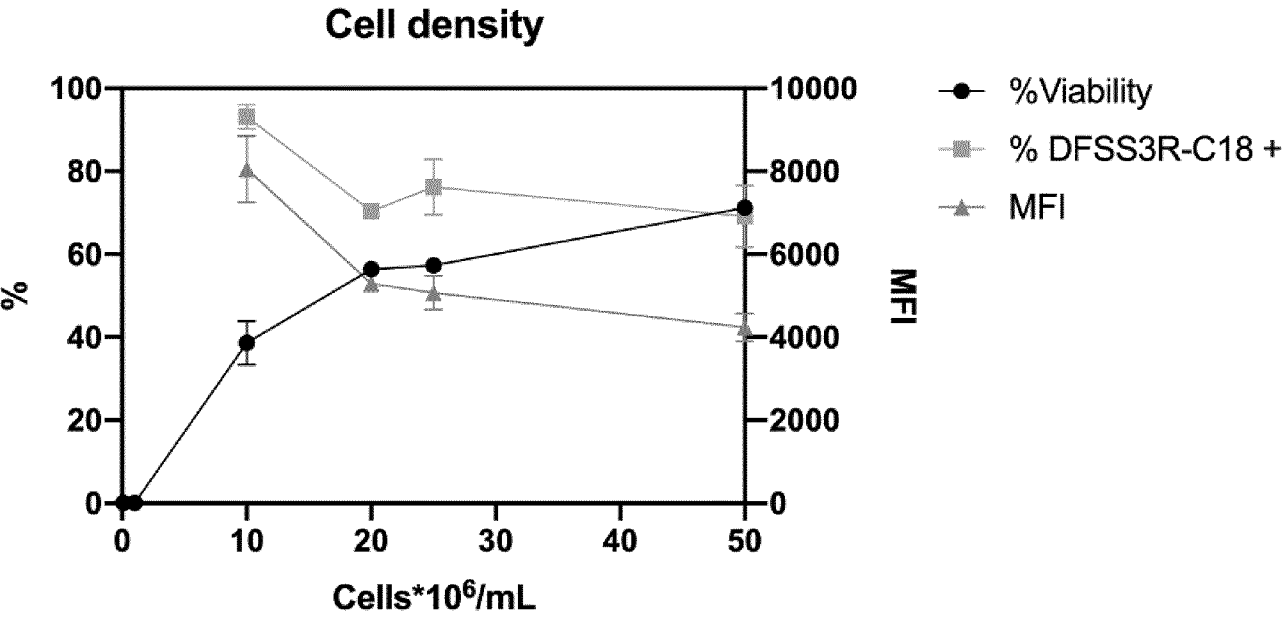


Fig. 12

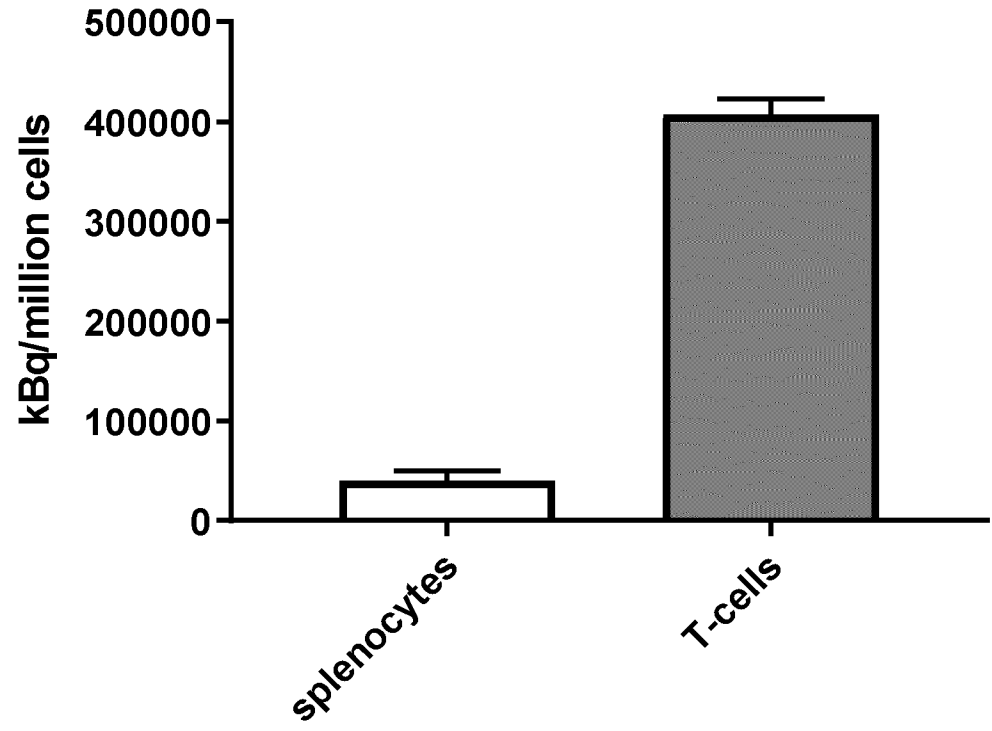


Fig. 13

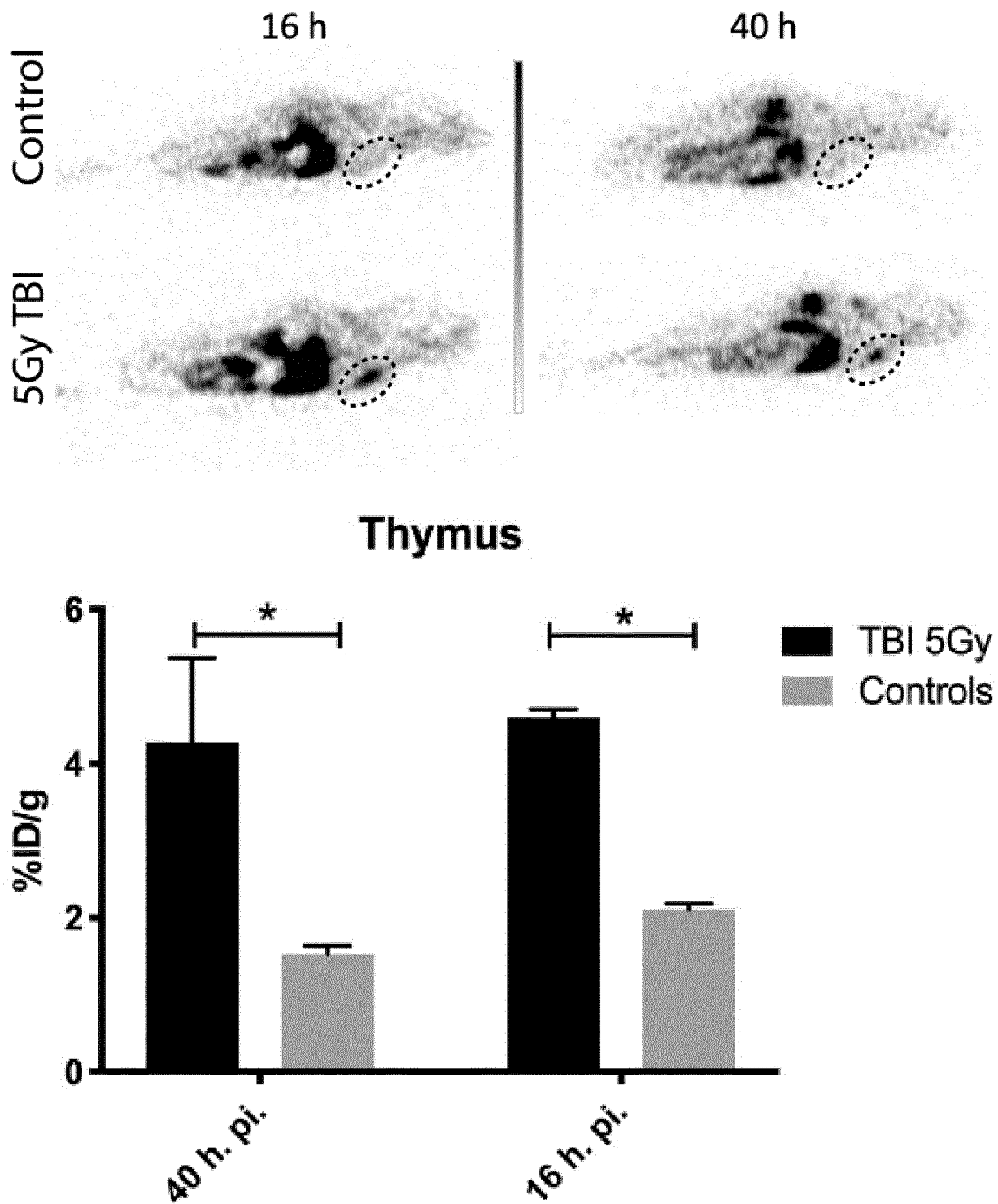


Fig. 14

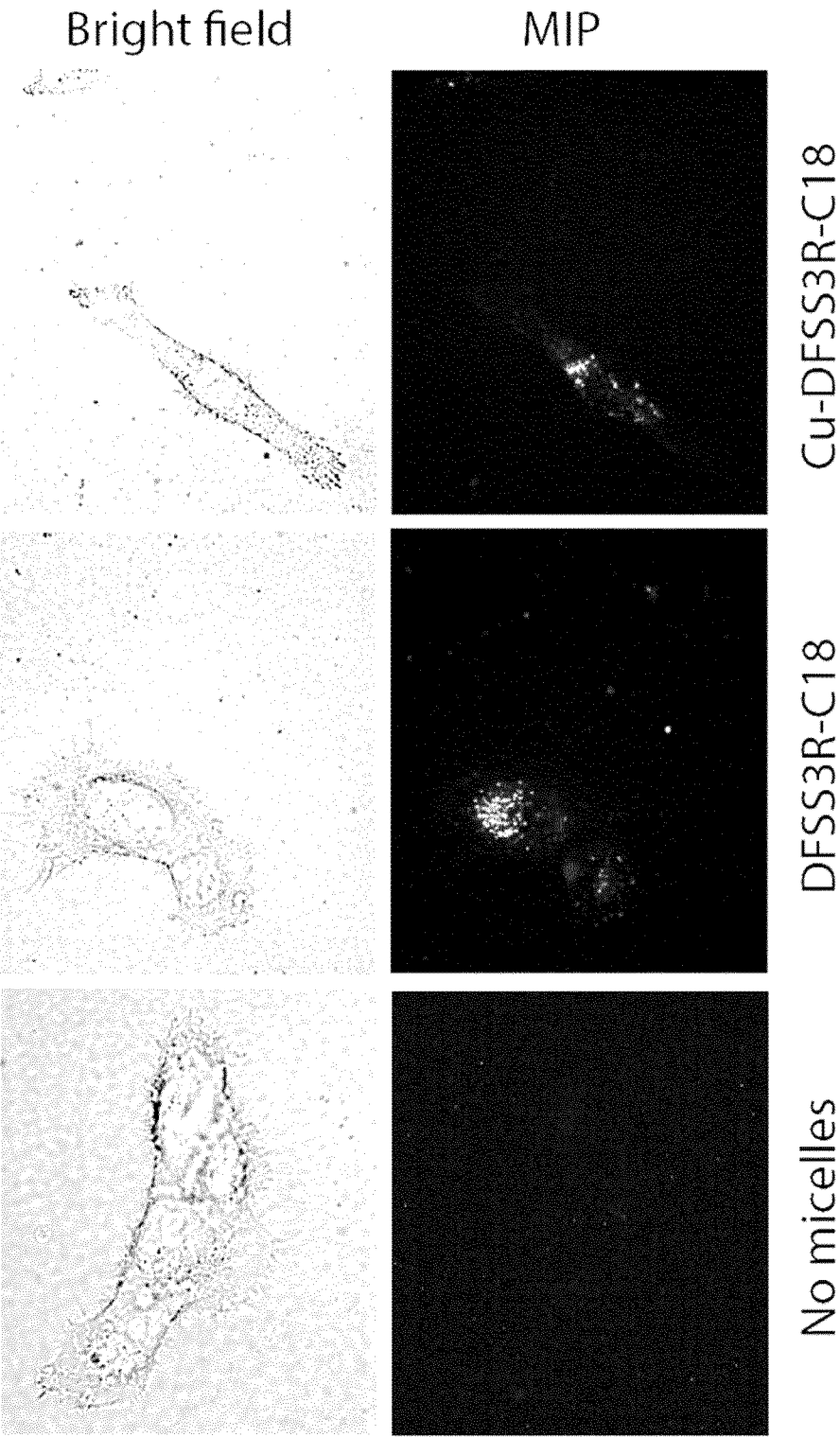


Fig. 15

A

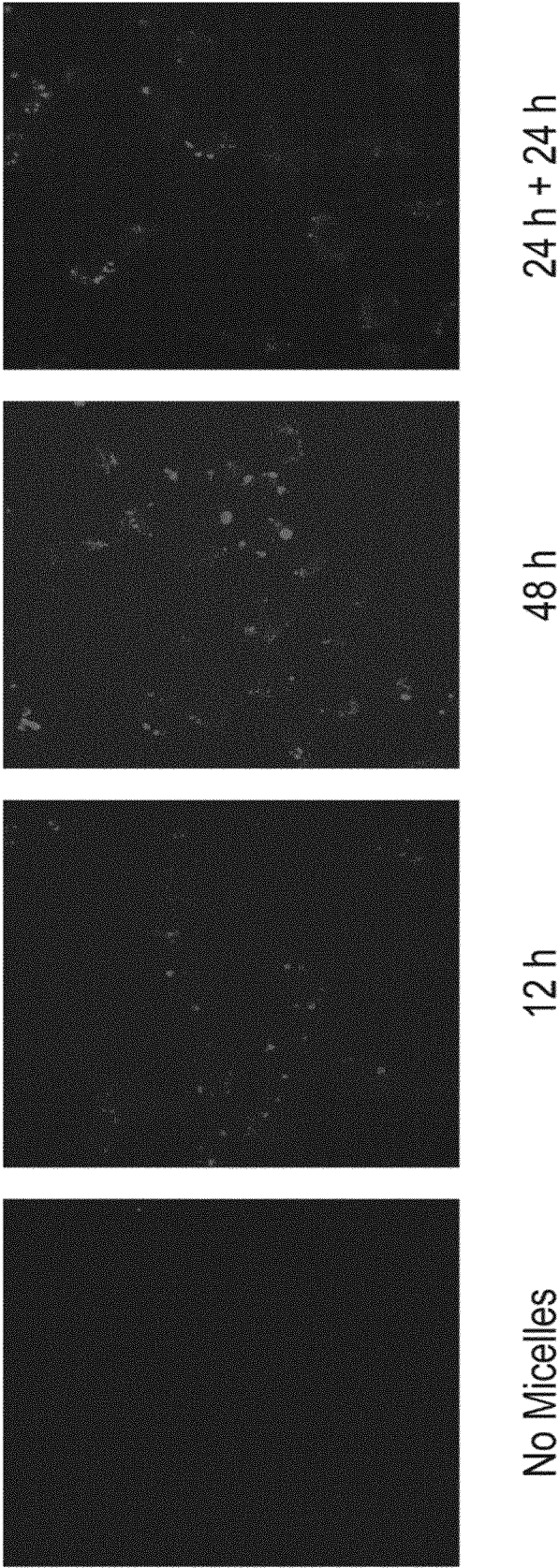


Fig. 16A

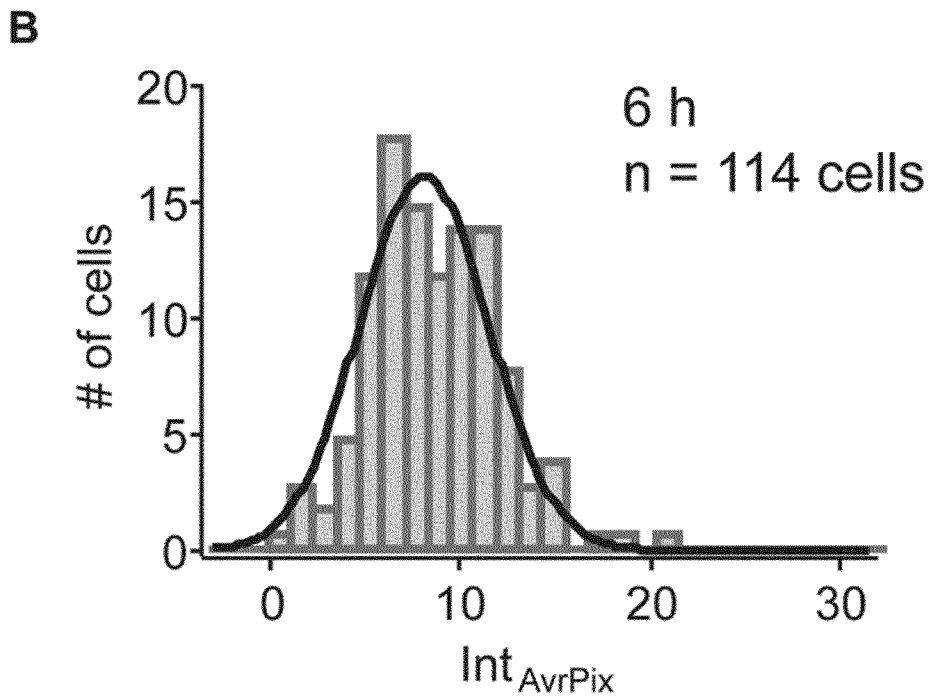


Fig. 16B

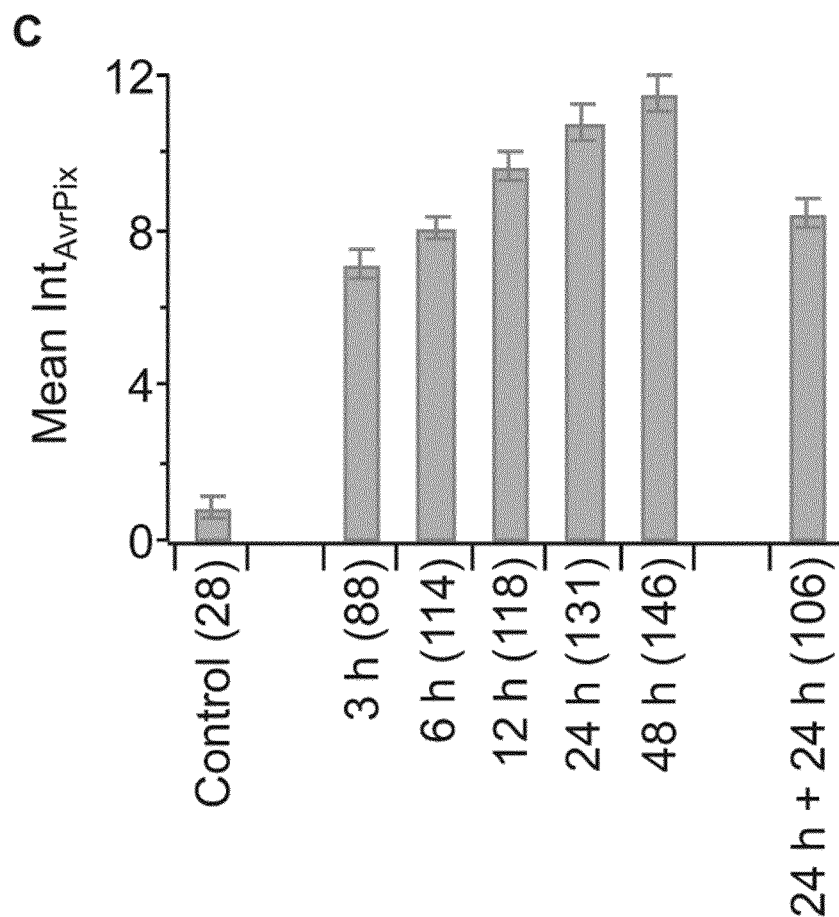


Fig. 16C

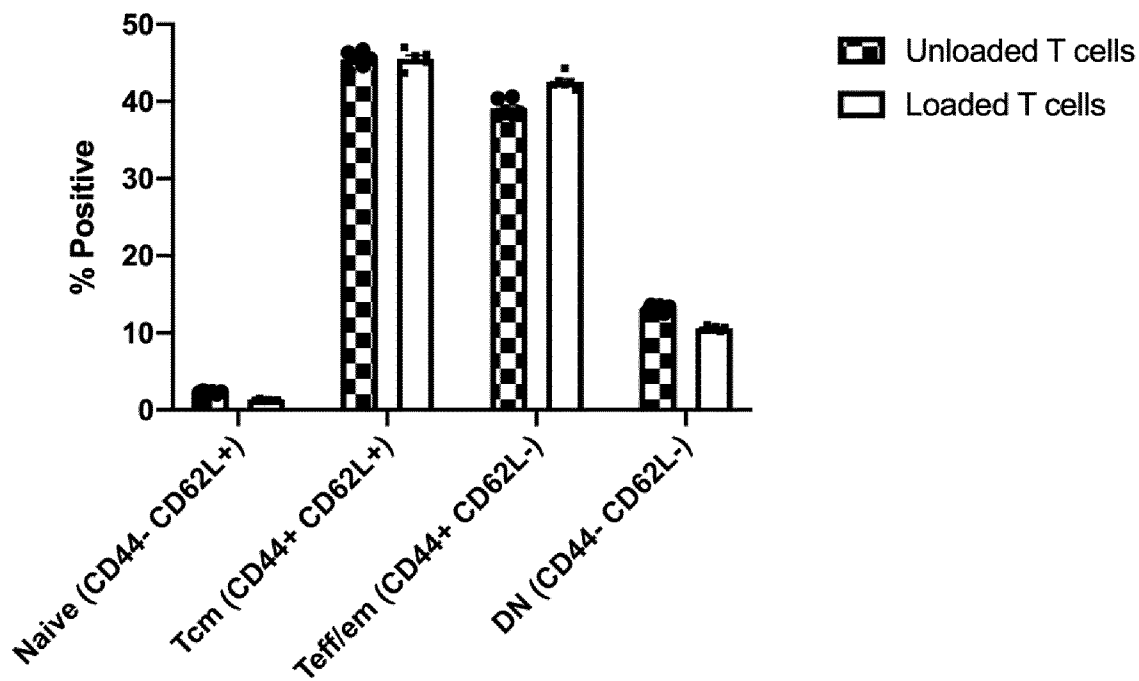
CD8⁺ T cell phenotype 3 days after loading

Fig. 17A

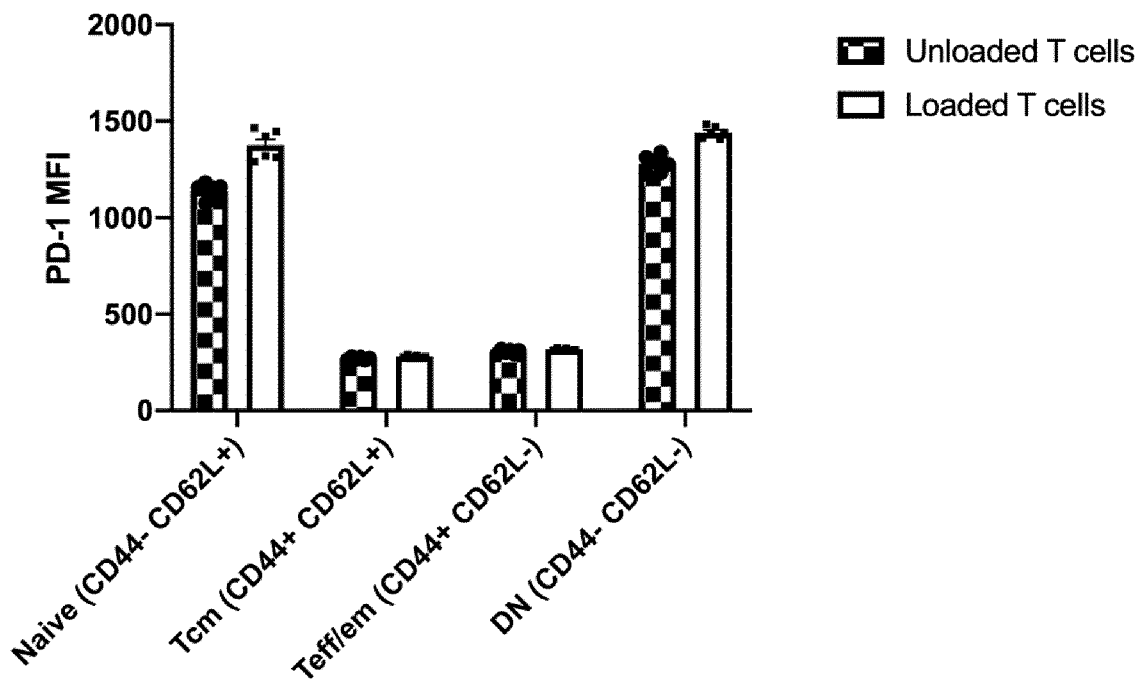
PD-1 expression

Fig. 17B

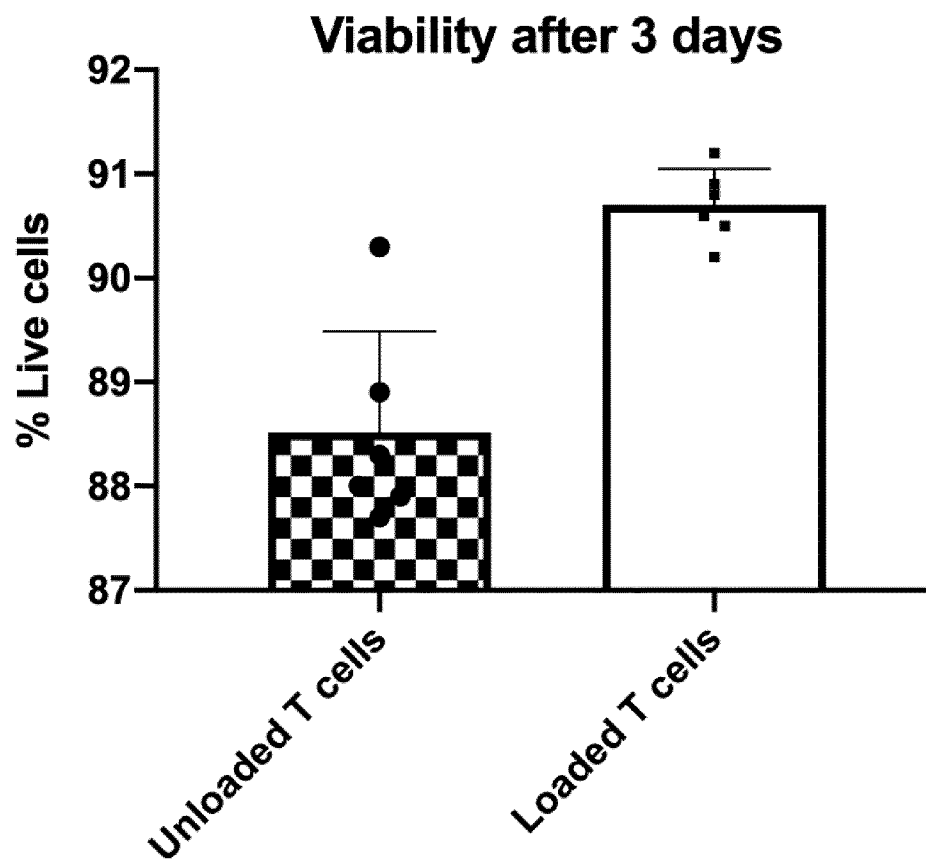


Fig. 17C

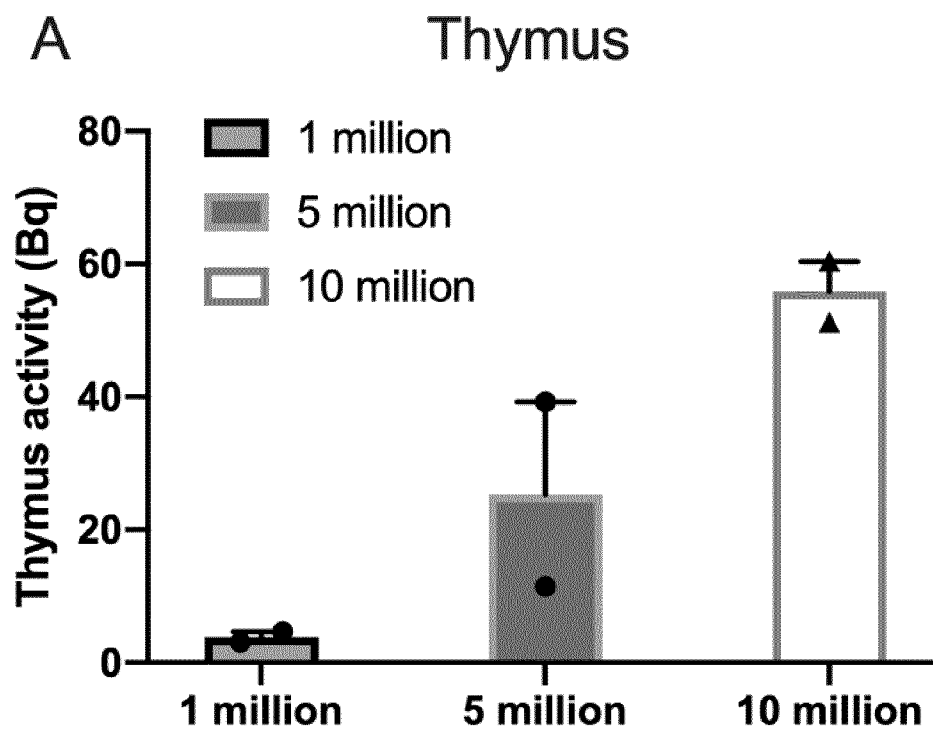


Fig. 18A

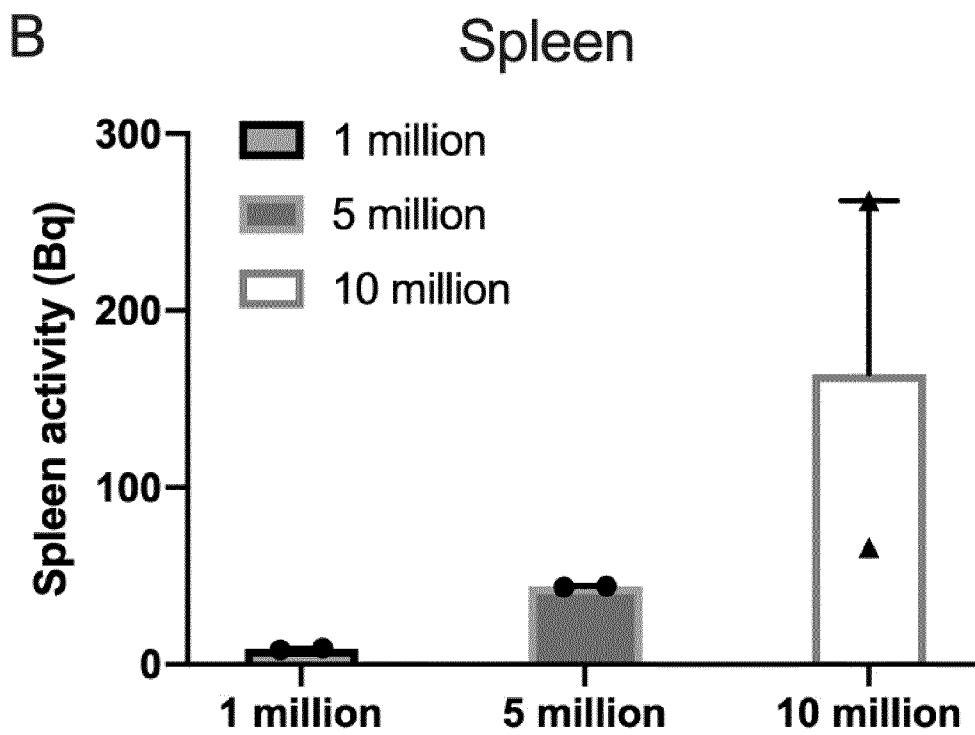


Fig. 18B

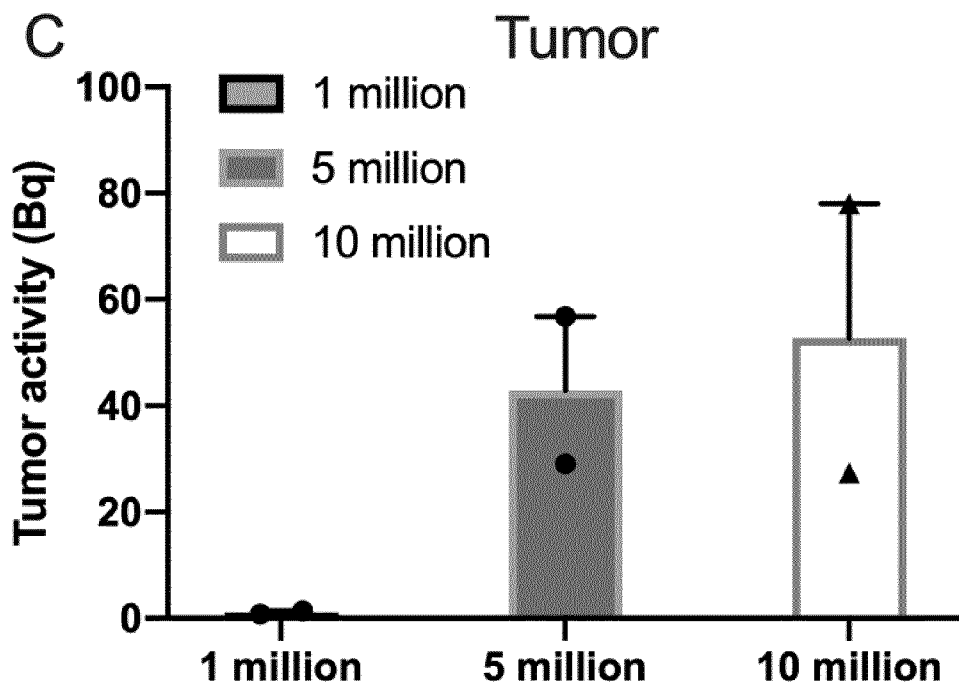


Fig. 18C

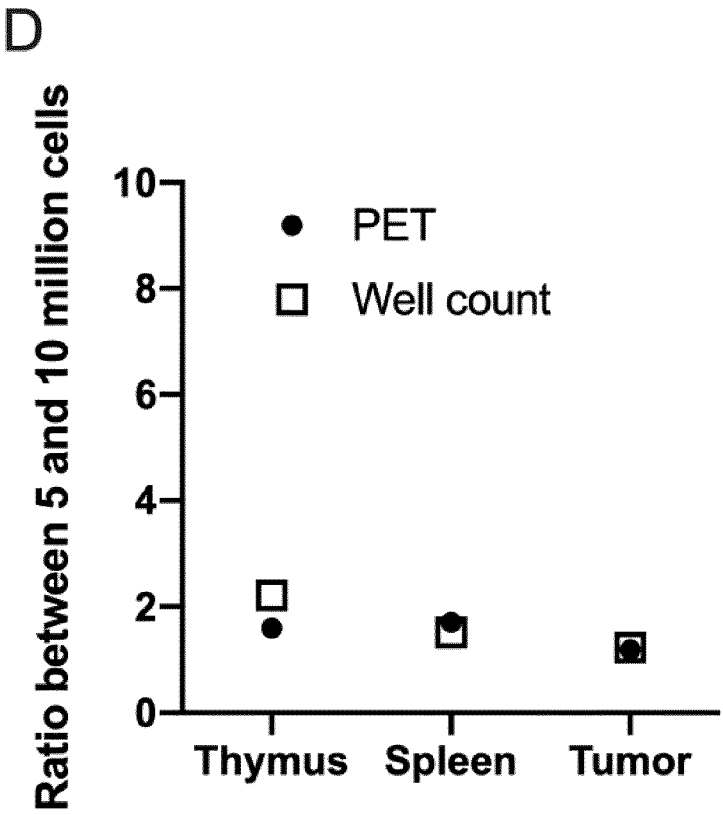


Fig. 18D

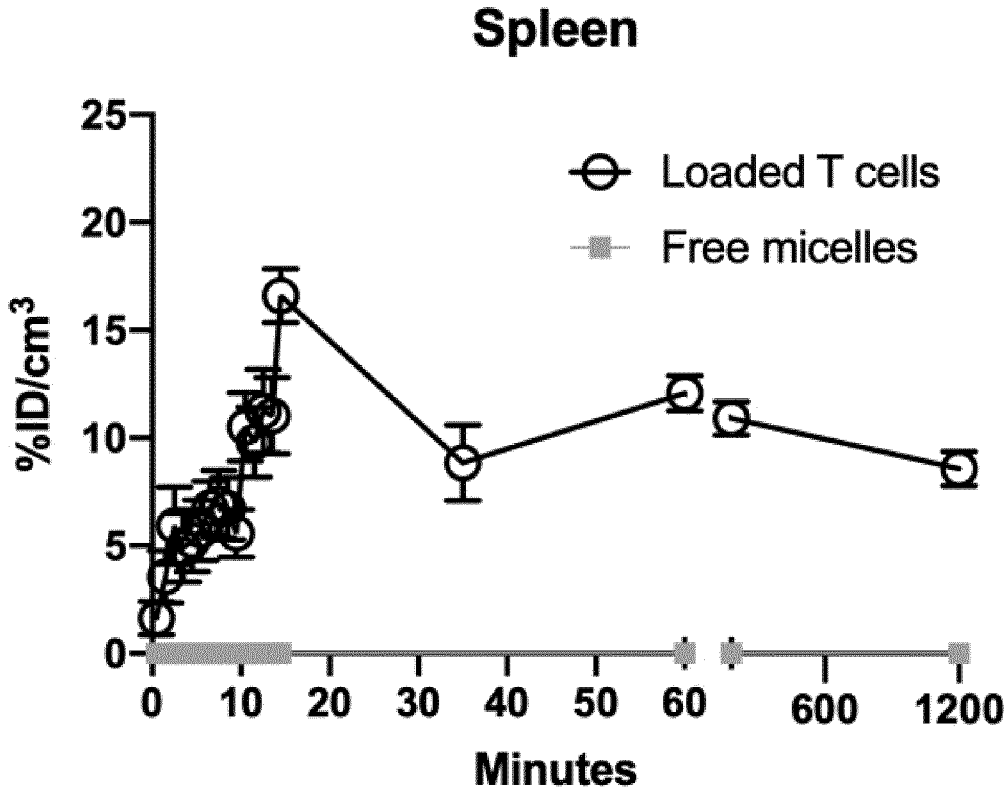


Fig. 19A

Lungs

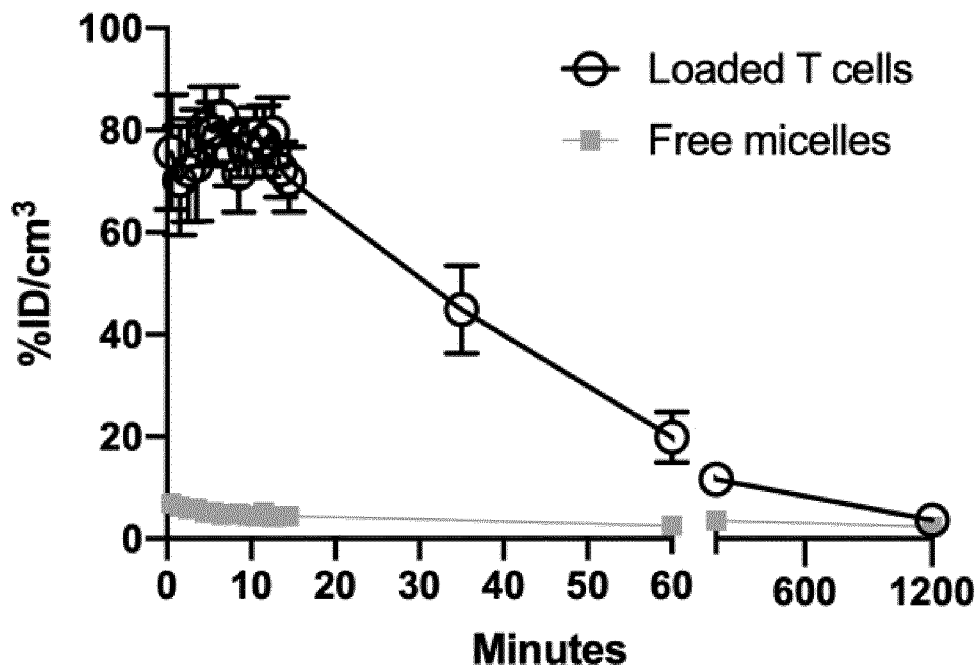


Fig. 19B

Blood

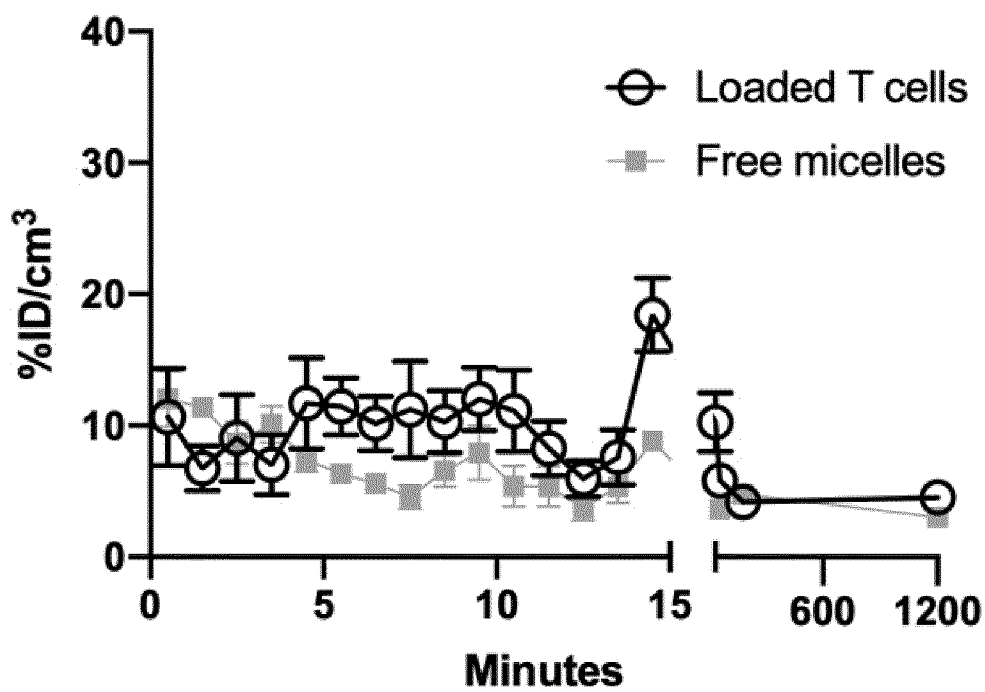


Fig. 19C

Liver

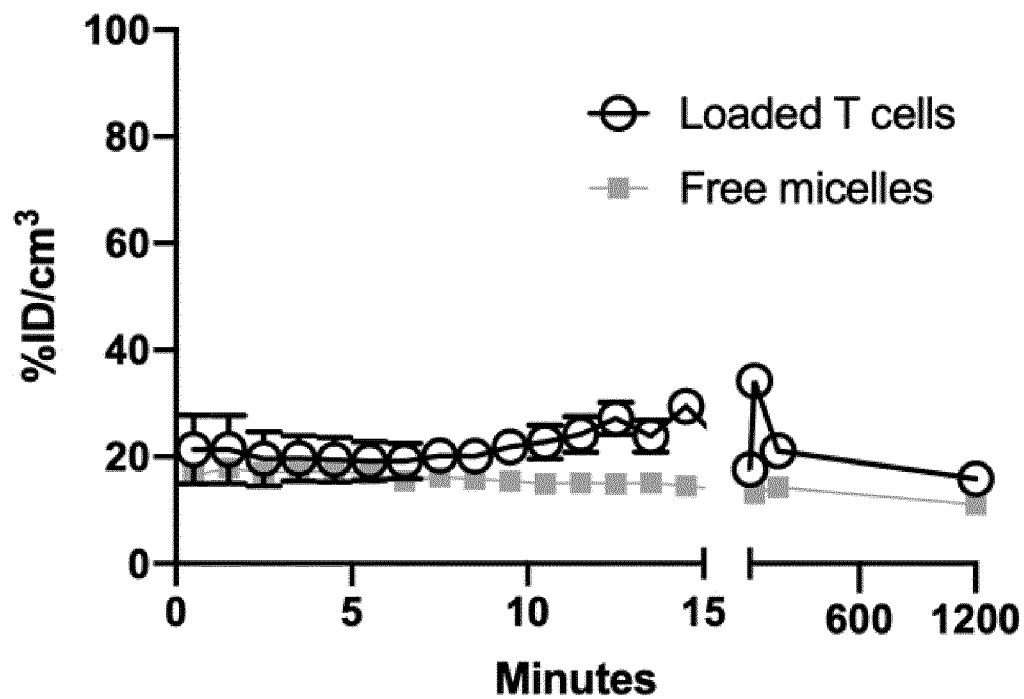


Fig. 19D

Tumor

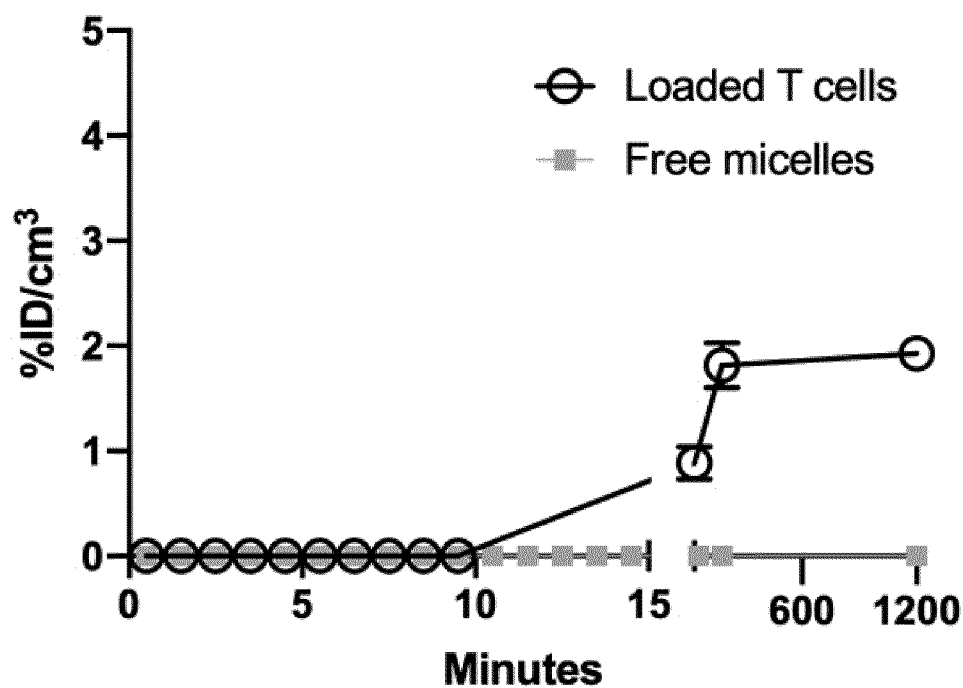


Fig. 19E

Bladder

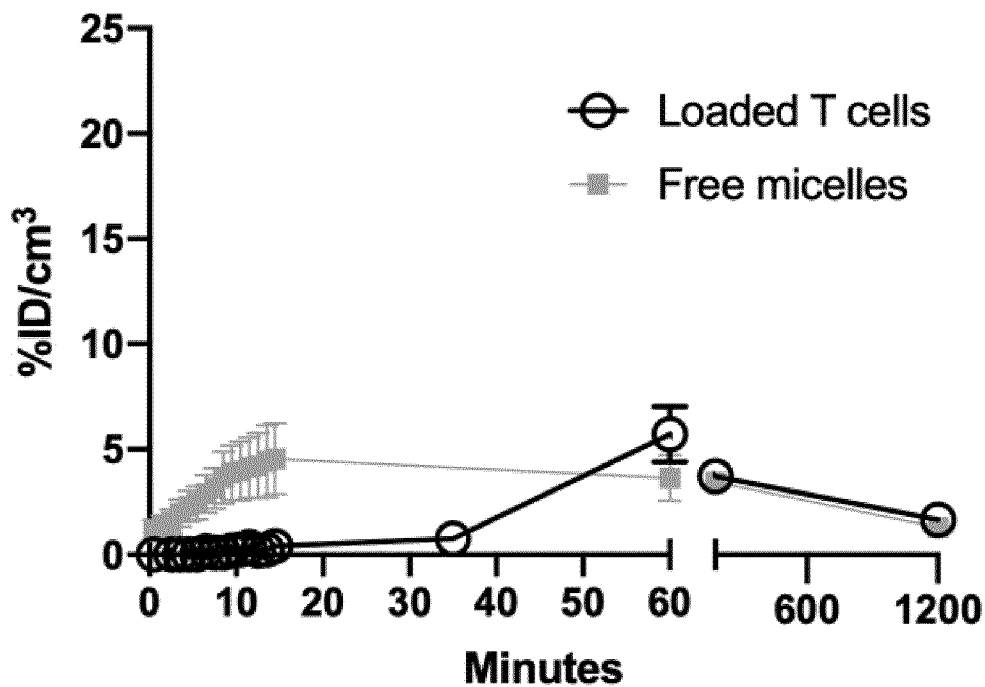


Fig. 19F

Overall whole body radioactivity

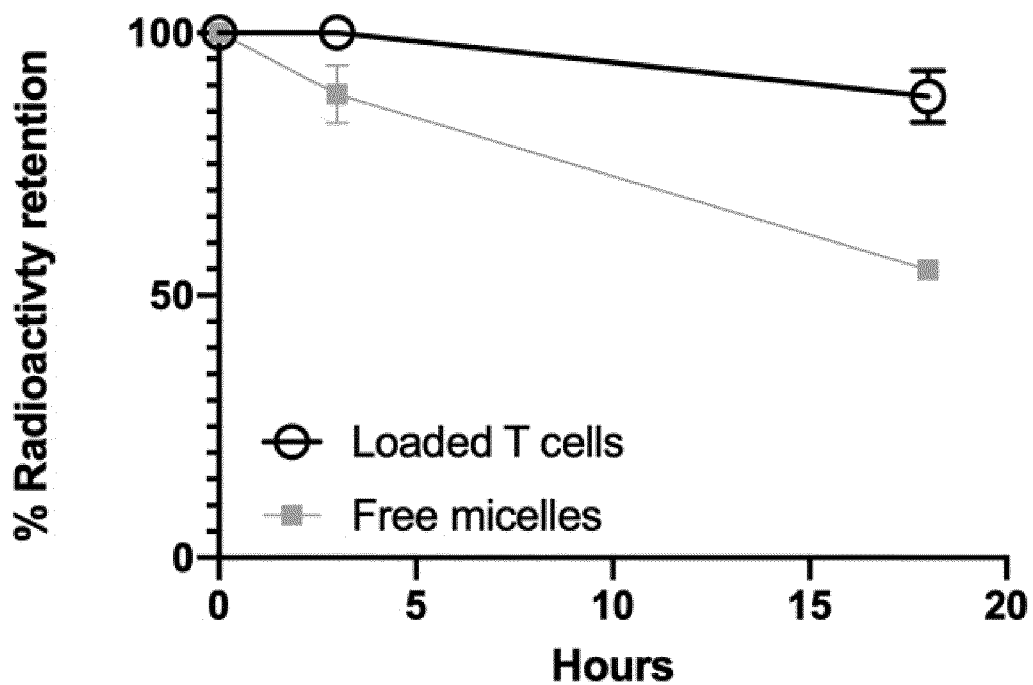


Fig. 19G

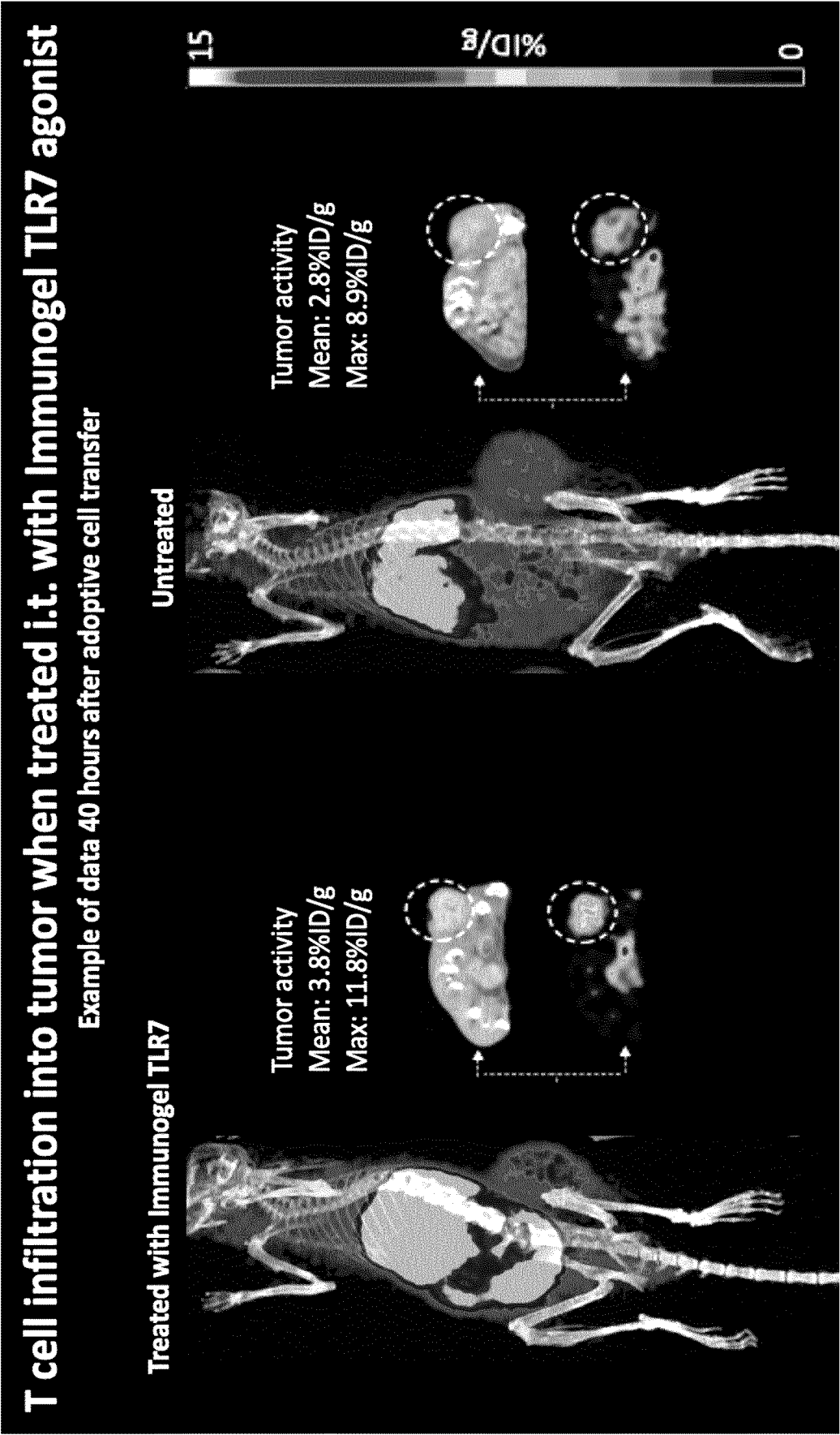


Fig. 20

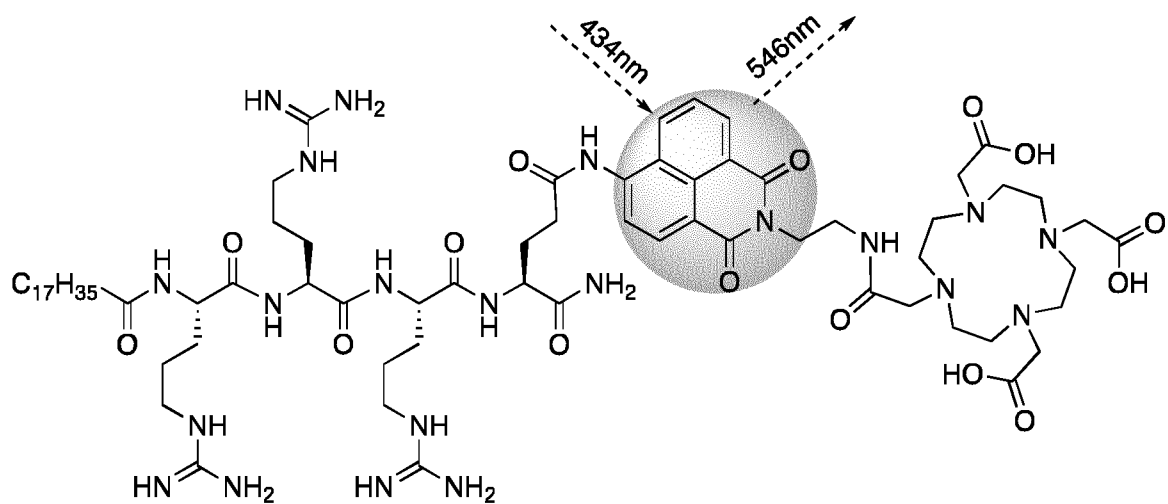


Fig. 21

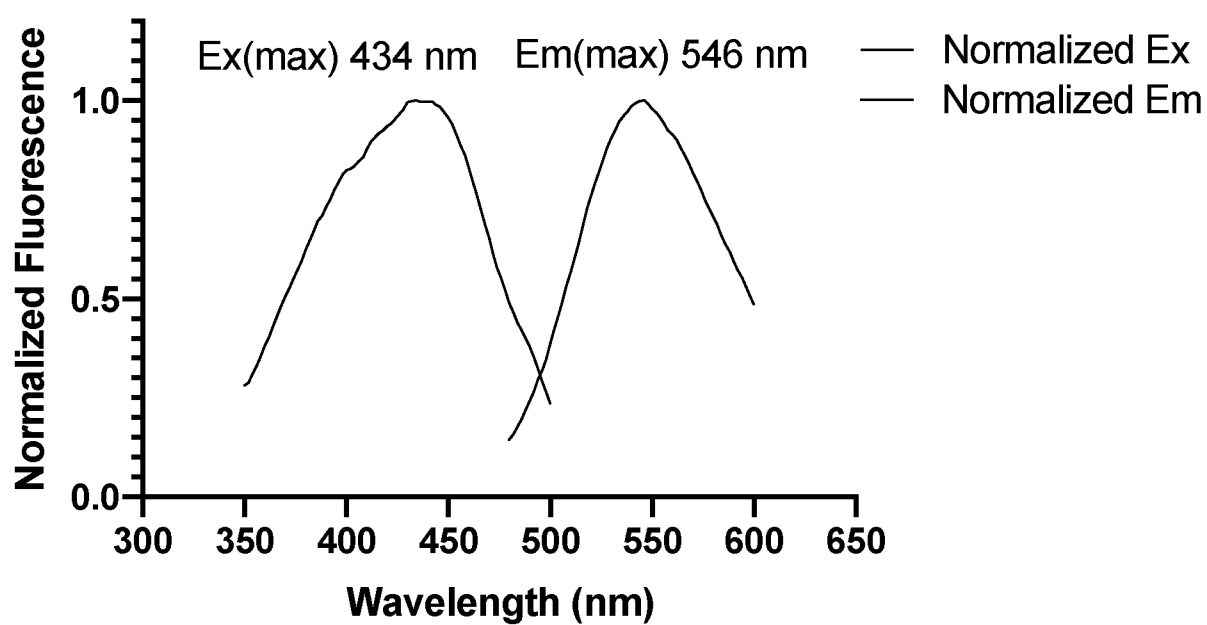


Fig. 22

INTERNATIONAL SEARCH REPORT

International application No
PCT/EP2020/066328

A. CLASSIFICATION OF SUBJECT MATTER

INV. A61K51/12 A61K51/08 A61K49/00 A61K51/04 C07K5/072
C07K5/09 C07K5/11 G01N33/58

ADD.

According to International Patent Classification (IPC) or to both national classification and IPC

B. FIELDS SEARCHED

Minimum documentation searched (classification system followed by classification symbols)

G01N A61K C07K

Documentation searched other than minimum documentation to the extent that such documents are included in the fields searched

Electronic data base consulted during the international search (name of data base and, where practicable, search terms used)

EPO-Internal, BIOSIS, EMBASE, WPI Data

C. DOCUMENTS CONSIDERED TO BE RELEVANT

Category*	Citation of document, with indication, where appropriate, of the relevant passages	Relevant to claim No.
X	<p>WILLIAM O'MALLEY ET AL: "Cellular Uptake and Photo-Cytotoxicity of a Gadolinium(III)-DOTA-Naphthalimide Complex "Clicked" to a Lipidated Tat Peptide", MOLECULES ONLINE, vol. 21, no. 2, 1 February 2016 (2016-02-01), page 194, XP055720797, DE ISSN: 1433-1373, DOI: 10.3390/molecules21020194 abstract table 1 figures 2,4</p> <p>----- -/--</p>	<p>1-34, 39-55,60</p>



Further documents are listed in the continuation of Box C.



See patent family annex.

* Special categories of cited documents :

"A" document defining the general state of the art which is not considered to be of particular relevance

"E" earlier application or patent but published on or after the international filing date

"L" document which may throw doubts on priority claim(s) or which is cited to establish the publication date of another citation or other special reason (as specified)

"O" document referring to an oral disclosure, use, exhibition or other means

"P" document published prior to the international filing date but later than the priority date claimed

"T" later document published after the international filing date or priority date and not in conflict with the application but cited to understand the principle or theory underlying the invention

"X" document of particular relevance; the claimed invention cannot be considered novel or cannot be considered to involve an inventive step when the document is taken alone

"Y" document of particular relevance; the claimed invention cannot be considered to involve an inventive step when the document is combined with one or more other such documents, such combination being obvious to a person skilled in the art

"&" document member of the same patent family

Date of the actual completion of the international search

7 August 2020

Date of mailing of the international search report

18/08/2020

Name and mailing address of the ISA/

European Patent Office, P.B. 5818 Patentlaan 2
NL - 2280 HV Rijswijk
Tel. (+31-70) 340-2040,
Fax: (+31-70) 340-3016

Authorized officer

Bliem, Barbara

INTERNATIONAL SEARCH REPORT

International application No

PCT/EP2020/066328

C(Continuation). DOCUMENTS CONSIDERED TO BE RELEVANT

Category*	Citation of document, with indication, where appropriate, of the relevant passages	Relevant to claim No.
X	ANNA LEONIDOVA ET AL: "Enhanced Cytotoxicity through Conjugation of a "Clickable" Luminescent Re(I) Complex to a Cell-Penetrating Lipopeptide", ACS MEDICINAL CHEMISTRY LETTERS, vol. 5, no. 7, 19 May 2014 (2014-05-19), pages 809-814, XP055720915, US ISSN: 1948-5875, DOI: 10.1021/ml500158w abstract	1,3-6, 9-12,14, 15,19, 23,45, 48,51,60
X	----- GIANOLIO E ET AL: "A Novel Method of Cellular Labeling: Anchoring MR-Imaging Reporter Particles on the Outer Cell Surface", CHEMMEDCHEM, vol. 3, no. 1, 11 January 2008 (2008-01-11), pages 60-62, XP055099329, ISSN: 1860-7179, DOI: 10.1002/cmdc.200700182 the whole document figures 1,2	1-34, 39-44, 56-60
X,P	----- WENBO WANG ET AL: "Preclinical evaluation of cationic DOTA-triarginine-lipid conjugates for theranostic liquid brachytherapy", NANOTHERANOSTICS, vol. 4, no. 3, 1 January 2020 (2020-01-01), pages 142-155, XP055720762, ISSN: 2206-7418, DOI: 10.7150/ntno.44562 the whole document -----	1-60